Addressing The Potential of Alternative Configurations for CO$_2$ER Supply Chains

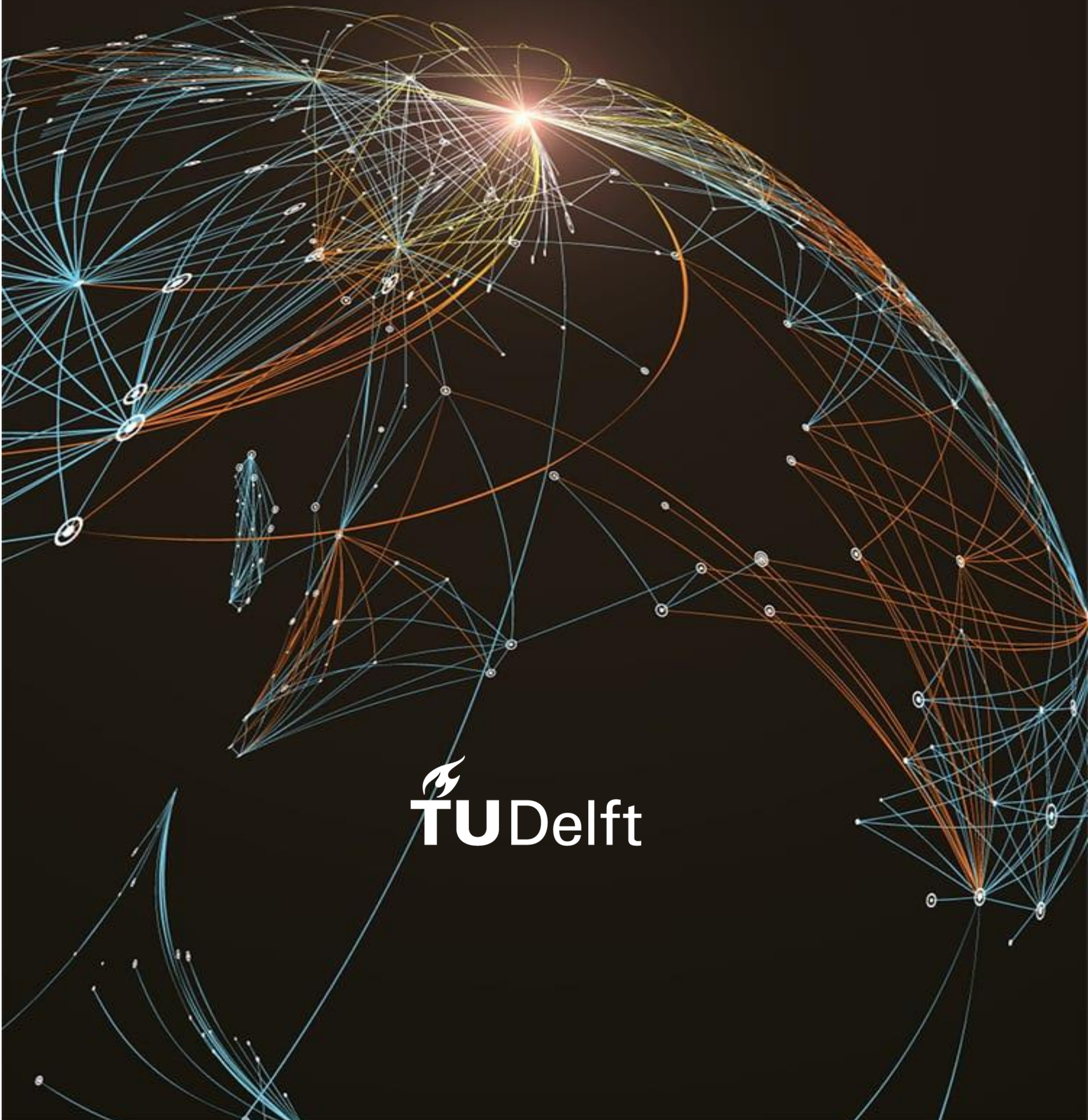

TU Delft

Addressing the Potential of Alternative Configurations for CO_2ER Supply Chains

Master thesis submitted to Delft University of Technology

in partial fulfilment of the requirements for the degree of

MASTER OF SCIENCE

in **Complex Systems Engineering and Management**

Faculty of Technology, Policy and Management

by

Stijn Yska

Student number: 5414156

To be defended in public on 21/12/2022

Graduation committee

Chairperson: Prof. dr. ir., C.A., Ramirez Ramirez, Energy & Industry
First Supervisor: Dr. ir., M.d.M., Pérez-Fortes, Energy & Industry
Second Supervisor: Dr., M.Y., Maknoon, Transport and Logistics

This page is intentionally left blank.

Abstract

As global climate change concerns intensify, the search for renewable-based alternatives to products and processes that rely on fossil fuels becomes ever more important. A process that has been championed is the co-electrolysis of carbon dioxide and water, under the supply of renewable energy, via high-temperature solid oxide electrolyser systems. The technological combination can produce syngas directly. This syngas is a renewable-based alternative to fossil-based syngas, which has a widely established market and can directly be used for the generation of energy in power plants, or as a precursor for the production of carbon-based chemicals and fuels. Although many technology-specific improvements have been made in recent years that contributed to the creation of a promising outlook and an increasing number of demonstration projects, the feasibility and implications of implementing the process on an industrial scale remain largely unaddressed. Since many technologies fail in the transition from benchtop to industrial scale, a deeper understanding of the requirements that are opposed at an industrial scale should be obtained, to this end, this work applies an exploratory research approach to investigate the feasibility and opportunities of the supply chain that supports the production of syngas via co-electrolysis. To delineate the feasibility of the supply chain, this work considers two perspectives of feasibility; (i) the feasibility of the horizontal supply chain which encompasses the requirements and availability of feedstocks, technology and process scales, and market potential, and (ii) the feasibility of the vertical supply chain which encompasses the availability of materials required for the operation of solid oxide electrolyser systems. To investigate the opportunities of the supply chain, this work considers decentralised and centralised supply chain configurations. To initiate the research the individual supply chain units that are required for the process to be operatable at industrial scales were assessed. The requirements and scales of the individual units are matched with the current and expected future scales of technologies, feedstocks and markets. From this scale match, it can be concluded that based on feedstock availability and syngas market size, it is technically feasible to completely replace fossil-based syngas with renewable-based syngas produced by solid oxide electrolyser technology. However, several aspects such as the renewable energy requirements and the number of high-temperature solid oxide electrolyser systems that are required, impose practical limitations on the large-scale rollout. The influence of these practical limitations is aggravated after an assessment of the opportunities of decentralised and centralised supply chains, as both possibilities require capital investments on the scale of 1 Billion Euros and no positive return. A smaller implementation scale was also considered, and the limitations opposed to such a scale, seem much easier to overcome, highlighting potential future research directions. To delineate the feasibility from the vertical supply chain perspective, the material requirements of solid oxide electrolyser systems and the corresponding material availability were investigated. From this investigation, it can be concluded that from a global point of view, only Gadolinium opposes feasibility limitations. However, from a European point of view, the limitations seem much more severe. Based on the findings of this work, future research should focus on detailed analyses of the potential of solid oxide electrolyser supply chains at smaller scales, as there exist many opportunities that could improve overall supply chain performance, and smaller scales oppose less severe problems.

This page is intentionally left blank.

Acknowledgements

This work represents the outline of my Master's Thesis project at the TU Delft, and throughout this research project, I benefitted from knowledge and guidance from various people. To this end, this section aims to identify, acknowledge, and thank these people.

First of all, I would like to express my gratitude to Mar Perez-Fortes, who spent much time reviewing my work and created the time to have weekly discussions. These discussions were both meaningful and allowed for some humour at the same time, the combination of which made my research project a pleasant and educational time. Secondly, I would like to express graduate to Andrea Ramirez and Yousef Maknoon, for providing me with guidance during the early and final stages of the project. Besides my graduation committee, Josephine Vos, Thijmen Wiltink and Jeroen Janssen helped me with some fruitful discussions. Additionally, I would like to thank Alexandra Kolbeins for providing me with useful literature throughout the entire thesis project.

This page is intentionally left blank.

Contents

List of Figures

List of Tables

List of Acronyms

AEL	Alkaline electrolyser
CAPEX	Capital expenditures
CDU	Carbon dioxide utilisation
CoSEM	Complex Systems Engineering and Management
CO	Carbon monoxide
CO_2	Carbon dioxide
CO_2ER	Carbon dioxide electrochemical reduction
CCS	Carbon capture and storage
CCU	Carbon capture and utilisation
CCUS	Carbon capture, utilisation and storage
DAC	Direct air capture
EC	European Commission
EOR	Enhanced oil recovery
ER	Electrochemical reduction
EU	European Union
FE	Faradaic efficiency
GHG	Greenhouse gas
HT	High temperature
H_2	Hydrogen
H_2O	Water
KPI	Key performance indicator
Ktpa	Kilo tonnes per anum
MILP	Mixed integer linear programming
Mtpa	Mega tonnes per anum
NG	Natural gas
OPEX	Operational expenditures
O&M	Operation and maintenance
PCC	Post-combustion capture
PSC	Point source capture
PEM	Proton exchange membrane
ppm	parts per million
PV	Photovoltaics
RE	Renewable energy
RES	Renewable energy sources
SOEC	Solid oxid electrolyser cell
SOFC	Solid oxid fuel cell
TEA	Techno-economic analysis
UK	United Kingdom
U.S.	United States

Chapter 1

Introduction

1.1 The Need for Carbon Dioxide Capture and Utilisation Processes

The melting of glaciers and the associated rise in sea level, deforestation, undesirable impacts on human health in large cities, and declining freshwater supplies (Pieri et al., 2018); are all examples of the negative results of global warming with a large societal impact. The rise in temperature, which can be identified as the origin of these problems, is primarily caused by the increasing amount of greenhouse gases (GHGs) emitted into the Earth's atmosphere. According to Gokhberg et al. (2013), approximately 80% of these GHGs consists of carbon dioxide (CO_2). The other GHGs are methane (10%), nitrous oxide (7%) and fluorinated gases (3%) (United States Environmental Protection Agency, 2022). Furthermore, research by Jin et al. (2021), identifies that the global atmospheric concentration of CO_2 has risen from 280 to 415 parts per million (ppm) between 1750 and 2021, this increasing concentration is primarily caused by human activities. Combining the given information with the maximum concentration of CO_2 which is required for the Earth to remain in a balanced state of energy; approximately 350 ppm (J. Hansen et al., 2013), one can easily delineate the urgency for actively pursuing the decrease of CO_2 concentrations on Earth. This urgency is translated into global energy and climate goals. To this end, the European Union (EU) formulated the European Green Deal, which is the EU's response strategy toward environmental and climate-related challenges setting out a vision for the EU, including the 2030 Climate Target Plan encompassing a GHG emission reduction of at least 55% in 2030 compared to 1990 levels, and the target for *net-zero GHG emissions by 2050* (European Commission, 2019b). Another example is the new target of the United States (U.S.) to achieve a 50-52% reduction in US GHG pollution from 2005 levels in 2030 and the intention to rejoin the Paris Agreement, reaching *net-zero emissions* economy-wide by no later than *2050* (The White House, 2021). Both examples of climate goals encompass the notion of "net zero" and according to the United Nations, this means "*cutting GHG emissions to as close to zero as possible, with any remaining emissions re-absorbed from the atmosphere*" (United Nations, 2022).

A branch of technological innovations that has the potential to play an important and diverse role in meeting global energy and climate goals is carbon capture, utilisation and storage (CCUS) (International Energy Agency, 2021). The technological branch of CCUS can be further divided into two sub-categories; Carbon Capture and Storage (CCS) and Carbon Capture and Utilization (CCU). In political discussions and between various geographical regions, these two concepts are often commingled and therefore it is important to identify the differences between them in the context of this work. The concept of CCS (also referred to as CO_2 capture and storage or CO_2 sequestration) was developed to deal with the substantial amount of anthropogenic CO_2 emissions originating from point sources, mostly fossil-fired power and fossil-based industrial plants. CCS processes have already been commercially adopted and commonly consist of three-step procedures: (i) capturing, drying and compressing CO_2; (ii) transportation of CO_2 to storage sites, commonly by, pipelines; (iii) and finally long-term storage of the CO_2 in, for example, deep saline formation, unminable coal beds, depleted oil or gas reserves, and mineralization (Bruhn et al., 2016) (Yaashikaa et al., 2019) (European Commission, 2022). Alternatively to CCS, the concept of CCU (also referred to as CO_2 capture and utilisation), aims to reduce fossil resource consumption, and consequently depletion, by reusing already emitted CO_2 as a substitute for carbon-based products (Bruhn et al., 2016). Like CCS, CCU technologies firstly require the capturing of CO_2, thereafter the CO_2 is either utilised directly (i.e. chemical structure is not changed), for example, in soft drinks, in greenhouses, used as a working fluid or solvent (e.g. for enhanced oil recovery (EOR)), or it is being used as a feedstock in which the CO_2 molecule is chemically changed and converted into value-added carbon-based products such as polymers, building materials, chemicals or synthetic fuels (Jones et al., 2017) (Jouny et al., 2018) (European Commission, 2022). Processes in the latter category of technological applications, that changes the chemical structure and utilise CO_2 as a feedstock for the production of carbon-based products, are referred to as carbon dioxide utilisation (CDU) processes (Pérez-Fortes et al., 2016). A schematic overview of the various pathways that could be followed to deal with captured CO_2 has been provided in Figure A. 1 in Appendix A.

The potential of CCUS applications in general, as a mitigating measure for high CO_2 concentrations, is also recognised worldwide (International Energy Agency, 2021) (Department of Energy, 2009) (K. Jiang et al., 2020). This recognition is quantified in Figure 1, displaying the global increase in the operation, development and planning of CCUS projects. According to the International Energy Agency (2021), the strengthened climate goals and new investment incentives result in positive momentum for the increased adoption of CCUS applications. They will play an important role in meeting the net-zero targets, including as one of the few solutions capable of tackling emissions from heavy industry. Having said that, even though the adoption of CCUS is increasing, the approximately 100 planned projects as depicted in Figure 1, have an annual CO_2 capture capacity that falls well short of the target capacity. Moreover, the number of CCUS facilities depicted in Figure 1 that were in operation in 2021, have a combined annual CO_2 capture capacity of approximately 40 Mega tonnes per anum (Mtpa) (International Energy Agency, 2020). Although Figure 1 does not depict the capture capacity of the facilities, comparing the 40 Mtpa with the targeted 1700 Mtpa of CO_2 capture capacity to be deployed globally by 2030 (International Energy Agency, 2021), it can be concluded that a significant increase in the number and possibly the size of CCUS projects is needed to reach the 2030 targets. However, it must be noted that the International Energy Agency (2021), refers to CCUS capacity, and in light of the previously defined discrepancy regarding the intertwined usage of the terms CCS and CCU, it is important to further highlight to what extent the CCUS facilities that have been depicted in Figure 1 are related to either of the two sub-categories. Moreover, although the International Energy Agency (2021), does not mention specific numbers, they do state that, in the *Net Zero Emissions by 2050 scenario*, the vast majority of the captured CO_2 will be stored and consequently can be assigned to CCS projects. Based on these claims, similar conclusions can be drawn for 2030.

Although CCS projects are perceived as the most prominent pathway to deal with high CO_2 concentrations for 2030 and 2050, CCU projects, and more specifically CDU projects, have significant potential to contribute to the circular economy and climate goals, not only by the actual reduction of CO_2 emissions and the possibility to decrease the atmospheric concentration of CO_2 (if certain CO_2 capture technologies are used), but also in other ways, for example, by avoiding environmental risks and side-effects caused by the exploitation and processing of fossil resources such as crude oil or gas, if the end-product can be used as a substitute for the fossil-based product (Von Der Assen & Bardow, 2014), or as CO_2-net-zero alternatives for nowadays fossil fuels in, for example, the transport sector (Pieri et al., 2018). If specific technologies are used to provide the CO_2 feedstock it addresses both aspects of the *net zero* notion that has been provided by the United Nations (2022); cutting GHG as close to zero as possible and reabsorbing emitted CO_2. Therefore, further research on technological, economic, social and political aspects that could enhance or oppose limitations to the increased adoption of CDU projects is required. However, to realize this, a further delineation of the different technological possibilities that fall within the CDU branch should be provided.

Figure 1 Global outline of commercial CCUS facilities operating and in development 2010-2021 (figure copied from IEA, 2021). Indicating the rapid and significant increase of global CCUS technology projects.

There exist multiple CDU pathways to convert CO_2 into value-added carbon-based products, a schematic overview of the different pathways has been provided in Figure A. 1 (in Appendix A.1). This work focuses on *carbon dioxide electrochemical reduction*, henceforth referred to as *CO_2ER*. A CO_2ER process utilises electrolyser technology, and under the supply of electricity, electrolysers convert CO_2 into reduced carbon-containing products (C. Chen et al., 2018). Additionally, to synthesise carbon-based products, there is usually hydrogen (H_2) feedstock required (Pérez-Fortes et al., 2016). CO_2ER is selected as the process that will be investigated in this work, since it is one of the most promising CDU conversion pathways, mainly because (i) the electrolyser and the alternation of its operating conditions offer the opportunity to tune the CO_2 reduction process to produce the desired products (Yun Zheng et al., 2017) (Jouny et al., 2018) (Mohammed et al., 2021), (ii) it can be integrated with renewable energy sources (RES), and as such deal with the associated intermittency whilst synthesizing saleable products (Garg et al., 2020), and (iii) the electrolyser is associated with modular reactor design, in turn, this modularity has intrinsic diversification, flexibility, and scalability properties (Dahlgren et al., 2013) (Yun Zheng et al., 2017) (Jouny et al., 2018). Furthermore, the electrical energy efficiency and potential cost-effectiveness are mentioned in the literature as factors that make CO_2ER one of the most promising technologies, not only within the CDU category but as a technology for mitigating CO_2 emissions whilst utilizing the captured carbon in general (Yun Zheng et al., 2017) (Park et al., 2021).

Despite its potential, CO_2ER is an emerging technology which is still in its infancy. Consequently, it has not been commercially adopted yet and there exists a significant gap between today's situation and the desired situation in which commercial CO_2ER supply chains are adopted and embedded into energy and carbon-based product production systems such that they contribute to the desired 1700 Mtpa of global installed CO_2 capture capacity by 2030 and the Net Zero Emissions targets for 2050, whilst producing saleable products. For the process to become a viable way to produce carbon-based products in the long term, there exist three types of limitations that must be understood and confronted: (i) thermodynamics, (ii) kinetics, and (iii) infrastructure (C. Chen et al., 2018). Moreover, according to W. A. Smith et al. (2019) most studies on CO_2ER focus on improving the performance of specific technological problems, as such, they revolve around the first and second limitations that have been identified by Chen et al., (2018), whilst the third limitation remains largely unaddressed. Consequently, a shift in research efforts towards the broader technological application that includes complete system integration, including the geographical components of its supply and demand units, and matching the scales of the various supply chain units, is required for the technology to be adopted into future energy systems (W. A. Smith et al., 2019).

1.2 Economies of Centralisation

For any of the value-added carbon-based products that could be produced by CO_2ER processes, the potential of scaling up the supply chain, its economic performance, and the availability of feedstocks that are required to produce these products are crucial. Since CO_2ER is an emerging technology, favourable technology implementation conditions remain unknown, and compared to conventional carbon-based product production processes, the utilisation of a CO_2ER process might oppose different *challenges* but could also create other *opportunities*. Moreover, conventionally, the production of carbon-based products is done in large-scale production facilities that follow the economies-of-scale model. This encompasses the idea of “bigger is better”, in which the capital costs per unit of capacity decline with increasing unit size (Dahlgren et al., 2013). An example of such a conventional large industrial chemical plant is provided by W. A. Smith et al. (2019), who refers to Shell’s Pearl Gas-to-Liquid (GTL) plant[1] that has a production capacity of 16.500 tons/day. The Pearl plant utilises oil and gas feedstocks from various wells and gas fields, these feedstocks are transported to the production site and the products that are being produced (e.g. kerosene, naphtha and base oils for chemicals) are transported to markets around the globe (Shell Global, 2012). Such a supply chain can be classified as a *centralised supply chain* since its products are being produced at one location, whilst the feedstocks are obtained from multiple supply points and the produced products are transported to various points of demand (i.e. markets) around the world. In a *centralised configuration*, the plant size and transportation costs of both feedstocks and products are proportional to the served area (i.e. they are dependent on the shipping and rate of transportation). Several advantages and disadvantages of centralised supply chain configurations that have been mentioned in the literature are provided in Table 1.

Table 1 Identification of possible advantages and disadvantages of centralised supply chain configurations

Centralised Supply Chain Configuration	
Advantages	**Reference(s)**
Spread out fixed cost-components of a system, that need to be included anyway, over a larger output	(Dahlgren et al., 2013)
Lower material requirements (construction)	(Dahlgren et al., 2013)
Decrease fixed OPEX (e.g., administrative costs, security costs and infrastructure costs, increased labour productivity)	(Dahlgren et al., 2013)
Possibility of better forecasting	(Garrehy, 2016)
Usage of local personnel	(Garrehy, 2016)
Consistent production	(Garrehy, 2016)
Improved efficiency in the usage of limited resources	(Bouffard & Kirschen, 2008)

---

[1] Shell’s Pearl plant is located in Ras Laffan Industrial City, Qatar and utilises natural gas to produce a wide variety of carbon-based liquid products such as gasoil, kerosene, naphta, normal paraffin and base oils for lubricants. (Shell Global, 2012).

Lower manufacturing costs	(Garrehy, 2016)
Decrease per unit transportation costs	(Bouffard & Kirschen, 2008)
Disadvantages	**-**
Ageing of highly complex infrastructure	(Bouffard & Kirschen, 2008)
Inflexibility to adjust the production process	(Garrehy, 2016) (Dahlgren et al., 2013)
Regulatory and economic risks	(Bouffard & Kirschen, 2008)
Terrorist threats	(Bouffard & Kirschen, 2008)
Climate change	(Bouffard & Kirschen, 2008)
Geopolitical disruptions	(Bouffard & Kirschen, 2008)
Natural disasters	(Bouffard & Kirschen, 2008)

Opposed to a centralised supply chain there exists the possibility of a *decentralised supply chain*. In a *decentralised configuration*, multiple smaller-sized plants located at various locations can serve the same area as centralised supply chains. However, unlike centralised configurations that generally require the transportation of both feedstocks and products over longer distances, in decentralised configurations, the production plant can be located close to sources of supply and/or points of demand, eradicating the need for costly (long-distance) transportation (Dahlgren et al., 2013). An example of such a decentralised configuration is provided by Dahlgren et al. (2013), who mention several companies (e.g. MIOX and AkzoNobel) that have designed small modular chlorine plants that can be placed close to points of demand, such that the need for storage and transportation of chlorine (a substance that is highly toxic and dangerous to store and transport) is eliminated. The chlorine plants designed by AkzoNobel can produce up to 15.000 tonnes of chlorine per year and are module-based and skit-mounted (i.e. assembled on-site) (CHEManager, 2011). Moreover, they are manufactured off-site, which reduces the on-site construction requirements, in turn, shortening the time needed to bring a plant online (Dahlgren et al., 2013). Several advantages and disadvantages of decentralised supply chain configurations that have been mentioned in the literature are provided in Table 2.

Table 2 Identification of possible advantages and disadvantages of decentralised supply chain configurations.

Decentralised Supply Chain Configuration	
Advantages	**Reference**
Flexibility in meeting demand	(Garrehy, 2016)
Being closer to customers reduces product transportation costs	(Garrehy, 2016)
Usage of local personnel	(Garrehy, 2016) (Lam et al., 2021)
The ability to take advantage of opportunities in different areas	(Garrehy, 2016)
Smaller initial CAPEX requirements	(Dahlgren et al., 2013)
Eliminating the need for the transportation of dangerous substances	(Dahlgren et al., 2013)
Disadvantages	**-**
Higher total CAPEX	(Garrehy, 2016)
Higher per-unit cost	(Garrehy, 2016)

A comparison of the advantages and disadvantages that have been provided in Table 1 and Table 2 respectively, identifies that the research by Garrehy (2016), assigns the advantage of "*usage of local personnel*" to both centralised and decentralised supply chain configurations. Moreover, in centralised supply chain configurations, this advantage is primarily related to the potential social benefits associated with the usage of local personnel at a single geographical location. In turn, this could enhance the relationship between the plant and the local community. In decentralised supply chain configurations, the advantage of "usage of local personnel" is related to other aspects. Moreover, Garrehy (2016) identify that in a decentralised configuration, there exists the possibility to take advantage of low labour costs in different areas, but also the possibility to locate plants close to areas where there exists a high degree of expertise and talent (i.e. research centres and universities), which could be attracted (Lam et al., 2021).

Another aspect that requires clarification is related to the possible advantages and disadvantages associated with capital expenses (CAPEX), operational expenses (OPEX), and fixed costs. Moreover, according to Dahlgren et al. (2013), centralised configurations can benefit from the advantage of "*spreading out fixed costs components of a system*", which is primarily related to control and monitoring systems that need to be included (at each location), but also the costs incurred during the design phase. This advantage relies on the assumption that, in a decentralised configuration, control and monitoring systems need to be available at each plant location whereas in a centralised configuration these systems only need to be available at a single location, resulting in decreased fixed costs. Furthermore, Dahlgren et al. (2013), identify that decentralised configurations could benefit from the advantage of "*smaller initial CAPEX requirements*", whereas Garrehy (2016), identifies "*higher total CAPEX*" as a disadvantage associated with decentralised configurations. The advantage revolves around the possibility of gradually deploying additional plants in a decentralised configuration which in turn results in reduced initial investment and risk since smaller plants generally result in lower construction costs and faster project completion (Garrehy, 2016) (Dahlgren et al., 2013). In turn, this advantage results in a disadvantage in the long run (i.e. when the total capacity of decentralised configurations approaches the total capacity of centralised configurations), since the construction of additional plants requires additional investments.

Based on Table 1 and Table 2, it can be concluded that both supply chain configurations have certain advantages and disadvantages, and since CO_2ER processes rely on electrolyser technology, which is modular by nature, the supply chain of a CO_2ER process can be configured in either a centralised or decentralised manner. However, due to the lack of research that is available on the broader technological application of CO_2ER, including system integration, the required infrastructure, and the broader limits of such supply chains, a detailed assessment of centralised versus decentralised configurations is not possible at the current research stage.

1.3 Problem Description

The broader context of the research and the associated need for increased adoption of CCUS projects that are capable of tackling CO_2 emissions have been identified in section 1.1. Additionally, considering the climate targets for 2030 and the target of Net Zero Emissions by 2050, section 1.1 identifies that, at the current stage, most of the CCUS projects are expected to focus on carbon storage and consequently fall within the CCS category. However, given the high potential of CDU projects and especially the CO_2ER process, further investigating the potential of CO_2ER processes and their ability to become a viable way to produce carbon-based products by utilising captured carbon in the long term, is an interesting and highly relevant research topic.

Most of the research on CO_2ER focuses on the thermodynamics and kinetics of the process, whilst aspects associated with the infrastructure and consequently the supply chain that is required for the operation of a CO_2ER process, remain largely unaddressed. The importance of considering the infrastructure and the supply chain for the production of carbon-based products, thus also for CO_2ER processes, has been identified in section 1.2. Apart from the importance, section 1.2 also identifies the opportunities that arise when considering CO_2ER technology from a broader perspective; centralised versus decentralised supply chain configurations, however, due to the lack of knowledge of an integrated supply chain, favourable technology implementation conditions, including potentially preferred supply chain configurations, remain unknown.

Since many technologies fail in the transition from benchtop to industrial scale, it is important that, at an early research stage, a deeper understanding is developed of the limitations or boundaries of technologies from an integrated system perspective. These limitations or boundaries have not been addressed for CO_2ER supply chains. This lack of knowledge on the upper and lower limits of CO_2ER supply chains can be identified as the *main problem* of this research. Based on the possible advantages and disadvantages of centralised and decentralised supply chains, this problem should be addressed whilst considering the notion of economies of centralisation. By considering alternative supply chain configurations during the exploration of limits, the possibility to utilise alternative supply chain configurations for future adoption of the technology can be further assessed.

1.4 Scientific Contribution and Societal Relevance

The exploration of integrated CO_2ER supply chains provides preliminary insights into the limits that should be considered in future research on the topic, but also on aspects that do not oppose any limits. The limits revolve around the availability of feedstocks for the CO_2ER process (e.g., H_2O and RE), the quantification of the market of the carbon-based product it produces, the availability of infrastructure to transport feedstocks and the carbon-based product, and the availability of high-temperature heat. Additionally, the consideration of an integrated supply chain perspective provides insights into the bottlenecks, both technical and economic, that are present considering state-of-the-art process technology, such as carbon capture technology and electrolyser technology, and consequently, hinder commercial adoption. The supply chain perspective also provides some preliminary insights into the opportunities associated with centralised and decentralised supply chains. The identification of limitations and opportunities are *scientific contributions* as they provide valuable insights for future research directions. Apart from the identification of boundaries and directions for future research, this work also provides a *scientific contribution* in another way. Moreover, since CO_2ER has not been commercially adopted, the integration of the supply chain requires a scale match between the various supply chain units. To match the scales of the respective supply chain units, this study requires the homogenisation of large amounts of data. The homogenised data is readily available for researchers in the field of CO_2 reduction processes and their supply chains.

Apart from the scientific contribution, tackling the problem that has been delineated in the previous section also has *societal relevance*. Moreover, the exploration of the limits of CO_2ER supply chains contributes to the information that policymakers can use in their decision-making for regulatory aspects associated with, for example, subsidizing and funding various aspects of the CO_2ER supply chain. Apart from policymakers, other stakeholders, such as technology developers and investors could also use the information for their decision-making processes. Furthermore, various demonstration projects, funded by governmental bodies, focus on the integration of electrolyser technology and carbon capture technology to produce carbon-based products. Such demonstration projects generally focus on demonstrating and examining the performance of integrated systems. The exploration of limits adds *societal relevance*, as it provides a preliminary identification of the potential of CO_2ER technology and its supply chain, in terms of its local and global requirements and potential. As such it provides a context for these demonstration projects.

1.5 Link to CoSEM Program and Energy Track

A *Complex Systems Engineering and Management* (CoSEM) master thesis, with *energy* as the selected track, should revolve around the design of solutions for large and complex contemporary socio-technical problems related to the energy domain. The CO_2ER process, which is the technology at the heart of the supply chain that is being investigated in this work, is a relatively novel technology that has not been commercially adopted. The technology, and its supply chain, have the potential to contribute to future energy systems by converting renewable energy into saleable carbon-based products, which highlights the link between this work and the energy track. Furthermore, the research problem that is being investigated is multidisciplinary by nature. Moreover, it has a clear technical component as it requires analytical calculations for both scale-matching within the supply chain and the determination of material requirements for the supply chain. It has a clear economic component as it involves market quantification and economic analysis of the CO_2ER supply chain. To assess the technical limits and economics of the CO_2ER supply chains that are being investigated, several existing regulations and actors have also been addressed, consequently, this work also considers institutional and social aspects.

1.6 Thesis Structure

To deal with the problem that has been defined in section 1.3, Chapter 2 focuses on providing a further outline of the state-of-the-art on CO_2ER supply chains. Based on the available literature a specific supply chain is selected as the scope of this work, which in turn, allows for further assessing the performance of alternative supply chain configurations. After delineating the state-of-the-art, the knowledge gaps and the associated research questions that will be treated in this work are identified. Subsequently, Chapter 3 focuses on delineating the research approach and methods that will be used in this work to provide answers to the main- and sub-research questions. Chapters 4, 5 and 6 will focus on answering the sub-research questions. Thereafter, Chapter 7 provides an overall conclusion combining the results from Chapters 4, 5 and 6 to answer the main research question. Finally, the research methods, the results of the research, and their implications for future research directions will be discussed in Chapter 8.

Chapter 2

State-of-the-Art and Research Specification

The introduction identified the potential of a CO_2ER process and the opportunities for its supply chain. Additionally, a primary indication of the problem has been provided, which revolves around the lack of knowledge on the limits of CO_2ER supply chains. To tackle this problem, a further outline of the CO_2ER process and its supply chain is required. Hence, this chapter aims to provide an overview of the state-of-the-art on technological possibilities within a CO_2ER supply chain and, based on the characteristics of these possibilities, a technological scope is selected. After delineating the scope, a further assessment of the state-of-the-art on transportation supply chain units that are deemed necessary for an industrial-scale CO_2ER supply chain will be provided and based on the scope and state-of-the-art, three knowledge gaps will be identified. This Chapter is concluded by formulating research questions that address these knowledge gaps and the formulation of the goal of this work.

2.1 Delineating the CO_2ER Supply Chain

This section aims to identify the scope of this work. Section 1.1 briefly touches upon the feedstocks that are required and the products that can be produced by a CO_2ER process. Additionally, the importance of the electrolyser and the operating conditions are mentioned. To provide structure to this section, Figure 2 depicts the selected supply chain units and the technologies that comprise them, forming the scope of this work. The argumentation to select this scope, which will be provided in the following subsections, relies on two aspects; (ii) the performance of supply chain units, and (ii) the possibility to explore and compare decentralised and centralised supply chains.

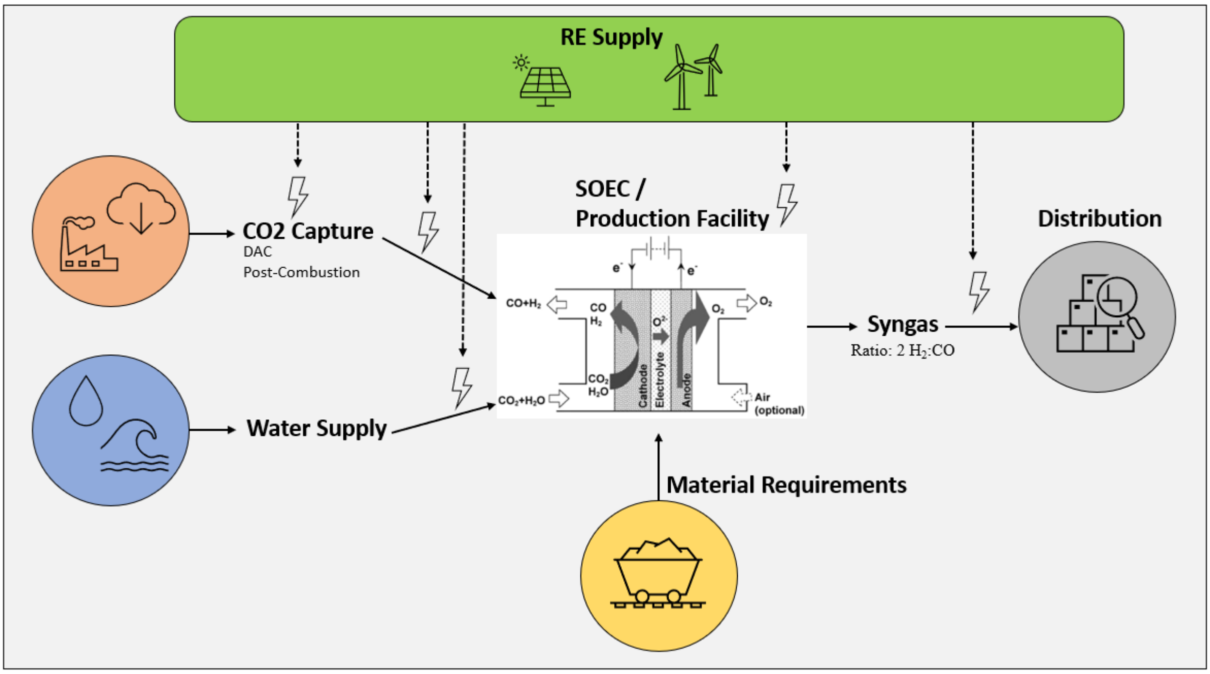

Figure 2 Schematic representation of the CO_2ER supply chain units; the technology, its inputs, outputs and requirements (picture for electrolyser obtained from Bedon (2018)).

2.1.1 The Type of Electrolyser and Production of Syngas, and Material Requirements

CO_2ER can be performed utilising various electrolyser types and the type of electrolyser technology determines a significant share of the process requirements, its energy efficiency and the reaction rate

(Mehmeti et al., 2018), and the composition and stability of the product (Ozden et al., 2022). There exist three main types of electrolysers: (i) proton exchange membrane (PEM), (ii) alkaline electrolyser (AEL), and (iii) *solid oxide electrolyser cell* (*SOEC*), a general overview of their key operating parameters is provided in Table 3. Generally, electrolysers have the same working principles; under the supply of electricity, the CO_2 reduction reaction (CO_2RR) occurs on the cathode side and if water (or steam) is used, the water oxidation takes place on the anode side (Mohammed et al., 2021). However, unlike PEMs and AELs, which have moderate operating temperatures of 40 - 80 ˚C and 65 - 220 ˚C respectively (Gallandat et al., 2017), SOECs use a solid oxide electrolyte, which allows operation at high temperatures (HTs). In HT-SOECs, the electrolyte is a ceramic material, and from temperatures above 600 ˚C, the electrolyte materials start to conduct oxide ions but remain impermeable to gaseous oxygen and electrons. As the temperature increases, the ionic conductivity of the electrolyte materials increases exponentially, resulting in higher reaction kinetics and favourable thermodynamics which, in turn, result in higher conversion efficiencies for HT-SOECs (> 80%), compared to PEM and AEL electrolysers (< 70%) (Münch, 2018).

Apart from the increasing ionic conductivity, by definition, higher temperatures increase the thermal energy of the reaction, consequently, the electrical energy component of HT-SOECs that is required to maintain the process is smaller than that of PEM and AEL (Elder et al., 2015). Due to the improved reaction kinetics at higher temperatures, the operating temperature of SOECs is typically chosen between 600 ˚C and 1000 ˚C (Hauch et al., 2020) (other research mentions temperatures in a slightly smaller range; 700 ˚C to 900 ˚C (Küngas, 2020)). However, although the higher temperatures that are used in HT-SOECs result in smaller electric energy requirements and higher conversion efficiencies, compared to PEMs and AELs, they also impose additional heat requirements. To save energy and money, in industrial processes, it is preferable to excess heat from hot streams to supply heat to cold streams (Ebbehøj, 2015). As such, in an ideal scenario, the large heat requirements of HT-SOECs are supplied by the excessive heat that is produced by other (industrial) processes. However, such external heat sources are not always available and as such, they might oppose limitations to, or result in certain preferences within CO_2ER supply chains that rely on HT-SOEC technology (N. Gao et al., 2020). Nevertheless, compared to PEM and AEL electrolysers, which have a higher technology readiness level (TRL) than SOEC electrolysers (TRL 8-9 and TRL 5-6 respectively), HT-SOEC is frequently mentioned as the most promising technology, especially when considering co-electrolysis for the production of *syngas*, which is a combination of carbon monoxide (CO) and hydrogen (H_2) (Ebbehøj, 2015) (Zhang et al., 2019) (Küngas, 2020) (Schreiber et al., 2020) (Hussain & Yangping, 2020).

Syngas is a versatile commodity that can be used directly for power generation (N. Gao et al., 2020), for the production of chemicals, or as a precursor for a wide range of processes in the petrochemical industry, such as methanol, formic acid, dimethyl ether, and hydrocarbon liquid which can be produced through, for example, the Fischer-Tropsch process (Ebbehøj, 2015) (Choe et al., 2022). It must be noted that the specific composition of the syngas mixture is key for further processing and according to various research, syngas with an H_2:CO ratio in the range of 1-3 is relevant for industrial applications (Schreiber et al., 2020). Although syngas can be further processed into chemicals with higher market prices (for instance, according to Jouny et al. (2018) the market price of syngas is 60 $/ton, the market price for methanol is 580 $/ton, and the market price for formic acid is 740 $/ton) in this work, syngas is considered as the product of the CO_2ER process. Syngas has a large global production (150 Mtpa according to N. Gao et al. (2020)), which also indicates the potential market of the CO_2-to-syngas process (N. Gao et al., 2020). Moreover, steam and CO_2 could be split via separate electrolysis processes whereafter the reaction products (CO and H_2) can be mixed to form syngas. However, according to Wang et al. (2017), there exist some significant advantages to splitting them simultaneously via a *co-*

electrolysis process. This claim is supported by Andika et al. (2018), who state that a co-electrolysis process has two principle advantages over separate electrolysis processes; (i) the need for a reverse water-gas shift (RWGS) unit is eliminated since CO_2 reduction occurs during electrolysis, and (ii) less solid carbon is formed during a co-electrolysis process. Consequently, the reason for selecting syngas as a product is threefold; (i) it does not need further processing (by for example the Fischer-Tropsch process) since it has a well-established market, and (ii) currently only the production of carbon monoxide (CO) has a high yield and high Faradaic Efficiency (FE) due to the selectivity of the process (Jin et al., 2021), and (iii) syngas can directly be produced via SOECs. Hence, the combination of SOECs as electrolyser technology and syngas as the product is selected as the scope of this work. Additionally, the ideal ratio for most industrial applications, including further processing by Fischer-Tropsch processes, is 2 H_2:CO (Yao Wang et al., 2017) (European Commission, 2019a), consequently, this work will focus on syngas with a ratio of 2 H_2:CO. Also, it must be noted that a single SOEC is composed of a solid electrolyte, an anode and a cathode and between these two electrodes with catalytic active sites, ion species migrate (this migration results in the reduction of CO_2 to CO and the reduction of H_2O to H_2). Consequently, a single cell can produce syngas. However, to obtain a larger overall output, single cells are connected in series forming either planar or (flat) tubular stacks (Bianchi & Bosio, 2021). The reason for connecting single cells into stacks and systems is that the area of a single cell cannot be increased endlessly, mainly due to the difficulties associated with controlling the temperature over larger areas (Elder et al., 2015). Consequently, to produce syngas on an industrial scale *HT-SOEC systems* are required.

Table 3 A general overview of the key operating parameters and characteristics of the alternative electrolysers based on the literature that has been provided above.

Operating Parameters & Characteristics	**PEM**	**AEL**	**SOE**
Operating Temperature	40 ˚C – 80 ˚C	65 ˚C – 220 ˚C	600 ˚C – 1000 ˚C
Operating Pressure	< 30 bar	< 30 bar	< 10 bar
Electrolyte	Liquid	Liquid	Solid (ceramic)
Conversion Efficiency	< 70 %	< 70 %	> 80 %
TRL	8-9 (commercial)	8-9 (commercial)	5-6 (demonstration)
Modular	Yes	Yes	Yes
Co-electrolysis	No	No	Yes

Apart from the research towards increased performance, another important aspect lately gaining much attention is the role of *critical materials* in the energy transition (Valero et al., 2021). Moreover, on 7 May 2021, the International Energy Agency (IEA) presented a report named "*The Role of Critical Minerals in Clean Energy Transitions*" (IEA, 2021). In this report, the IEA addresses the urgency of assessing the availability of certain materials that are used in novel technologies, such as SOECs that are being used in CO_2ER processes. The increased adoption of a technology results in a rapid increase in demand for the materials it requires. Consequently, the availability and reliability of the supply of these materials might hinder the feasibility of the CO_2ER process when the materials in question are critical. This availability and criticality aspect of the materials that are, or might be used in the CO_2ER supply chain, is represented in Figure 2 by the material requirements and henceforth referred to as the *vertical supply chain* of the process. In conclusion, based on the high potential of a CO_2ER process with an HT-SOEC as electrolyser technology and syngas as a product, from now on forth this work will focus on this combination. Furthermore, the CO_2 supply, water supply, RE supply, and the product (syngas) will, henceforth, be referred to as the *horizontal supply chain* of the CO_2ER process. The requirements and working principles of the horizontal supply chain, except for syngas, will be treated in the subsequent sections.

2.1.2 CO_2 Feedstocks and Supply

The CO_2ER process requires a CO_2 input stream to be electrochemically reduced such that syngas can be produced. This CO_2 feedstock can be obtained through multiple methods; it can be captured from the atmosphere (or ambient air) or from waste emissions. Both possibilities are considered in this work; capturing CO_2 from ambient air, most commonly referred to as *Direct Air Capture* (*DAC*), and capturing CO_2 from waste emissions, most commonly referred to as *point source capture* (PSC). DAC is selected to be part of the scope of this work since it is not limited to a specific location, which allows for the possibility of a *decentralised supply chain*. Moreover, Jouny et al. (2018) state that one of the advantages of DAC is the portability of the process, which allows for decentralised use, which couples well with RESs. Additionally, tackling CO_2 emissions from certain sectors such as long-distance aviation and marine transport cannot be done through conventional point source capture methods, since these emissions are not emitted at one specific location (Budinis, 2022). PSC is selected since its operation is geographically limited to the location of point sources, consequently, it allows for the possibility of a *centralised supply chain*.

Today there are a total of 18 DAC plants in operation worldwide, with a combined CO_2 capture capacity of almost 0.01 Mtpa (Budinis, 2022). Based on the combined capture capacity it can be concluded that all of these DAC plants are of relatively small scale. Moreover, according to W. A. Smith et al. (2019), the largest DAC plant that is currently in operation is developed and operated by Climeworks[2] and has a capture capacity of 900 tonnes of CO_2 per year (almost 10% of total capture capacity). However, Climeworks has recently announced the start of construction of their largest plant to date, with a capture capacity of 36 ktpa, which is planned to become operational by 2024. Furthermore, in June 2022, two companies[3] announced their plans to deploy 70 large-scale high-temperature DAC facilities, with capacities of up to 1 Mtpa each, by 2035 (Budinis, 2022). As such, it can be concluded that currently operating DAC units are still of a relatively small scale, however, larger-scale DAC units will become operational soon. Moreover, there is a rapid increase in DAC installations, and if all of the planned projects were to go ahead, the total CO_2 capture capacity would be around 5.5 Mt-CO_2 p.a. by 2030 (Budinis, 2022), indicating the prospects of the technology. For DAC technology, two technological approaches are currently being used; (i) solid DAC, the approach that Climeworks utilises, which uses solid absorbents and operates at ambient to low pressure and medium temperature (80-120˚C), and (ii) liquid DAC or HT-DAC, the approach that Carbon Engineering and 1PointFive utilise, which uses an aqueous basic solution and operates at atmospheric pressure and high temperatures (between 300-900˚C) (Budinis, 2022). Due to these high operating temperatures, liquid DAC is commonly referred to as high-temperature DAC (HT-DAC) (Budinis, 2022). In Figure A. 2 (in Appendix A.2), a comparison of the energy needs, including the electrical energy for compression and capturing and thermal energy of these two approaches is provided, from which it can be concluded that HT-DAC requires significantly less electricity for the capturing process than solid DAC. Additionally, due to the operation at HTs there exist potential synergies with HT-SOEC technology. Based on these aspects, this work will focus on HT-DAC technology. However, it must be noted that

● Low-temperature heat ● High-temperature heat ● Electricity ● Electricity for CO2 compression only

---

[2] Climeworks is a Swiss company that develops and operates DAC plants with subsequent carbon storage.

[3] The two companies are 1PointFive and Carbon Engineering. 1PointFive is a U.S. based company that develops industrial scale decarbonization projects and Carbon engineering is a Canadian based clean energy company that focuses on the production and commercialisation of DAC technology.

Alternatively to DAC, CO_2 capture from point sources is a method that is already deployed on a larger scale, especially for CCS and EOR applications, and it can be categorized based on three categories; (i) *post-combustion capture* (PCC); capturing flue gasses emitted by power plants or heavy industries after the combustion of carbon-based fuels (e.g., steel production, cement production, coal-fired power plants) (ii) pre-combustion; carbon is removed from the fuel before it is combusted (e.g., pre-treatment of natural gas or coal using reactions such as steam reforming or gasification to convert the fuel to syngas and subsequently followed by a water-gas shift reaction to convert CO to CO_2, or, naturally occurring as from natural gas extraction), and (iii) oxyfuel combustion; fuel is combusted using pure oxygen instead of ambient air, producing a flue gas with a high CO_2 concentration (Pérez-Fortes et al., 2016) (Ingvarsdóttir, 2020) (Daneshvar et al., 2022).

Selecting one of the explained point source carbon capture methods depends on the characteristics of the gas stream, the CO_2 recovery requirements, sensitivity to impurities of the transportation equipment and the equipment used in subsequent processes (if any), and the desired purity of CO_2 (Ingvarsdóttir, 2020). According to Daneshvar et al. (2022), PCC is the most widely adopted method for already existing factories or processes aiming to adopt CO_2 capture technologies into their processes. The wide adoption is primarily caused by the ease of retrofitting to existing infrastructure and consequently minimal change requirements. However, the method is also prone to some disadvantages; it requires CO_2 separation from flue gas with high N_2 concentrations (70%) and low CO_2 concentrations (>15%), and consequently, a potentially energy-intensive separation step is required. Also, the low CO_2 concentration requires additional purification steps depending on the CO_2 inlet requirements of the HT-SOEC technology and the required composition for syngas. Compared to PCC, pre-combustion and oxyfuel combustion both result in higher concentrations of CO_2 (>20% for pre-combustion and 80-98% for oxyfuel combustion) (Daneshvar et al., 2022). However, like post-combustion, these methods are also prone to some disadvantages. Pre-combustion methods primarily focus on the production of H_2 and require fundamental modifications to existing systems. Oxyfuel combustion methods also require additional equipment and have a high thermal energy consumption due to the pure oxygen requirements of the technology. Based on the ease of retrofitting, and the fact that PCC is linked to a single location which matches a *centralised supply chain*, this work will focus on PCC as a method for PSC of CO_2. It must be noted that, within current European legislation, CO_2 capture for industrial use is not eligible for exceptions on the Emissions Unit Allowance, since the CO_2 is not removed from the carbon cycle. Any CO_2 emitting plant that captures its flue gasses and aims to utilize the captured CO_2 within products that will emit CO_2 at a later stage in their lifecycle, would have to purchase emission allowances. As such, with current legislation, the application of PCC technologies would not benefit from avoiding such costs. When DAC is used as a capture technology, the air is captured from atmospheric air and as such CO_2 is deducted from the environment, which makes it eligible for exceptions on the Emissions Unit Allowance (Bellona, 2020).

After capturing the CO_2 via either DAC or PCC technology, several aspects, such as the desired composition of syngas, the equipment used for transport, and the specifics of the HT-SOEC technology that is used, determine the required purity of the CO_2 inlet stream and consequently the purification, drying and pressurising processes that are required after capture (Pieri et al., 2018). In the CO_2ER supply chain, these processes prepare the CO_2 stream for transportation to the production facility that houses the electrolyser (as depicted in Figure 2). The various transportation modes; waterborne (ships), pipelines, and land borne (trains & trucks) are important considerations for the transportation of purified CO_2 in the CO_2ER supply chain and consequently will be taken into consideration in this work (European Commission, 2022).

2.1.3 H_2O Supply and Requirements

Since this work focuses on syngas production through co-electrolysis via HT-SOEC technology, the CO_2ER process also requires an H_2O input in the form of steam. According to Mehmeti et al. (2018), water consumption is one of the emerging categories in Life Cycle Analysis (LCA) studies that analyse the potential of alternative fuel production through water-intensive H_2 production, like co-electrolysis. Particularly the consideration of water consumption and other water-related effects on the environment become more crucial due to increasing global water demand and declining freshwater reserves as a result of global warming (Smedley, 2017) (Mehmeti et al., 2018). Besides the environmental importance of assessing the water requirements of the CO_2ER supply chain, there are also technical and economic considerations that must be accounted for. Examples of these are; (i) the existing water infrastructure and available points of supply, (ii) the required purity or composition of the H_2O input stream, and the possible purification processes that are required, (iii) possible means of transportation, and (iv) the price and required quantity of H_2O. Some literature suggests that the environmental and financial impact of H_2O in the CO_2ER supply chain is negligible compared to other components (Schreiber et al., 2020). However, the increasing demand and decreasing availability of H_2O make it an important aspect to consider.

2.1.4 Electricity Supply and Requirements

When considering the requirements of the HT-SOEC CO_2ER supply chain as depicted in Figure 2, various aspects require electrical energy input. Moreover, whether DAC or PSC is used to provide the required CO_2 feedstock, both technologies require electricity for purification, drying and compression processes (Pieri et al., 2018). Also, the CO_2 needs to be transported to the production facility utilising earlier stated pipelines, waterborne or land-born transportation means which also require an electricity input, primarily for compression and/or liquefaction. Furthermore, the purification of the H_2O feedstock and the pressure required for its transportation, but also its vaporization to steam require electrical (or thermal for vaporization) energy input. Once the CO_2 and H_2O of the desired composition arrive at the production facility, the co-electrolysis of these feedstocks through HT-SOEC requires an electricity input during the electrochemical reduction process (Fernández-González et al., 2022) (Jouny et al., 2018). Since this work focuses on HT co-electrolysis, there are also significant heat requirements, which could be met by electricity or with excessive heat from industrial processes. Nevertheless, the availability and consumption of electricity play a vital role in the supply chain at hand.

The electricity supply that is required for the HT-SOEC CO_2ER process and the other aspects of its supply chain, need to originate from *RES*s, such as wind, solar photovoltaics, or tidal energy, for the process to environmentally outperform syngas generation via alternative fossil-fuel-based synthesis paths (D. Y. Lee et al., 2020). According to Smith et al. (2019), the currently available technology to produce syngas via electrolysis has a larger electricity consumption than the available alternative fossil fuel-based synthesis routes. Alternatively, a lifecycle analysis study performed by Schreiber et al. (2020) focuses on comparing one of today's most utilized fossil benchmark technologies for the production of syngas; steam methane reforming (SMR), with syngas production via co-electrolysis with HT-SOEC technology. They conclude that, for the production of 1 kg of syngas, HT-SOECs require 8.82 kWh of electricity whilst SMRs require 0.826 kg of natural gas and 0.23 kWh of electricity. From their research, it can be concluded that the electricity consumption of using HT-SOEC technology to produce syngas, is indeed larger than fossil fuel-based synthesis routes for the production of syngas, however, the fossil fuel-based route does use a fossil-fuel thermal energy supply, which possibly leads to increased GHG emissions. To determine the potential of a CO_2ER supply chain that utilises HT-SOEC technology, electricity consumption is of great importance and is frequently mentioned as the biggest cost contributor to the entire supply chain (M. Li et al., 2021) (M. Y. Lee et al., 2020). Thus, all electricity (and other energy) requirements within the CO_2ER supply chain that has been specified in the previous subsections must be identified and quantified to create an understanding of the feasibility of renewable syngas production through HT-SOEC in terms of RE availability and economics.

2.2 The Feasibility of Transportation

Due to the lack of already existing commercialized CO_2ER supply chains, the feasibility of such supply chains remains largely unaddressed. To this end, this section aims to review the literature that is available on the transportation of the feedstocks (CO_2 and H_2O) and the product (syngas). Hence it aims to identify the feasibility of a CO_2ER supply chain from a transportation point of view.

2.2.1 State-of-the-art on CO_2 Transportation

Today there already exists a significant transportation infrastructure for CO_2 (in the US alone approximately 70 Mtpa of CO_2 is transported by pipelines) primarily for CCS and EOR projects (Kearns et al., 2021). The large-scale transport of CO_2 for CCS (and EOR) projects is currently done via pipelines. Nowadays, this transportation means is commonly selected, since it is a mature technology (TRL 8-9), as can be seen in Figure 3. The costs of pipeline transportation of CO_2 vary widely and depend on several factors including the quantity transported (commonly in Mega tonne per anum (Mtpa)), the diameter, material, and length of the pipe, the planned lifetime of the system, and factors related to geography, such as labour costs and location (IEA, 2020). The most efficient way to transport CO_2 via pipelines (both on- and offshore) is in its supercritical phase (i.e. dense phase). To transport CO_2 in its supercritical phase, (almost) all H_2O that is normally present must be removed to prevent corrosion of the pipelines and other equipment (Hong, 2022). The supercritical phase can be reached between temperature and pressure ranges of 12 ˚C and 44 ˚C and 85 bar and 150 bar respectively as can be seen in Figure A. 3 (in Appendix A.3) (Zero Emissions Platform, 2010). The lower pressure limit is set by the phase behaviour of CO_2 and should be sufficient to maintain the desired supercritical condition, whilst the upper limit is primarily related to transport economics (Serpa et al., 2011). Whereas the pressure range is related to the ease and costs of transportation, the temperature range is related to the material limits of the pipeline. The upper limit is selected to avoid damage to the internal and external coating material of the pipe, while the lower limit is determined by (winter) ground temperature (Serpa et al., 2011).

Although large-scale transport of CO_2 is currently done by pipelines, various pieces of research indicate that transportation of CO_2 by ship may be more economical when CO_2 needs to be transported on a large scale, over large distances, and overseas (Kearns et al., 2021) (Durusut & Joos, 2018) (Hong, 2022). As opposed to capital-intensive pipelines, which benefit from economies-of-scale, however, the transport of CO_2 by ship is less capital-intensive since the transportation capacity can be built out gradually by simply adding more ships to the fleet. Additionally, ships are cost-competitive for trans-oceanic transportation of CO_2. As can be seen in Figure 3, the TRL of CO_2 transportation by ship varies between TRL 3 and TRL 9 for the ship design, and TRL 2 and TRL 9 for the ship infrastructure. The high TRLs are based on the shipping experience of CO_2 in the food and beverages industry, commonly associated with small-scale transport of only up to 3 Mtpa (Hong, 2022). Besides the food and beverages industry, there exist many commonalities between shipping CO_2 and other gasses, such as liquified natural gas (LNG) and liquified petroleum gas (LPG). Consequently, much of the large-scale shipping infrastructure can be based on the experience obtained with the transport of, for example, LNG and LPG. Although there is much research that focuses on assessing the possible adaptation of the shipping infrastructure of LNG/LPG to CO_2 shipping, tankers that are specifically designed for CO_2 transport can be better optimized for maximum capacity and investment costs (E. Smith et al., 2021). Consequently, The repurposing of the infrastructure and ships has not been implemented on a commercial scale, resulting in the lower TRLs as depicted in Figure 3. For the operation of large-scale CO_2 transport, the National Petroleum Council (2019) estimated that an average ship can carry 45 kt of liquified CO_2, at an operating temperature and pressure of -40 ˚C and 17 bar respectively. Under these conditions, the CO_2 is in its liquid phase as can be seen in Figure A. 3. Other research by L. Gao et al. (2011), states that large-scale transport of CO_2 by ship should be done at a temperature and pressure of -52 ˚C and 6.5 bar respectively because these operating conditions give the highest density in the liquid state, which reduces transport unit costs. Alternatively, research by Durusut & Joos (2018), mentions operating temperatures and pressures in the range of -60 ˚C – +30 ˚C and 5.2 bar – 72 bar. They classify possible operating conditions in terms of high, medium and low-pressure designs, in which the higher pressures are combined with higher temperatures and lower pressures with lower temperatures (based on the density). Although they mention these wide ranges for temperature and pressure, they conclude that for large ships with capacities > 10 $ktCO_2$, the most cost-effective way of transportation is generally around 5.2 bar and -56.6 ˚C, since this provides sufficient margin to avoid solid formation.

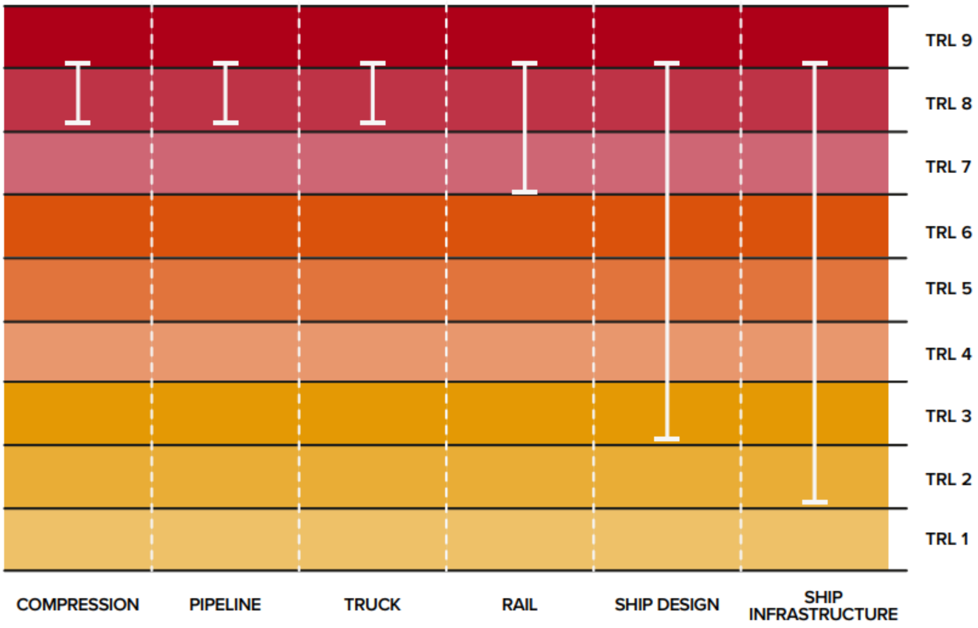

Figure 3 The technology readiness levels (TRL) of the various CO_2 transportation means and the processes and infrastructure required for the various modes of transportation (copied from Kearns et al. (2021)).

As stated, the transport of CO_2 can also be done via trains and trucks (Gutiérrez-Sánchez et al., 2022). However, unlike the vast amount of research that is available on CO_2 transport by pipelines and ships, there is less research available on the transport of CO_2 by trucks and especially by trains. The underlying reason is that most of the research on CO_2 transport aims to assess the possible transportation means from the perspective of large-scale CCS (and EOR) projects, in which large volumes of CO_2 have to be transported over long distances. Moreover, according to Hong (2022), transport by truck is only a viable method for small quantities, from 4 tonnes to a few hundred, and over short distances up to 322 km. Transport by train is economically viable for the same quantities as trucks, however, for longer distances up to 1.609 km. Hong (2022) also states that trucks can be a complementary transportation means to pipeline and ship options, for the intermediate transportation of small quantities of up to 10 kt between various CCS sites and ports that are inaccessible for pipelines and ships. According to Metz et al. (2005), the typical operating temperature and pressure for both trucks and trains are -20 ˚C and 20 bar respectively, corresponding to liquefied CO_2 (as can be seen in Figure A. 3). Alternatively, the research by Psarras et al. (2020a) is one of the few scientific studies that consider truck transport for CCS applications. Within their research, they use operating conditions of -30 ˚C and 17 bar, which also correspond to liquefied CO_2.

2.1.2 State-of-the-art H_2O Usage and Transportation

Unlike the transportation of CO_2, which needs an energy-intensive (electrical energy and possibly thermal energy) capturing process before it can be transported, and which has specific transport operating conditions, the transportation of H_2O is less complex since it can be done at atmospheric pressure and room temperature, and H_2O does not need to be captured from atmospheric air or flue gasses. However, there are different sources of water, and there exist discrepancies in the literature on the type of water (and its purity) that should be used during electrolysis. Moreover, in general, the possible sources of water are surface water (rivers, streams and lakes), groundwater, industrial wastewater, urban wastewater, seawater, estuary, water supply network, cooling towers and rainwater (Simoes et al., 2021). In addition to the identification of the source of water, the water that is used in a CO_2ER process is either used as it is or can be treated via a fine screening process, treated via coagulation-flocculation and filtration, treated via ultrafiltration or treated via reverse osmoses (Simoes et al., 2021). To delineate which type(s) of water can be used in theory and whether additional purification processes are required for the CO_2ER process that uses HT-SOEC technology, several studies have been reviewed.

Recent research by van ’t Noordende & Ripson (2022), on an advanced design for a greenfield 1-GW green-H_2 plant that will be built in 2030 and utilises AEL and PEM electrolysers, mention different water requirements for the two types of electrolysers. For AEL, demineralised water is suitable as process water, however, PEM electrolysers need ultrapure water. For the demineralised water feedstock, they include a demineralisation plant in the design, which is capable of producing 230 m^3-demineralised water/hr. Demineralised water (also known as deionised water or demi water) is water that is purified in such a way that (most of) its mineral- and salt ions are removed (Witvoet, 2018). This demineralised water is used directly in AELs but also for the production of ultrapure water for PEMs. This ultrapure water is produced by a reverse-osmosis plant followed by a post-treatment process. Although the research by van ’t Noordende & Ripson (2022), provides insights into the water purity requirements of different commercial-scale electrolysers, no specifications are provided on how the initial H_2O feedstock is transported to the production facility, nor do they include the type of water (and purity) that should be used for co-electrolysis via HT-SOECs. Moreover, unlike AEL and especially PEM technology, HT-SOECs are more resistant to variable feedstock compositions. According to Bianchi & Bosio (2021), HT-SOECs reach the required catalyst activity without needing cost noble metals. They state that, because there is no usage of cost noble metals, HT-SOECs are more resistant to variable feed compositions, and therefore, their operation is not limited to pure H_2, H_2O or inert mixtures. Additionally, they mention that sea chlorine-based salts volatilize at temperatures from 1073 K (=800 ˚C), as such, an operating temperature of at least 800 ˚C results in avoiding the risk of these sea chlorine-based salts deposition on electrode active sites, and theoretically avoiding the need for desalinisation of seawater. These claims are to some extent supported by the research by Lim et al. (2017), who investigate the effects of the usage of synthetic seawater in HT-SOECs, and conclude that an operating temperature of 800 ˚C, results in almost identical performance and degradation rates for the synthetic seawater and pure water. Despite, the information provided by Bianchi & Bosio (2021) and Lim et al. (2017), other literature that focuses on HT-SOEC technology use desalinated water as feedstock, and to this end, includes a desalinisation process (Ebbehøj, 2015). Moreover, according to Ebbehøj (2015), who research the integration of CO_2 air capture and SOECs to produce methane, a CO_2ER process with access to freshwaters, such as groundwater, or access to seawater, requires a desalination process, which typically operates at less than 10 kJ/mol, and compared to other cost-factors, this would only add minor costs. Although they mention the usage of seawater and a desalination process, they do not specify the costs (or means) for the transportation of water. Alternatively, Fu et al. (2010), perform an economic assessment of the production of syngas via HT-SOEC co-electrolysis. Within their assessment, they assume that demineralised water is required for the production process. They do not mention any means of transportation for the water, however, they do provide some cost specifications.

Apart from a reverse osmosis process, the treatment processes that have been mentioned in the introduction of this section (fine screening process, coagulation-flocculation and filtration process, ultrafiltration process, and reverse osmoses process) have not been mentioned in the reviewed literature. Moreover, the H_2O treatment processes that have been mentioned are demineralisation and desalinisation. Additionally, based on the reviewed literature, it can be concluded that, theoretically, seawater could be used for the CO_2ER process. If this would be the case, the process requires an operating temperature of at least 800 ˚C. Nevertheless, no literature that assesses electrolysis technology for large-scale application focuses on seawater as a feedstock without adding a desalination process or a demineralisation process before the co-electrolysis of H_2O and CO_2.

2.1.3 State-of-the-art on Syngas Transportation

According to Ridjan et al. (2013), some micro syngas grids exist in the chemical and petrochemical industry, nevertheless, no information on these grids can be found. The lack of literature available on the topic is emphasized by Ridjan et al. (2013), who states that the only identified literature available on the topic is a report[4] by the European Industrial Gasses Association (2004), which intends to harmonise the industry standards for the transportation of CO and syngas via pipelines. This document does indicate some aspects that should be accounted for in pipelines that are used for CO and syngas transportation. The report states that such systems are limited to gaseous products with a temperature range between -40 C – +150 C and pressures in the range of 1 bar – 150 bar. Nevertheless, the document mainly focuses on delineating the design process rather than designing a syngas pipeline. Furthermore, according to Newcomer & Apt (2007), in 2007 there were eight gasification facilities in operation, producing approximately 1.7 GW of electricity from syngas that is produced by the gasification of coal or petroleum coke. In these facilities, the syngas that results from the gasification processes is used immediately after production to generate electricity. Consequently, there is no information provided on the transportation of syngas. It is this difficulty of transportation, but also the fact that syngas is often directly used, that causes the lack of existence of commercial scale syngas transportation networks. This claim is supported by more recent research by Lo et al. (2021), who investigate the economic performance of a biomass gasification supply chain that produces syngas in Malaysia. They state that, due to safety concerns of syngas transportation and the lack of literature available on syngas transportation, their case study only considers a biomass gasification plant that is in close proximity (i.e. 1 km) to the power plant in which the syngas is used, however, they do not provide estimations for this 1 km pipeline. Furthermore, Ridjan (2015), researched the possible integration of electrofuels in renewable energy systems, they also state that there are no cost assessments of syngas transportation available since the properties of the gas require research into appropriate construction materials for new pipelines. To this end, they also exclude the transportation of syngas from their system design.

According to N. Gao et al. (2020), syngas with a low concentration of CO_2 eliminates the need for further downstream product separation. Consequently, syngas production processes generally produce syngas with low CO_2 concentrations. However, N. Gao et al. (2020), also state that for syngas

---

[4] The report by the European Industrial Gasses Association (2004), is titled "*carbon monoxide and syngas pipeline systems*" and its purpose is to improve understanding of such pipeline systems for those engaged in safe design, piping, valves and equipment, construction, operation and monitoring.

applications such as its conversion to fuels or chemicals, there is a tolerance for small amounts of remaining CO_2 if the H_2:CO ratio is above 2. Additionally, Ridjan et al. (2013) mention that, for syngas with an H_2:CO_2 ratio of 3, the syngas would not be toxic and would be lighter than air. These properties would cause the syngas to disperse if there were any leakages during transportation and therefore would not result in potential human harm. Also, they state that it is expected that CO_2 would (at least for some part) resolve the self-ignition problem associated with H_2. Moreover, the research by Ridjan (2015), states that syngas cannot be transported in existing NG pipelines, because they can only handle up to 15-20 % of H_2 by volume. However, with volume concentrations below 15%, very few modifications are necessary. This is also mentioned by Newcomer & Apt (2007), and they conclude that, if the H_2 volume rate of the syngas that is to be transported is lower than 15%, its transportion (and storage) is feasible, by increasing the operating pressure of the transport (or storage) system (either pipeline or vessel). In theory, alternating the composition of syngas and increasing the operating pressure of already existing gas infrastructure, enables the transportation of syngas. However, this work specifically focuses on a CO_2ER supply chain that produces syngas with a molar ratio of 2 H_2:CO. Consequently, with the available knowledge, syngas transportation should be excluded from the supply chain, resulting in the requirement that the production facility is in close proximity to the syngas demand location.

2.3 Identification of Knowledge Gaps

The need for a shift in research efforts towards the broader technological application of CO_2ER, including its infrastructure and complete system integration has been identified in the introduction. The main problem of further investigating the broader application of CO_2ER supply chains revolves around the lack of knowledge of its limits. To further explore the solution space, a specific scope (provided in Figure 2) has been selected based on the state-of-the-art performance of the various supply chain units and the possibility to benefit from the possible opportunities associated with centralised and decentralised supply chain configurations. Nevertheless, based on the literature that has been reviewed, several remaining knowledge gaps can be identified and need to be filled to explore the limits of alternative configurations for industrial-scale CO_2ER supply chains.

2.3.1 Limited Understanding of Feasibility, Scalability and Interrelations

The individual supply chain units and a primary indication of their performance and requirements have been provided in the previous sections. Although some research (W. A. Smith et al., 2019), addresses the required size of the various supply chain units of an industrial-sized CO_2-to-fuel process based on their interrelations, no research addresses the requirements of the supply chain that has been identified as the scope of this work. Consequently, there is a lack of knowledge on the feasibility to integrate the various supply chain units on an industrial scale and vice versa a lack of knowledge on the requirements that are opposed by implementation on an industrial scale. Additionally, the research by W. A. Smith et al. (2019), provides a quantification of the requirements of a single large-scale production facility (focused on producing methanol), however, the feasibility to implement a CO_2ER process that relies on HT-SOEC technology for the production of syngas to meet global and/or European demand levels remains unaddressed. It is this knowledge gap associated with matching the scales of the various supply chain units of this specific supply chain and whether such supply chains can produce syngas in the large quantities such as on a global and/or European level, that needs to be solved to identify the feasibility but especially the implementation potential of CO_2ER supply chains that produce syngas. The importance of addressing this knowledge gap is also stressed by various researchers, who state that much effort is focused on problem-solving on a small scale, whilst commercialisation of the technology can only be reached by investigating integrated system design (W. A. Smith et al., 2019) (Yao Zheng et al., 2019).

2.3.2 Lack of Knowledge of Performance of Supply Chain Configurations

As highlighted in Chapter 1, centralised and decentralised supply chain configurations have certain theoretical advantages and disadvantages. However, whether such alternative configurations influence the economic performance of CO_2ER supply chains remains unaddressed. The state-of-the-art on the feasibility of transportation identifies that there exist various CO_2 transportation means and from an economic perspective, the preferred transportation means are dependent on the quantity and distance over which the CO_2 needs to be transported (Psarras et al., 2020) (Hong, 2022). Additionally, the various capture technologies (DAC & PCC) allow for a centralised and decentralised supply chain configuration. Apart from the costs associated with the transportation of CO_2, it has been identified that H_2O needs to be transported (and purified) as well. Since the H_2O feedstock can be obtained from various supply sources, decentralised supply chain configurations could benefit from the dispersed nature of the feedstocks by lowering the costs of transportation. However, due to the lack of knowledge of the influence of the individual supply chain units on the total costs of an integrated CO_2ER supply chain, the opportunities for centralised and decentralised supply chain configurations cannot be quantified. It is this knowledge gap associated with the economic performance of alternative configurations that need to be solved to provide some preliminary insights into possible economies of centralisation opportunities at an industrial scale.

2.3.3 Limited Understanding of Implications of Increased Adoption

The previous knowledge gaps focus specifically on the horizontal supply chain of the CO_2ER process. However, this work also incorporates some aspects of the vertical supply chain. Moreover, in section 2.2.1, the research by Valero et al. (2021) and the report published by the IEA (2021), stress the importance of assessing the availability of certain materials that are used in novel technologies. Consequently, to assess the potential of the specific CO_2ER supply chain of this work, further investigating whether the increased material requirements associated with a rapid increase in adoption of the technology might cause additional challenges, is an important aspect of the feasibility of an industrial-scale CO_2ER supply chain. The limited understanding of the material requirements could endanger the future potential of the technology and consequently, is a knowledge gap that needs to be filled.

2.4 Research Questions

To assess the potential and limitations of alternative CO_2ER supply chain configurations that produce syngas, the following main research question is formulated:

> **"How do alternative supply chain configurations impact the technical feasibility and economic performance of carbon dioxide electrochemical reduction plants that produce syngas?"**

Hereafter, in turn, three sub-research questions have been formulated, providing structure and guidance in answering the formulated main research question. These sub-questions are formulated below.

1. What are the theoretical and practical limitations of a HT-SOEC CO_2ER supply chain focused on producing syngas?
2. How do the different supply chain units influence the performance of decentralised and centralised configurations and which supply chain units have the highest impact when comparing these configurations?
3. What are the implications of increased syngas demand scenarios for the vertical supply chain and the usage of critical materials?

2.5 Research Goal

This work aims to explore the limits of alternative supply chain configurations for CO_2ER processes that utilise SOEC technology. As such, it aims to identify the *feasibility* of an industrial-scale CO_2ER supply chain and its potential to meet *global* and *European* syngas production. Additionally, this work aims to identify the *opportunities* associated with potential alternative configurations that might result in the improved economic performance of CO_2ER supply chains. Moreover, the goal is not to find a specific quantification of a single optimal supply chain configuration (either centralised or decentralised), rather it is to map the supply chain requirements and delineate potentially favourable technology implementation conditions. To this end, it aims to find the trade-offs and limitations of the possible alternative configurations by exploring the solution space of CO_2ER supply chains implemented at an industrial scale.

Chapter 3

Methodology

This chapter aims to argue for an approach that aligns with the goal of this work and enables the answering of the formulated research questions. In section 3.1, multiple approaches that could be used to reach this goal are compared, and finally, an *exploratory research approach* is selected. After the selection of a research approach, section 3.2 further delineates the specific methods that align with this approach and will be used to answer the research questions.

3.1 Research Approach

The selection of a research approach should be based on the possibility to include several research aspects. Moreover, this work aims to address the *horizontal supply chain* and its *feasibility* and *opportunities*, and the *vertical supply chain* and its *feasibility*. Within currently existing scientific research, countless challenges revolve around the analysis of networked systems, including supply chains, their characteristics and their optimisation. Present-day, these challenges are often related to energy infrastructure networks that focus on RE-technology implementation and technologies that contribute to CO_2 mitigation. Examples of research on infrastructure networks that also include the notion of economies of centralisation are biogas production (Marufuzzaman et al., 2016) (Pérez-Fortes et al., 2012) and the integration of complementary energy technologies in nowadays energy mix (Capuder & Mancarella, 2014) (Parra & Patel, 2016). The stated examples utilise a mathematical mixed integer linear programming (MILP) modelling approach. As such, to address the opportunities for alternative supply chain configurations, a mathematical MILP modelling approach seems a suitable research approach.

However, the research of Marufuzzaman et al. (2016), has readily available technical and economic data for biogasification facilities (provided by Mississippi State University). Additionally, bio gasification and its required infrastructure have been researched extensively (Q. Li & Hu, 2016). Moreover, the research by Marufuzzaman et al. (2016), refers to over 20 other researches that focus on various aspects including the production costs based on various feedstocks, plant sizes, conversion methods, operating conditions, plant locations, transportation issues and supply chain networks. Hence, many of the input parameters, trade-offs, and limitations associated with bio-gasification supply chains have been identified in previous research. Alternatively, the research by Parra & Patel (2016) assesses various technologies, including electrolysers with lower TRLs compared to biogasification, they also have readily available information on the model environment (based on the Swiss regulatory and operational context). Apart from the availability of detailed information, the stated research examples aim to provide insights into the optimal supply chain or system configuration. Since the goal of this work is not to provide an optimisation of a supply chain, but rather to provide insights into its feasibility on a global/European scale and quantification of the potential opportunities at such scales, a modelling approach seems less appealing. Additionally, several supply chain units (e.g. DAC technology, SOEC technology) are at relatively low TRLs, and according to Heijnen et al. (2014), who provide an overview of several modelling approaches and their advantages and disadvantages, MILP modelling approaches rely on complete, pre-specified information to ensure optimisation. In turn, it is this information that determines the accuracy of the optimal solution that is generated. Consequently, due to the incipient stage of the general understanding of the various supply chain units and their interrelations, a mathematical modelling approach is deemed unsuitable at the current research stage.

Although the phenomenon of centralised versus decentralised supply chain networks is well known in the literature, it has not received any attention in the context of implementing CO_2ER supply chains on an industrial scale and not the least in the context of the specific technologies and material requirements of the supply chain that together form the scope of this work. Moreover, based on the reviewed literature, addressing the potential of alternative supply chain configurations is usually a research topic that is being investigated at a later research stage, when there is abundant quantitative data available. Nevertheless, the identification of the feasibility and opportunities associated with alternative configurations at an early research stage could lead to valuable insights. Due to the incipient stage of the general understanding of the combination of these concepts, but also the discrepancies that exist in current research on CO_2ER processes and supporting supply chains, an *exploratory research approach* seems most suitable for this work.

An exploratory research approach is often applied when the issue that is being studied is new or when the data collection process is challenging for some reason (Berlin et al., 2022). Additionally, exploratory research approaches can lay a strong foundation for any future study that is being carried out in the same research environment, as it tends to tackle new problems on which little or no previous research has been done (Voxco, 2021) (Rahman et al., 2022). Such approaches can be used if there is a general idea or specific question that should be researched, but there is no or lacking preexisting knowledge or paradigm with which to study it. Moreover, based on the literature that has been reviewed, it can be concluded that there is lacking preexisting knowledge on the interrelations between the various supply chain units, also there is not a single research paradigm that could be used to address all of the knowledge gaps that have been identified. Additionally, in section 2.5 it has been identified that the research goal is to *explore* the solution space of CO_2ER supply chains on a global and European level, which aligns with an exploratory research approach. It must be noted that such research approaches are prone to limitations. Moreover, a frequently mentioned limitation of exploratory research, is that it brings up tentative results and is therefore inconclusive (Berlin et al., 2022) (Rahman et al., 2022). This limitation results in the issue that the research insights are not reliable for effective decision-making. To (at least partly) address this limitation, the exploratory research approach in this work should make use of several methods that result in conclusive results. These methods will be further explained in the following section.

3.2 Research Methods

This section aims to describe the specific research methods that will be used to evaluate the feasibility and opportunities for industrial-sized CO_2ER supply chains with alternative configurations. In the previous section, it has been identified that there is not a single research paradigm that could be used to address all the knowledge gaps, consequently, section 3.3.1 addresses the methods for the horizontal supply chain and section 3.3.2 addresses the methods for the vertical supply chain.

3.2.1 Methods to Adress the Horizontal Supply Chain

According to Rahman et al. (2022), exploratory research can be conducted in three steps; identifying the problem, delineating the research focus, and conducting the research using suitable methods. They identify suitable research methods as (i) a review or survey of the literature, (ii) an experience survey, (iii) a focus group, and (iv) an analysis of stimulating cases. Although experience surveys and focus groups could be useful methods if they include experts in the fields, for this work, *literature reviews* and the *analysis of stimulating cases* are deemed more suitable. Moreover, a comprehensive literature review will be used and based on the information that has been found in Chapter 2, the following aspects should be treated; (i) the costs and requirements for transporting various quantities of CO_2 and H_2O (ii) the costs and requirements to capture CO_2 by DAC and PCC methods, (iii) the costs and requirements of various SOE systems, (iv) the characteristics of the syngas market.

Since this work aims to assess the trade-offs and limitations of alternative CO_2ER supply chain configurations, uniform cost estimations for various transportation means and processes are undesirable. In general, there exists a great deal of variability and ambiguity in the existing literature that focuses on the documentation of transportation, processes, and associated costs. Consequently, a literature review to compare these costs across studies is a challenging research activity. To analyse the data that will be obtained from the available literature, the units must be comparable. To this end, this research uses *Euro in the year 2020* as a reference year. Additionally, *kilometres* will be used as the unit for distances, and *metric tonnes* as the unit for quantities. If another unit or currency is provided these must be converted to units that have been specified. To accommodate the conversion of cost estimations, an InflationTool[5] and a US$ (2020) to € (2020) exchange rate of 0.877[6] are used.

Based on the quantification of the costs associated with the supply chain units that have been depicted in Figure 2, and the delineation of the available sizes and operating requirements of these supply chain units, the practical and theoretical limitations of individual supply chain units can be found. Hereafter, a *back-of-the-envelope calculation*, aiming to integrate the individual supply chain units, will be used to determine whether any additional practical and theoretical limitations will be opposed by integrating the individual supply chain units. A similar method has been used by W. A. Smith et al. (2019), who provide valuable insights into the required improvements for various supply chain units of a CO_2-to-methanol process. Consequently, to answer the first sub-research question, a combination of literature reviews and a back-of-the-envelope calculation are the methods that will be used in this work. Since this work aims to integrate the individual supply chain units and determine the overall feasibility based on the quantities, costs and sizes, the limitation that exploratory research often brings up inconclusive results, is therefore partly addressed. Nevertheless, due to the incipient stage of research, it is expected that many assumptions have to be made, resulting in higher uncertainty.

To answer the second sub-research question, an *analysis of stimulating cases* is the method of choice, as it aligns with part of the research goal; the identification of opportunities associated with alternative supply chain configurations. The quantification of the operating parameters of the individual supply chain units can be used to formulate alternative supply chain configurations. To analyse the opportunities of such alternative configurations, an *economic analysis* will be performed. Moreover, the key performance indicator (KPI) of the economic analysis is chosen to be the *simple payback time*, which can be calculated via Equation (i) (Towler & Sinnott, 2022). To assess the impact of the supply chain units the alternative configurations should be changed in terms of quantity and distance of the transportation of feedstocks and the quantity of production/demand.

$$\text{(i)} \qquad \text{Simple Payback Time} = \frac{Total\ Investment}{Average\ Annual\ Cash\ Flow}$$

3.2.2 Methods to Adress the Vertical Supply Chain

To answer the third sub-research question, a definition of criticality and a method for assessing it must be provided. According to the EU criticality method, all critical materials are classified as a combination of two main parameters: economic importance and supply risk (HyTechCycling, 2019). The prior parameter aims to quantify the importance of a specific material for the EU economy in terms of end-

---

[5] The inflation tool that is used is called "InflationTool" and is available at: www.inflationtool.com

[6] The exchange rate for US$ (2020) to € (2020) is based on the average spot exchange rate in 2020 available at: www.exchangerates.org.uk

use applications and the value added by the corresponding EU manufacturing sectors. The latter reflects the risk of a supply disruption of the specific material and is based on the concentration of supply from raw materials producing-countries, and the governance and trade aspects of these producing countries. Blengini et al. (2020), use ratings for economic importance and supply risk to assess the criticality of 83 individual raw materials from the perspective of the EU. They created a report for the EC, titled "*Study on the EU's list of Critical Raw Materials (2020)*", which identifies that 30 of the 83 raw materials that have been assessed, should be listed as critical. The report of Blengini et al. (2020), encompasses the fourth technical assessment[7] of CRMs that was conducted for the EC. Compared to the previous assessment, which was conducted in 2017, Helium was taken off the list whilst Bauxite, Lithium, Titanium and Strontium were added. As such, the list changes over time, and consequently, its future validity (e.g. the critical materials in 2030) is unknown.

Nevertheless, to assess whether material availability might hinder increased adoption of the CO_2ER supply chain that relies on SOEC technology from the EU's perspective, the CRMs that have been identified by Blengini et al. (2020) can be compared with materials that have been or could be used in SOEC technology. To this end, the *literature review* of the research papers that have been used throughout this work should be reviewed with a focus on the materials that are used in SOECs. Furthermore, according to Elder et al. (2015), many of the electrode compositions and structures used for the construction and operation of SOFCs (i.e. in fuel cell mode, generating electricity) have shown equally good performance compared to electrolysis operation (i.e. in SOEC mode). Bianchi & Bosio (2021) support this claim, however, they do mention that there are still some aspects, such as the differences in thermal behaviour during fuel cell and electrolysis modes, which might favour the usage of different materials for the different applications.

Apart from a claim, of whether a material is critical or not, that is based on a comparison between the EU perspective on critical materials and the materials that are used in SOECs, it is common practice that, during the assessment of a specific technology, scenarios for the increased adoption of this technology are transposed into its material usage. Examples of research that apply such methodology are the research by Kiemel et al. (2021), who assess CRM usage in water electrolysers at the example of the energy transition in Germany for 2030 and 2050 scenarios, the research by Junne et al. (2020), who assess the usage and availability of various materials (such as lithium and cobalt) for power generation-, storage-, and transport technology applications on a global scale by 2050, and the research by Davidsson & Höök (2017), who assess the material requirements and availability for large-scale (multi-terawatt) deployment of solar photovoltaics via scenarios that predict technological-growth up to 2070. The stated examples all follow similar methods, in which scenarios for future demand of technology are either developed in the research itself, using tools (e.g. Kiemel et al. (2021) use a simulation tool called REMod-D), or readily available scenarios from previous studies are used (e.g. Davidsson & Höök (2017) use the Advanced Energy (R)evolution scenario presented by Greenpeace). Hereafter, a specific share of a given market, such as electrolyser technology for hydrogen production, or solar PV for renewable electricity generation, is dedicated to the technology in question. Based on this share and the projected future demand, the material requirements are determined. Once these material requirements have been determined, the availability of the materials that could be used for the specific technology is assessed based on, for example, their global availability, or other parameters such

---

[7] The first assessment on CRMs for the EC was conducted in 2011 and listed 14 CRMs out of 41 materials in total. The second assessment was conducted in 2014 and identified 20 CRMs out of 54 in total. The third assessment was conducted in 2017 and listed 27 CRMs among 78 candidate materials.

as economic importance and supply risk, as was done in the CRM assessment for the EC conducted by Blengini et al., (2020).

Although this method is frequently used, it is prone to some limitations. Moreover, due to ongoing research towards novel technologies, the prediction of their share in future systems is prone to high uncertainties. As such, either winner-picking or discarding technologies by increasing or decreasing their respective share would be premature (Kiemel et al., 2021). This limitation can (at least partially) be overcome by developing many scenarios and altering the projected technology share in each scenario. However, this is a time-consuming process and does not take into account the possibility of emerging novel technologies that compete in the same market segments. To this end, this work will not dedicate a specific market share of electrolyser technology to SOECs, rather it aims to identify the feasibility to deliver global and European syngas demand by SOEC technology. Consequently, the required installed SOE system capacity to deliver global/European syngas demand should be used to address the material requirements and compare these with the material availability, which corresponds to a *critical material analysis* method.

Chapter 4

Exploring and Quantifying the Horizontal Supply Chain

This Chapter aims to answer the first sub-research question of this work; "*What are the theoretical and practical limitations of an HT-SOEC CO_2ER supply chain focused on producing syngas?*" The methodology that will be used to answer this question has been identified in Chapter 3 and consists of two core elements: (i) a comprehensive literature review on the individual supply chain units, and (ii) a back-of-the-envelope calculation to address the implications and feasibility of CO_2ER supply chains that produce syngas at local and global sales. Section 4.1 reviews the literature to quantify the costs and scales of the transportation of the feedstocks. Thereafter, section 4.2 reviews the literature to quantify the processes on which the CO_2ER supply chain relies and the market it aims to supply. Consequently, sections 4.1 and 4.2 address the first element. The theoretical and practical limitations that have been found will be used for a back-of-the-envelope calculation in section 4.3, resulting in the identification of theoretical and practical limitations of the CO_2ER supply chain, providing an answer to the first sub-research question.

4.1 The Quantification of Feedstock Transportation

Within the CO_2ER supply chain, CO_2 and H_2O need to be transported over short- and/or long distances, depending on the specific supply chain configuration. To this end, the conceptualisation of the possible supply chain requires the quantification of all the possible transportation means.

4.1.1 The Transportation of CO_2

The availability of infrastructure that enables safe and reliable transportation of CO_2 is an essential aspect of a CO_2ER supply chain, and in Chapter 2 it has been identified that the two main options for large-scale transport of CO_2 are pipelines (both on- and offshore) and ships. Alternatively, the transportation of smaller quantities of CO_2, over shorter distances, can also be done via rail (i.e. trains) or road (i.e. trucks) (Gutiérrez-Sánchez et al., 2022). The CO_2 transportation costs associated with the various means of transportation are generally stated using one of several common metrics. These common metrics are: (i) the unitary transport cost per unit of distance and/or quantity reported, (ii) the Levelized cost of transport (EUR/tCO_2), measuring the transportation costs amortised over the project lifetime, and (iii) the cost of CO_2 avoided (EUR/tCO_2) including the total costs of CO_2 captured and stored (E. Smith et al., 2021). According to the specified research methodology, cost quantifications will be used for the economic analysis that will be provided in Chapter 5. Consequently, the first and second metrics are the main focus of this section.

4.1.1.1 Quantification of CO_2 Transportation

The cost of CO_2 transport will be based on the literature that is available on the topic. To this end, all assumptions that have been stated in the respective articles must be noted and compared, to form a general understanding of the cost associated with the transportation of CO_2 and what factors influence these costs. Based on the selected metrics, all costs as stated in the literature must be transposed to a standard metric, and based on the methodology that has been explained in Chapter 3 this is chosen to be in Euro (2020) per tonne CO_2 (taking into account a specified system lifetime). The section below provides an overview of the most important findings from the literature that has been reviewed and provides the converted costs in Table 4. The assumptions that have been used in the various literature are specified in Appendix B.1, whereas the conversion of the costs is provided in Appendix B.2.

Psarras et al. (2020), perform a cost analysis on the transport of CO_2 transport via trucks and onshore pipelines. They state that transport by truck only becomes cost-competitive to onshore pipelines at volumes of lower than 500 ktCO_2/yr, and trucking becomes the favoured transportation means at volumes in the range of < 200-300 ktCO_2/yr. They conclude that the costs for trucking transport are mainly dominated by two factors: hauling capacity and travelled distance, however, at very low capacities (< 5 ktpa of CO_2) the costs are dominated by truck lease or purchase, since hauling remains well below capacity (Psarras et al., 2020). Additionally, they conclude that, as delivery closes in on the maximum capacity, both in terms of distance and maximum capacity for each trip, economies of scale are optimized. Psarras et al. (2020a), also provide a generalized cost calculation for CO_2 transportation via onshore pipelines, for transportation quantities larger than 750 ktpa. According to their research, the pipeline transport costs change linearly for fixed volumes (variable distance) and nonlinearly for fixed distance hauls (i.e. a variable load). This is because the increased distance hauling requires a linear increase in pipeline infrastructure (piping and pumps), as well as fixed and variable operating expenses and maintenance, while variable load haul costs are more sensitive to the optimal pipeline diameter, which is determined from the desired pipeline capacity. The costs that have been calculated by Psarras et al. (2020), are provided in Table 4. They also provide an energy requirement of 140 kWh/tCO_2 for compression during transportation, the specifications are provided in Appendix B.1 and B.2.

Alternatively, the research by McCollum & Ogden (2006), creates techno-economic model equations to estimate the costs of CCS systems. In their research, they use estimations for equipment size, costs of compression, costs of pipeline transport, and injection costs to calculate the overall costs of CCS systems that use onshore pipelines to transport CO_2 in the U.S. The CO_2 transportation costs that have been estimated by them, at quantities of 0.73 and 7.3 Mtpa and distances of 100 and 500 km respectively, have been provided in Table 4. Their estimations are based on several variable model inputs including CO_2 viscosity and density in the pipeline, the roughness of the pipeline, location and terrain factors, and required inlet, outlet and intermediate pipeline pressures.

The research by the Zero Emissions Platform (2010), also focuses on a cost assessment for CO_2 transportation means, including shipping and on- and offshore pipelines. The calculated transportation costs have been converted and provided in Table 4. The cost calculations are based on the assumption of full capacity utilisation from the start, which may very well prove to be unrealistic, as large infrastructures generally deal with ramping up over time, which would lead to an increase in unit costs for the networks that utilise pipelines as CO2 transportation means. They conclude that such ramp-up aspects influence transportation by ships significantly less since ramp-up is achieved by adding additional ships. Furthermore, they conclude that the offshore pipeline costs are roughly proportional to the distance, which is comparable to the conclusion by Psarras et al. (2020a) for the costs of onshore pipelines.

Research by Durusut & Joos (2018) focuses on estimating the costs of shipping CO_2 from different terminals, at a range of scales (both distance and capacity), to CO_2 storage sites in the UK. Additionally, they aim to provide a comparison between shipping (port-to-port) and the usage of an offshore pipeline for the transportation of CO_2. They conclude that, for large distances and low capacity, the transportation of CO_2 by ship is cheaper than the usage of offshore pipelines. Moreover, for a capacity of 500 ktpa (=0.5 Mtpa), shipping CO_2 is cheaper than pipeline transport for all distances above 200 km. Whereas for a large capacity of 5 Mtpa, the breakeven distance for shipping to become cheaper than offshore pipeline transport is 500 km. To this end, they conclude that the usage of ships for CO_2 transportation is more favourable for a project with a capacity lower than 5 Mtpa, a project duration shorter than 20 years and transportation distances over 500 km. Additionally, they conclude that economies of scale can be realised in shipping across many components of the supply chain, including the CAPEX of ships, the usage of fuel during transportation and harbour fees. The provided costs have been converted to the appropriate units and are provided in Table 4. Alternatively, the research by Kujanpää et al. (2011) also calculates the shipping costs for CCS projects, but for Finland specifically. They provide a CO_2 transportation cost estimation for a specific distance of 1950 kilometres. This cost estimation is converted and provided in Table 4. Their main conclusion is that ship transportation allows much flexibility in the planning and operation and to this end, should be selected for projects with significant amounts of uncertainty.

Fu et al. (2010), provide an economic assessment of a syngas production process via co-electrolysis with HT-SOEC technology. They state that offshore pipelines are 40-70% more expensive than onshore pipelines of the same size, these higher costs are primarily related to increased construction and operation difficulty. Furthermore, they provide a cost for the transportation of CO_2 through pipelines or shipping, for mass flow rates of 5 – 40 Mtpa and a distance of 250 km. Although the research is interesting due to the similarities with this work, they generalise pipelines and shipping into one class of costs and do not provide the underlying assumptions for these costs. Such generalisations do not align with the research approach of this work, consequently, the stated costs have not been provided in Table 4. However, they also mention transportation costs for distances of 60 km and 250 km, if the means of transportation is a truck. They state that these costs are based on commercially available information, however, no further specification is provided on this commercial information. Nevertheless, since these costs are transportation mean-specific and based on variable distances, they have been included in Table 4. Opposed to the research of Fu et al. (2010), which provides transportation cost quantifications for large annual capacities, Fasihi et al. (2019), provide cost quantifications for small annual capacities of 15 – 20 tonnes of CO_2 per year. Like the research of Fu et al. (2010), the research by Fasihi et al. (2019), does not state the underlying assumptions for these costs. Nevertheless, these costs are based on a specific distance and quantity, and consequently, they can be used to compare the costs that have been stated in other research and to this end have been converted to the appropriate units and provided in Table 4.

Trucks, ships, and onshore- and offshore pipelines have been reviewed and their respective cost assumptions have been provided in Table 4. However, there are no estimations for the costs associated with the transportation of CO_2 by train. To this end, Thorvaldson Aursland (2016), mentions that there are several benefits associated with the transportation of CO_2 by train. First, they claim that train transport has similar cost trends to ship transport, which makes it attractive for small to medium quantities of CO_2 over medium to long distances. Second, train transport can take advantage of the already existing railway infrastructure, and as such, for regions with a strong railway infrastructure, can be a flexible option for CO_2 transportation without having additional infrastructure investment costs. Third and final, it is mentioned that pipelines face larger challenges in terms of social acceptance, as tanked transport of gas and liquid such as train or truck transport are generally receiving broader public acceptance. Although they mention these favourable terms for train transport, they are not based on calculations. Alternatively, the research by L. Gao et al. (2011), does include cost calculations of the transportation of CO_2 by trains, which have been provided in Table 4. Their research focuses on a specific case in China, and they compare rail transport with ship- and onshore pipeline transportation respectively. They conclude that ship transport of CO_2 provides a more flexible, and in many cases, more cost-effective transport solution than pipelines with distances over 1000 km. However, in their research, they do not include the possibility of off-shore pipeline transport. Furthermore, they provide a cost-function for the usage of rail transport, which is significantly higher than the costs for shipping and onshore pipelines respectively.

Table 4 The converted transportation costs for specific quantities of CO_2 over specific distances, that have been obtained from the literature. *These costs include liquefaction (5.3 €/tCO_2).

Tp. Mean	Capacity MtCO_2/pa	Distance km	Cost €/tCO_2	Ref.
Truck	15 – 20 x 10^{-6}	>100	13.0	(Fasihi et al., 2019)
	1 x 10^{-3}	32.2	47.4	(Psarras et al., 2020)
		80.5	50.0	(Psarras et al., 2020)
		160.9	53.5	(Psarras et al., 2020)
	1 x 10^{-2}	32.2	7.0	(Psarras et al., 2020)
		80.5	9.6	(Psarras et al., 2020)
		160.9	14.0	(Psarras et al., 2020)
	1 x 10^{-1}	32.2	3.5	(Psarras et al., 2020)
		80.5	7.5	(Psarras et al., 2020)
		160.9	14.0	(Psarras et al., 2020)
	1 x 10^{-1} – 1	n.a.	0.076 (in €/tCO_2-km)	(Psarras et al., 2020)
	5 – 40	60	17.0	(Fu et al., 2010)
		250	73.4	(Fu et al., 2010)
Train	1.46	598	10.4	(L. Gao et al., 2011)
Shipping	0.5	>200	12.7	(Durusut & Joos, 2018)
	1.46	300	5.7	(L. Gao et al., 2011)
	2	750	11.1	(Fasihi et al., 2019)
	2.5	180	9.3 | 15.3*	(Zero Emissions Platform, 2010)
		500	10.7 | 16.7*	(Zero Emissions Platform, 2010)
		750	12.0 | 18.0*	(Zero Emissions Platform, 2010)
		1500	16.4 | 22.4*	(Zero Emissions Platform, 2010)
	3	1950	13.0*	(Kujanpää et al., 2011)
	5	500	8.1	(Durusut & Joos, 2018)
	20	180	12.5*	(Zero Emissions Platform, 2010)
		500	13.8*	(Zero Emissions Platform, 2010)
		750	14.9*	(Zero Emissions Platform, 2010)
		1500	18.2*	(Zero Emissions Platform, 2010)
Onshore pipeline	0.73	100	7.9	(McCollum & Ogden, 2006)
		500	50.9	(McCollum & Ogden, 2006)
	>0.75	n.a	0.038 (in €/tCO_2-km)	(Psarras et al., 2020)
	1.46	300	6.6	(L. Gao et al., 2011)
	2.5	180	6.1	(Zero Emissions Platform, 2010)
	7.3	100	1.7	McCollum & Ogden 2006
		500	11.4	McCollum & Ogden 2006
	20	180	1.7	(Zero Emissions Platform, 2010)
		500	4.2	(Zero Emissions Platform, 2010)
		750	6.0	(Zero Emissions Platform, 2010)
Offshore pipeline	2.5	180	10.5	(Zero Emissions Platform, 2010)
		500	23.1	(Zero Emissions Platform, 2010)
		750	32.4	(Zero Emissions Platform, 2010)
		1500	58.4	(Zero Emissions Platform, 2010)
	20	180	3.8	(Zero Emissions Platform, 2010)
		500	6.8	(Zero Emissions Platform, 2010)
		750	9.3	(Zero Emissions Platform, 2010)
		1500	18.4	(Zero Emissions Platform, 2010)

4.1.1.2 Theoretical and Practical Limitations of CO_2 Transportation

To provide a partial answer to the first sub-research question, this section aims to delineate the theoretical and practical limitations associated with the transportation of CO_2 within the CO_2ER supply chain. Firstly, a specific geographic location (either feedstock or demand for CO_2) might hinder the possibility of transporting CO_2 by pipeline (e.g. located at a high altitude making compression infeasible, densely populated areas prohibiting the construction of CO_2 pipelines) or ship (e.g. not close to open water such as rivers or seas/oceans) (Hong, 2022). Furthermore, the transportation means are limited by the capacity they can transport and the required operating conditions of the various transportation means. The annual capacities for CO_2 transportation that have been found are in the range of 15 tonnes per year – 10 Mega tonnes per year. Additionally, although it is not a limitation but rather an opportunity, the measure of economies of scale for the various transportation means is calculated in detail in Appendix B.3, the results of which have been provided in Table 5.

Table 5 Assessing the measure of economies of scale for the different transportation means based on the transportation costs provided by McCollum & Ogden (2006), Psarras et al. (2020) and the Zero Emissions Platform (2010).

TM	**Percentual increase in transportation capacity ($\boldsymbol{\Delta Q_{capacity}}$)**	**Distance (km)**	**Percentual decrease in per unit costs ($\boldsymbol{\Delta C}$) – Measure of economies of scale**
Ship	700 % $_{\text{2.5 Mtpa – 20 Mtpa}}$	180 | 500 | 750 | 1500	18.3 % | 17.4 % | 17.2 % | 18.8 %
Offshore pipeline	700 % $_{\text{2.5 Mtpa – 20 Mtpa}}$	180 | 500 | 750 | 1500	63.8 % | 70.6 % | 71.3 % | 68.5 %
Onshore pipeline	700 % $_{\text{2.5 Mtpa – 20 Mtpa}}$ || 900 % $_{\text{0.73 Mtpa – 7.3 Mtpa}}$	180 100 | 500	72.1 % 78.5 % | 77.6 %
Train	-	-	-
Truck	900% $_{\text{1ktpa – 10ktpa}}$ 900% $_{\text{10ktpa – 100ktpa}}$	32.2 | 80.5 | 160.9 32.2 | 80.5 | 160.9	85.2 % | 80.8 % | 73.8 % 50.0 % | 21.9 % | 0.0 %

From Table 5 it can be concluded that pipelines benefit significantly more from economies of scale than ships. According to the Zero Emissions Platform (2010), pipeline costs consist mainly of CAPEX (~90%), while shipping costs are less CAPEX-intense (~50%). For pipelines, CAPEX increases when the capacity is increased, but only due to minor additional requirements such as a larger number of compressors and more construction material, and as such is roughly proportional to distance and consequently benefits more from economies of scale. Additionally, when comparing off- and onshore pipelines it can be concluded that onshore pipelines benefit slightly more from economies of scale than offshore pipelines. The CAPEX of offshore pipelines are significantly higher than the CAPEX of onshore pipelines, and since the Zero Emissions Platform (2010) uses an annual O&M cost of 6% of the CAPEX for both transportation means, the larger decrease in per unit costs of onshore pipelines can be attributed to this cost factor. Moreover, trucks also benefit significantly from economies of scale advantages, for all distances, when the capacity is increased from 1ktpa to 10ktpa. However, when the capacity is increased from 10 ktpa to 100 ktpa, the percentual decrease in per unit costs becomes smaller for increasing distances and even becomes 0% for a distance of 160.9 km. Since these capacities are small in comparison with the capacities of ships and pipelines, one could argue that economies of scale do not apply to trucks. Unfortunately, the lack of available literature on CO_2 transportation by trains does not allow an assessment of possible economies of scale advantages for trains. However, since trains and trucks use already existing infrastructure and have similar operating conditions one could argue that trains could have economies of scale advantages similar to trucks.

A true comparison between the various transportation means is rather complex since CO_2 transportation systems are most often designed and constructed for one specific application (i.e. customized for a supply chain). Especially the costs of pipeline systems are heavily dependent on the specific operating environment, whereas ships and trucks are more flexible. Nevertheless, the reviewed literature has identified some preferred transportation means for various capacities and distances. Psarras et al. (2020), state that the preferred transportation means for land transportation of CO_2 for quantities up to 300 ktCO_2/pa are trucks and above these quantities, onshore pipelines are the preferred means of transportation. Furthermore, Durusut & Joos (2018), state that for quantities under 500 ktCO_2/pa and a distance that is larger than 200 km, but also quantities above 5 MtCO_2/pa and distances larger than 500 km, ships are preferred over offshore pipelines. Although these preferences are not necessary limitations and are based on case-specific research, they align with the economies of scale calculations and within the CO_2ER supply chain of this work, the preferred CO_2 transportation mean and its costs can be based on these quantities and distances.

4.1.2 Transportation and Usage of H_2O

Comparable to the quantification of the costs of CO_2 transportation, the cost of H_2O consumption and transport will be based on the literature that is available on the topic. Moreover, based on the information that has been provided in section 2.1.2 (state-of-the-art H_2O usage and transportation), this section will focus on the quantification of costs of the water feedstock considering the possible required treatment processes. To ensure that the information that is found is comparable, all costs that have been stated in the literature must be transposed to a standard metric and based on the methodology that has been explained in Chapter 3, this is chosen to be Euro (2020) per m^3 of H_2O and, if quantities are mentioned, they will be converted to m^3/hr or tonnes/hr.

4.1.2.1 Quantification of H_2O Feedstock

This section reviews the literature and provides the costs and assumptions that have been mentioned in the respective research. The converted costs are provided in Table 6, and a detailed explanation of the conversion of these units is provided in Appendix B.4.

The research by Redissi & Bouallou (2013) performs an economic assessment to compare the price of 1 kg of syngas (with a molar ratio of 1.19 H_2:CO), which is produced through co-electrolysis via HT-SOEC technology, with the price of 1 kg of oil. In their research, they assume a water cost price of 0.87 €/m^3. They state that this price is based on the production cost of desalinized seawater. According to their research, the desalinisation process requires 0.1 kJ/mol of H_2O, and they assume an electricity price of 76.3 €/MWh. However, the provided cost of 0.87 €/m^3 is not calculated based on the stated energy requirements and electricity price but obtained from the research by Graves et al. (2011). No further information is provided on the quantity of H_2O to which this cost applies, nor is there any information on the production rate of syngas, however, in their research, they specify that the inlet flowrate of H_2O is 8107 kg/hr (at standard pressure and 25 ˚C). Additionally, it must be noted that they do not mention any specific geographic environment in which the assessed syngas production process operates. Nevertheless, the stated costs and quantity are converted and provided in Table 6.

Alternatively, the research by Fu et al. (2010), also provides an economic assessment of the production of syngas via HT-SOEC co-electrolysis. Within their assessment, they assume that deionised water is used as a feedstock, however, they do not specify a specific geographic environment in which the process operates. Also, they do not mention any means of transportation for the water, however, they do specify a cost of 1.15 €/tonne of deionised water, which is delivered at the HT-SOEC at a temperature of 20 ˚C and atmospheric pressure. Furthermore, they calculate that, to produce 5006 kg-syngas/day (with a molar ratio of 2 H_2:CO) 668 kg/day of H_2 must be produced, which corresponds to a system mass flow rate of water of 5984 kg-H_2O/day. The provided costs and quantities are converted and depicted in Table 6.

Mehmeti et al. (2018), perform a life cycle analysis for various hydrogen production methods, including SOECs. They assess several impact categories, including the water consumption potential and the water scarcity footprint. Furthermore, they differentiate between electrolysis via SOECs that use fossil-generated electricity (E-SOECs) and electrolysis with SOECs that solely use wind energy as input (E-SOEC-R). They conclude that, if fossil-fuel-powered plants are used for the provision of electricity, throughout the supply chain, the consumption of water for the generation of 1 kg of H_2 is approximately 17 times higher than when renewable (wind) energy is used (146.82 m^3/kg-H_2 versus 8.82 m^3/kg-H_2). Although their research provides valuable insights, it does not focus on co-electrolysis, and neither does it provide any price indications for water usage, nevertheless, the stated water requirements for H_2 production have been provided in Table 6.

Nicodemus et al. (2014), investigate the costs and policy considerations of solar syngas production by the zinc/zinc-oxide solar thermochemical fuel production cycle in New Mexico, the U.S. Although the technology that is used to produce syngas in their research is not an electrolysis technology, the fact that they focus on the production of syngas on a production location in the desert with scarcity in the supply of H_2O, makes it interesting research to review. Their research assumes a syngas production rate of 6166 kg/h, however, they do not specify an H_2:CO molar ratio, nor do they specify a quantification of the H_2O inlet flow. They do mention that the H_2O comes from a water supply network, and its associated costs are US$ 0.014/L of H_2O. They conclude that the cost of feedstock water is an important consideration for areas where water resource is scarce, such as the desert of New Mexico. Moreover, if certain areas lack water supply, the water needs to be transported from its sources to such desert regions, which also increases the price by factors up to an order of magnitude (i.e. US$ 0.14/L). This price increase is mainly caused by the electric energy required for the compression power, and according to Gómez et al. (2018), the simplest case for the transportation of water, which is also commonly applied, is the usage of pipelines in which the water is pumped from an aquifer to a tank. As such it is a connection between a source and an endpoint. They provide electric energy requirement calculations based on the following assumptions; elevation head (H) = 100 m, a flow (Q) = 0.1 m^3/s (=8640 m^3/day), and no pressure requirements at the delivery point (i.e., a tank), and a water specific weight (γ) = 9,810 kN, results in daily electric energy requirement (E_{el}) of 2354.4 kWh/day, calculated via Equation (ii).

$$\text{(ii)} \quad \text{Required Electric Energy } (E_{el}) = \gamma * Q * H$$

Schreiber et al. (2020), provide a life cycle assessment of power-to-syngas, in which they compare HT co-electrolysis with steam methane reforming. When HT-SOECs are used to produce 1 kg of syngas, with a molar ratio of 2 H_2:CO (with a corresponding density of 0.481 kg/m^3), they state that 1.13 kg of deionised H_2O is required as feedstock. They use a 150 kW HT-SOEC which produces 147 tonnes of syngas per year (assuming full load hours) and they assume that the deionised water supply is delivered at ambient temperature and atmospheric pressure. Although they do not state a cost price for the H_2O feedstock, they do mention that the environmental footprint of the deionised H_2O supply is negligible compared to other aspects of the supply chain, such as electricity requirements. Although the research of Schreiber et al. (2020) does not provide a quantification of the cost of the deionised water supply, they do provide insights into the H_2O requirements for the production of syngas with a molar ratio of 2 H_2:CO, which can be compared to the quantification that has been provided by Fu et al. (2010) whom use a similar molar ratio; 5006 kg-syngas/day / 403 kg-syngas/day = 12.4 and 0.25 m^3-H_2O/hr / 0.019 m^3-H_2O/hr = 13.2. From this comparison, it can be concluded that there is a small difference in the ratios of approximately 6%. Nevertheless, taking into account the 10 years between the two publications, the amount of H_2O required for the production of syngas with a molar ratio of 2 H_2:O, via co-electrolysis by HT-SOECs, can be deemed validated.

Table 6 The converted costs of water consumption that have been provided in the various research.

Process	Water source	Quantity (m^3-H_2O/hr)	Price (€/m^3)	Ref.
Co-electrolysis to produce syngas	Desalinized seawater	8.13	0.96	(Redissi & Bouallou, 2013)
Co-electrolysis to produce 5006 kg of syngas per day	Deionised water	0.25	1.30	(Fu et al., 2010)
Electrolysis to produce H_2 (E-SOEC & E-SOEC-R)	Water supply network	146.82 m^3/kg-H_2 (E-SOEC); 8.82 m^3/kg-H_2 (E-SOEC-R)	-	(Mehmeti et al., 2018)
Solar syngas production via Zinc/Zinc-Oxide cycle	Water supply network	-	13.38	(Nicodemus et al., 2014)
Co-electrolysis to produce 403 kg of syngas per day	Deionised water	0.019	-	(Schreiber et al., 2020)

The reviewed literature that addresses the costs of H_2O from the point of view of specific processes (i.e. co-electrolysis, electrolysis and zinc/zinc-oxide cycle as depicted in Table 6), does not consider price differences in volumes of a more general cost indication can be provided by considering the water price that is opposed by a water provision company for water consumption in a specific region. To this end, Figure A. 4 (in Appendix B.5) provides the cost of using water from the water supply network in the Netherlands for 2020, 2021 and 2022, which are transposed into Figure 4. Moreover, based on Figure 4 it can be seen that the costs of water follow a stepwise linear function for the ranges 0-300, 300-1.000, 1.000-10.000, 10.000-100.000 and >100.000. These costs are based on the costs in the Netherlands, consequently, it must be verified whether they are representative of a larger region such as the EU. To this end, the prices provided in Figure 4 are compared to the prices provided in a report by EurEau (2021), on the European drinking water and wastewater sectors which have been provided in Figure A. 5 (in Appendix B.6). According to EurEau (2021), the mean European price of H_2O is € 3.67/m^3 whereas the average price of H_2O in the Netherlands is € 4.33/m^3. This price is based on average consumption of 105 m^3/yr, which corresponds to a price of € 2.09/m^3 according to the 2021 price data of Waternet (2022). When comparing the prices provided by EurEau (2021) and Waternet (2022) it can be concluded that there is a significant difference (of € 2.24/m^3) between the two. The prices provided by EurEau (2021), include the costs associated with wastewater services, and according to the information provided in Figure A. 6 (in Appendix B.6), these costs account for approximately 55% of the total costs in the Netherlands. These costs are not included in the water prices that have been provided by Waternet (2022). Multiplying € 4.33/m^3 by 45% results in a price of € 1.95/m^3, which is still not identical to € 2.09/m^3, but much closer, and as such, can be used to explain the price difference. Consequently, it can be concluded that the water price provided by Waternet (2022) can be used, taking into account that it is slightly above the average price of water in Europe.

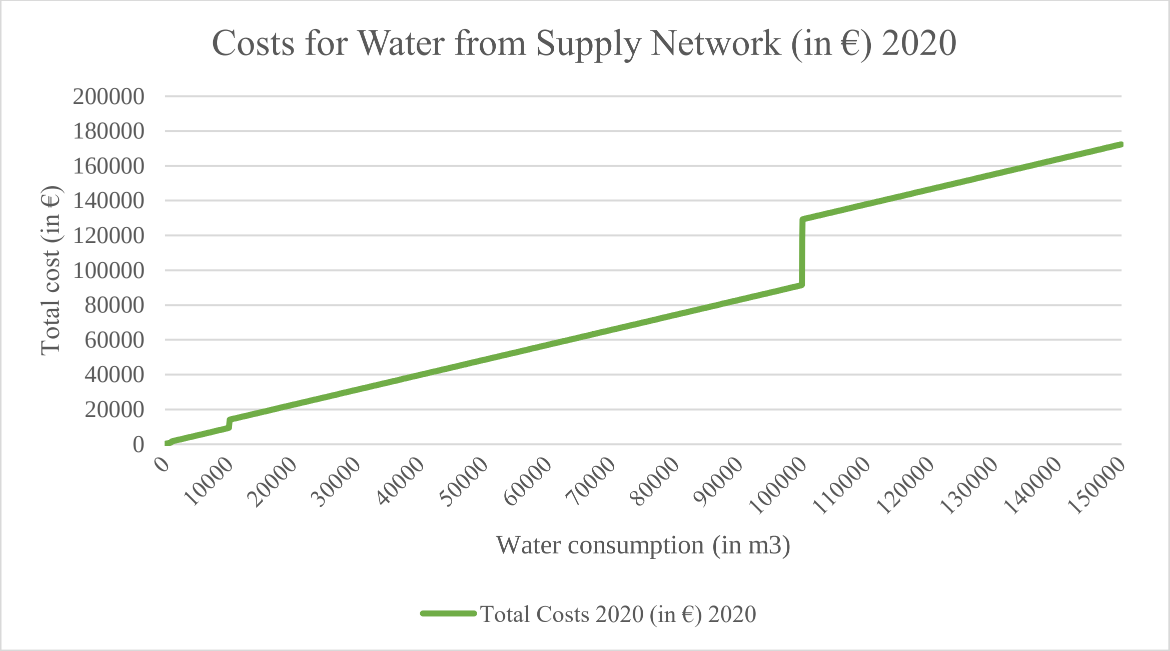

Figure 4 The price of H_2O if it is supplied by a water supply network and does not need additional treatment processes.

A comparison between the costs for deionised water, desalinated water and untreated water from a water supply network can now be made. For desalinated water, a quantity of 8.13 m^3/hr and a price of 0.96 €/m^3 have been provided in Table 6, which will be used for calculation purposes. Transposing this quantity into an annual feedstock requirement results in 71219 m^3/yr, which according to Equations iii-v, corresponds to a total cost of € 68370/yr ($C_{desalinated}$) for desalinated seawater. For untreated water from a water supply network, these costs are € 66747/yr ($C_{wsn[1.000\text{-}10.000]}$), and for deionised water, they are € 92585/yr ($C_{deionised}$).

(iii) $C_{desalinated} = 0.96 * Q_{annual}$

(iv) $C_{wsn[1.000-10.000]} = 1.09 * (712.7 + 0.79 * Q_{annual})$

(v) $C_{deionised} = 1.30 * Q_{annual}$

4.1.2.2 Theoretical and Practical Limitations for Water Usage and Transportation

To provide a partial answer to the first sub-research question, this section aims to delineate the theoretical limitations associated with the transportation and usage of H_2O within the CO_2ER supply chain. The research of Bianchi & Bosio (2021) and Lim et al. (2017) delineate that a CO_2ER supply chain that uses HT-SOEC technology with an operating temperature of at least 800 ˚C, could use seawater as a feedstock without the requirement of additional treatment processes such as desalination or demineralisation. Nevertheless, the reviewed literature that assesses the production of syngas via co-electrolysis use either desalinated seawater or deionised water. Beswick et al. (2021), calculate the water requirements for the green hydrogen economy. They estimate that the global green hydrogen economy requires 2.3 Gt of H_2 per year. Based on the estimation that the production of one kg-H_2 requires 9 kg of H_2O, the total water requirement to meet the global H_2 demand is 20.5 Gtpa (or 20.5 billion m3 per year). This amount accounts for only 1.5 ppm of the Earth's available freshwater. Since the SOECs can also use (desalinated) seawater, it is assumed that the total availability of water does not oppose any theoretical limitations. The costs of the alternative water feedstocks are compared and although deionised water is approximately 35% more expensive than desalinated water and 39% more expensive than water from the Dutch water supply network, the literature indicates that both the costs and the environmental impact of the water feedstock are negligible compared to other supply chain echelons.

However, these costs are based on geographic locations with an abundance of water supply. If the CO_2ER supply chain is located at a geographic location prone to water scarcity, the research by Nicodemus et al. (2014) identifies that the price of water from a water supply network is an order of magnitude higher, and could even be two orders of magnitude higher if there is no water availability and the feedstock must be transported over large distances. Consequently, the theoretical limitations associated with the usage and transportation of water are mainly determined by the geographic location of the CO_2ER supply chain. If there is access to seawater, there are ought to be no limitations, whereas, for alternative geographic locations, the potential limitations should be researched individually based on the availability, the amount of syngas that is to be produced, and the volume of water feedstock that is required to produce this amount of syngas.

4.2 The Quantification of Processes and Market

Having delineated the transportation of CO_2, the usage and transportation of H_2O, this section focuses on quantifying the remainder of the supply chain units that constitute the CO_2ER supply chain. This will be done by addressing the CO_2 capture process in section 4.2.1, the syngas production process which includes the HT-SOEC in section 4.2.2, and the syngas market in section 4.2.3.

4.2.1 The Quantification of CO_2 capture and Preparation for Transport

There exist various point sources and activities that result in a surplus of capturable CO_2. Examples of these are biofuel production, flue gases from biomass and fossil combustion plants, and industrial plants (e.g., iron and steel, pulp and paper, and cement) (Ingvarsdóttir, 2020), but also geothermal activity, seawater and air are mentioned in the literature (Brynolf et al., 2018). Moreover, although these sources all generate a surplus of CO_2, their respective CO_2 concentrations vary significantly. The smallest concentration of CO_2, approximately 415 ppm (0.0415%) in 2021, can be found in atmospheric air (Jin et al., 2021), whereas production plants that produce ethanol through fermentation of sugar, production plants that use anaerobic digestion of household waste to produce biogas, production plants that use gasification of biomass to produce syngas, and ammonia production plants can have CO_2 concentrations up to 100% (Brynolf et al., 2018). The CO_2 concentrations at the various sources affect the capture efficiency and the cost of capture, as such, the choice of capture technology is an important aspect. In section 1.3 the argumentation for selecting PCC and HT-DAC has been provided. To this end, this section aims to delineate the theoretical and practical limitations associated with these two CO_2 capture technologies in terms of availability, requirements and costs.

4.2.1.1 Quantification of High-Temperature Direct Air Capture

During the DAC process, atmospheric air flows (either by natural air speed or forced through fans) through a filter which removes the CO_2 from the air by either adsorption, absorption, or mineralization (Schreiber et al., 2020). Since this research focuses on HT-DAC specifically, the quantification that will be provided in this section solely considers an HT-DAC process. Such a process generally consists of two main cycles: the first cycle which is known as absorption and the second cycle which is known as regeneration (Fasihi et al., 2019). In the first cycle, atmospheric air is brought into contact with a solvent in the absorption column, either via the natural flow of air or assisted with fans. The CO_2 molecules react with the solvent, generally sprayed sodium hydroxide ($NaOH$) (alternatively KOH), and form a solution of sodium carbonate (Na_2CO_3). In the second cycle, the sodium carbonate solution is mixed with calcium hydroxide ($Ca(OH)_2$) (alternatively $Na_2O.3TiO_2$) and is formed into calcium carbonate ($CaCO_3$). In turn, the calcium carbonate is heated to a temperature of approximately 900 ˚C resulting in the release of CO_2. The outputs of the process are a pure stream of CO_2 and calcium oxide (CaO), from which the CO_2 is collected such that it can be transported, whereas the calcium oxide is mixed with water for regeneration to $Ca(OH)_2$ (Fasihi et al., 2019).

The HT-DAC process requires energy input in the form of high-temperature heat, mainly for the release of CO_2, and in the form of electricity for blowing air, spraying, and the transportation of solutions between units. Additionally, the compression and/or liquefaction that is required to transport CO_2 also requires electrical energy input. A literature review by Fasihi et al. (2019), provides typical ranges for these energy inputs, which are 1420-2250 kWh_{Th}/tonneCO_2 and 366-764kWh_{el}/tonneCO_2, the latter includes the electric energy required for CO_2 compression in a range of 58-150 bar. According to Fasihi et al. (2019), the minimum electrical energy requirement for CO_2 compression to 138 bar is 63.5 kWh/tCO_2, however, a compressor never works at 100% efficiency, consequently, the actual electrical energy demand is based on the compressor efficiency (approximately 60% in state-of-the-art compressors), resulting in an actual electrical energy requirement of 104 kWh/tCO_2. It must be noted that, according to McCollum & Ogden (2006), recoverable heat is generated during the compression of CO_2 which can be utilised to deliver part of the heat energy requirements of the system. However, it must be noted that the HT-DAC requires high-tempertature, and the excess heat resulting from the CO_2 compression will not be in the range of 900 ˚C. Alternatively, Budinis (2022), provide the total energy demand in GJ/tCO_2, which is converted to kWh/tCO_2 in Appendix B.7. The converted energy requirements are 1833 kWh/tCO_2 in total, consisting of 1472 kWh/tCO_2 for HT heat energy requirements, 222 kWh/tCO_2 for electrical energy requirements (for capturing and separation) and 139 kWh/tCO_2 of electrical energy for compression requirements. Yet other research by Schreiber et al. (2020), states that the thermal energy requirements of an HT-DAC process are 1500 kWh/tCO_2 and the electrical energy requirements are 500 kWh/tCO_2.

Apart from the energy input that is required to capture, process and compress CO_2 from ambient air, HT-DAC technology also consumes H_2O, both for the startup of the plant and to make up for the losses throughout the system (Mcqueen et al., 2021). Moreover, according to Fasihi et al. (2019), the water loss in HT-DAC systems could be in the range of 0 – 50 tonnes of H_2O per ton of CO_2 captured. The actual amount of H_2O that is lost depends on the temperature and humidity of the ambient air that is fed into the process and the concentration of the aqueous solution. An example of the quantification of H_2O consumption by a specific DAC process is provided by Keith et al. (2018), who state that the new HT-DAC design of Carbon Engineering needs 4.7 tonnes of H_2O per tonne of captured CO_2, at a temperature of 20 ˚C and relative humidity of 64%.

Since the CO_2 is captured from ambient air, naturally, another requirement for the HT-DAC process is the availability and flow of air. The air can either flow through the system based on the natural flow of air or be forced into the system, by using fans. To address the theoretical and practical limitations in terms of the required size and volume of air, the research of Bui et al. (2018), estimated that a DAC plant that operates on a Mtpa scale, at an average capture rate of 50% and a typical air velocity of 2-3 m/s (no fans), requires the processing of 80000 m^3/s of air. Such a large-scale process would need a surface area of 30000 m^2 (=0.03 km^2), which is about 600 times larger than the area that is generally used for the PCC of CO_2 at coal power plants (~50 m^2). Alternatively, W. A. Smith et al. (2019) propose a DAC capture system that provides the CO_2 feedstock for a 10000-tonneMeOH/day plant. They also assume a 50% capture efficiency by the KOH capture solvent and an air velocity (V_{wind}) of 2 m/s. Furthermore, they assume a CO_2 concentration in the air of 400 ppm. The MeOH plant requires 13750 tonnesCO_2/day (5.02 Mtpa), to this end they calculate that 27500 tonnesCO_2/day need to pass the air inlet for the DAC process. They use an air density of 1.184 kg/m^3 that contains 0.608 gCO_2/kg air. Using these numbers, they calculate that approximately 38.2 km^3 of air/day (=$V_{air,req}$) must pass through the capture area (see Equation (vii)). To support a process of such scale, Equation (viii) is used to calculate a required frontal surface area ($A_{capture}$) of 0.22 km^2.

(vi) $$\mathrm{V}_{\mathrm{air,req}} = \frac{1}{\rho_{air}} * \frac{m_{air}}{m_{CO2,air}} * \frac{m_{CO2,req}}{\eta_{cap}}\ [\mathrm{m}^3]$$

(vii) $$\mathrm{A}_{\mathrm{capture}} = \frac{Volume\ of\ air\ required\ per\ day}{V_{wind}}\ [\mathrm{m}^2]$$

Having delineated the requirements of an HT-DAC process, the range of possible sizes and the associated costs should be identified. According to the research of Ozkan et al. (2022), who summarize various papers and create a table that states the characteristics of the DAC technology that has been mentioned in these papers, the only company that focuses on HT-DAC, and plans to deliver this DAC technology for commercial use, is Carbon Engineering. Moreover, other research by Mcqueen et al. (2021) also provides an overview of the literature that provides cost estimates for HT-DAC. Although they mention five articles that focus on HT-DAC, only one of them is based on technology that is being developed instead of theoretical models, which is also the HT-DAC technology that is being developed by Carbon Engineering. A similar conclusion can be drawn from the research by Fasihi et al. (2019). Additionally, in Chapter 2 (section 2.1.2) it is mentioned that Carbon Engineering, in cooperation with 1PointFive, aims to develop 70 large-scale HT-DAC facilities by 2035 (Budinis, 2022). Consequently, this work will consider the sizes and costs that have been provided in the literature that focus on the HT-DAC technology developed by Carbon Engineering. Nevertheless, it must be noted that these systems have not been commercialised yet.

The performance of any large industrial process depends on matching the scales of the process to the environment in which it operates. For the HT-DAC technology developed by Carbon Engineering, both the air contactor and the pellet reactor are modular, as such, their performance varies little from capturing CO_2 at scales of 10 ktpa – 1 Mtpa (Keith et al., 2018), and their capital cost per unit capacity is nearly constant down to 100 $ktCO_2$-pa. At a scale of 100 ktpa, the energy intensity of the full process would be very close to a process at a scale of 1 Mtpa, however, the approximate capital costs for the latter would be 80% larger (Keith et al., 2018). Table 7 provides an overview of the CAPEX and OPEX of an HT-DAC unit, which has been mentioned in the research by Fasihi et al. (2019) and Keith et al. (2018), and the calculated costs for a smaller HT-DAC unit (0.1 Mtpa), based on the information provided by Keith et al. (2018). These costs will be used as quantification for the HT-DAC process. An overview of the conversions that have been applied and the operating parameters on which these costs are based are provided in detail in Appendix B.7.

Table 7 The converted CAPEX and OPEX for HT-DAC technology by Carbon Engineering that has been provided by Fasihi et al. (2019) and Keith et al. (2018), and calculated (0.1 Mtpa) based on Keith et al. (2018).

Capacity	CAPEX	OPEX (non-energy)	Lifetime	Energy demand	Ref.
1,0 Mtpa	€ 815/tCO_2 (over lifetime)	3.7% of CAPEX p.a.	25 years	1535 kWh_{el}/tCO_2 (E + H), (C) excluded	(Fasihi et al., 2019)
1.0 Mtpa	€ 657/tCO_2 (over lifetime)	3.7% of CAPEX p.a.	25 years	1460 kWh/tCO_2 (H) and 366 kWh/tCO_2 (E + C 150 bar)	(Keith et al., 2018)
1.0 Mtpa	€ 520/tCO_2 (over lifetime)	3.8% of CAPEX p.a.	25 years	1460 kWh/tCO_2 (H) and 77 kWh/tCO_2 (E), (C) excluded	(Keith et al., 2018)
0.1 Mtpa	€ 365/tCO_2 (over lifetime) (based on row 3)	3.7% of CAPEX p.a.	25 years	1460 kWh/tCO_2 (H) and 366 kWh/tCO_2 (E + C 150 bar)	Calculated based on (Keith et al., 2018)

0.1 Mtpa	€ 289/tCO_2 (over lifetime) (based on row 4)	3.8% of CAPEX p.a.	25 years	1460 GJ/tCO_2 (H) and 77 kWh/tCO_2 (E), (C) excluded	Calculated based on (Keith et al., 2018)

4.2.1.2 Conceptualisation of Post-Combustion Capture

The PCC process of CO_2 includes separation and capture from flue gas that is produced by a specific production process, such as the combustion of fossil fuels to generate electricity or the production of steel and iron. Although DAC technology is expected to increasingly be adopted into nowadays energy systems, PCC is a mature technology and it has already been applied to CO_2-emitting production plants for over a decade (Hong, 2022). The capture costs for PCC are dependent on the industrial process and its specific process conditions. However, in general, PCC processes follow similar steps as DAC processes; (i) separation of CO_2 from other gases of which the flue gas consists, (ii) removal of water from CO_2 (dehydration), (iii) ensuring that the transport conditions are met, consequently compression resulting in the supercritical phase or liquefaction resulting in the liquid phase of $CO_{2,}$ is done before transport. According to Pace & Sheehan (2021), there exist two commercialised technologies for the separation process: monoethanolamine (or simply amine adsorption) and solid sorbent. Both technologies have TRL9. Additionally, ammonia absorption is in the commercial demonstration phase, as such, it has TRL 6-9. Apart from these separation technologies, multiple other technologies are currently at the laboratory scale (TRL 3-5) or still in theoretical development (TRL 2-3). Examples of these technologies are vacuum swing adsorption, nonaqueous amine absorption, and activated carbon adsorption (Durán et al., 2017) (K. Jiang et al., 2020).

As stated, the different point sources are associated with different CO_2 concentrations in their exhaust gas. An overview of these sources and their respective CO_2 concentration is provided in Table 8. There are also reference plant sizes provided in Table 8, which are primarily based on the information provided by the National Petroleum Council (2019) and where necessary, supplemented by NETL (2014) and Environmental Protection Agency (2019). The National Petroleum Council (2019) reviewed a total of 7 studies that focus on the cost of CO_2 capture from various industrial process plants. The calculations and numbers that have been provided in their work are based on the usage of amine adsorption technology. Besides the point sources that are depicted in Table 8, there are additional point sources, such as refineries that use a fluidized catalytic cracking process, industrial furnaces for refining or chemical production, or the production of paper (Pieri et al., 2018), nevertheless, the information provided in Table 8 is deemed sufficient for this work, since it already indicates the wide variety of available point sources and the respective quantity of CO_2 that can be captured from them by PCC technology.

Table 8 An overview of the different types of point sources (i.e. industrial plants) where PCC can be used, their average CO_2 production, a reference size plant, the amount of CO_2 that can be captured from this reference size plant, and the respective energy requirements per tonne of CO_2. The data in the table is based on the work of the National Petroleum Council (2019) (which is based on calculations by NETL (2014), and the Environmental Protection Agency (2019)).

Point Source of CO_2 Emission	Concentration (mol% in exhaust gas)	Average CO_2 Produced per Plant (ktpa)	Reference Plant Size	CO_2 Capture Potential (ktonnes/year)	Energy requirements per tonne of CO_2
Ammonia production plants	99	710	907 ktonne-ammonia per year	389	0.10 MWh

Natural gas processing plants	99	1000	140 MMCF per day	24	0.10 MWh
(Bio)Ethanol production plants	100	410	150 Mgal per year	342	0.12 MWh
Steel and iron manufacturing plants	26	7150	2.54 Mtonnes per year	3324	0.16 MWh (E), 0.76 MWh (H)
Hydrogen production plants	45	600	87 MMCF/D	340	0.18 MWh (E), 0.76 MWh (H)
Cement production plants	21	355	1 Mtonne-cement per year	842	0.16 MWh (E), 0.76 MWh (H)
Coal power plants (>500 MW)	13	2644	550 MW (large)	1272 – 3089 (depending on capacity utilisation)	0.16 MWh (E), 0.76 MWh (H)
Gas power plants (>500 MW)	4	1109	560 MW (large)	527 – 1279 (depending on capacity utilisation)	0.16 MWh (E), 0.82 MWh (H)

From Table 8 it can be concluded that the industrial plants that have an exhaust gas CO_2 mol% which is close to 100% (i.e. > 95%), require an electrical energy input of 0.10 MWh or 0.12 MWh per tonne of CO_2 that is captured. These requirements are based on several assumptions that have been made by the National Petroleum Council (2019), including an electric energy requirement of 0.10 MWh per tonne of CO_2 for compression and dehydration and a required electrical energy input of 0.05 MWh per tonne of CO_2 for the operation of the amine system (with minor differences between various point sources (or facilities)). Detailed calculations of the respective energy requirements of the various point sources have not been provided in the research by the National Petroleum Council (2019), as such, it is not possible to identify why (bio)ethanol production plants, which have a higher exhaust gas CO_2 concentration than ammonia production plants and NG processing plants, require 0.02 MWh more of electrical energy per tonne of CO_2. Moreover, for the industrial plants that have an exhaust gas CO_2 mol% which is lower than 95%, the electrical energy inputs that have been provided by the National Petroleum Council (2019) are 0.16 MWh and 0.18 MWh respectively. Based on the assumptions that have been provided, the difference between these more diluted streams and the high-purity streams can be attributed to the requirement of 0.05 MWh per tonne of CO_2 for the operation of the amine system (with minor differences between various point sources). Additionally, the point sources with an exhaust molar concentration lower than 95% require a separation process. This separation process requires an additional energy input, generally provided in the form of heat. The National Petroleum Council (2019), provided these energy requirements in Million British Thermal Units (MMBTU), which have been converted to MWh (conversion provided in Appendix B.8). These requirements (0.76 MWh and 0.82 MWh respectively) are based on the usage of amine absorption technology, and fuel requirements in the range of 2.5 – 3.5 MMBTU, dependent on the facility and solvent type.

For dilute gas streams (i.e. with lower CO_2 concentrations < 95 mol%), more gas must move through the separation process to obtain similar amounts of CO_2, which results in additional costs (National Petroleum Council, 2019). Based on the information that has been provided in Table 8, it can be concluded that the National Petroleum Council (2019), differentiate between high (>95%) and low (<95%) purity streams based on the electrical energy requirements associated with amine adsorption, however, within these two categories of purity only a small differentiation has been provided. To delineate the differences in costs, Table 9 provides the converted CAPEX, OPEX excluding energy costs, and energy OPEX (or unit energy operating costs), for the same point sources (and medium/small coal and power plants) as depicted in Table 8 (these costs have been converted in Appendix B.8). Both the unit capital costs and the unit OPEX (non-energy), are given in low and high costs, which are developed with the intent to reflect differences in economies of scale between individual point sources (National Petroleum Council, 2019). According to the National Petroleum Council (2019), the unit capital costs (given a lifetime of 20 years) that have been provided in Table 9, are based on estimation for each reference plant within a facility type based on an assessment of historical studies, published industry experience, and insights from a wide range of industry. The non-energy unit OPEX consists of two major categories; annual fixed costs (taxes, insurance, overhead, general salaries) and semi-variable costs (major and minor repairs, maintenance and overhauls), and the energy costs have been explained in the discussion of Table 8 (National Petroleum Council, 2019).

From Table 9, it can be concluded that the cost differences between the various point sources with alternating exhaust stream CO_2 concentrations are primarily attributed to the unit capital costs and the non-energy unit OPEX. Moreover, the National Petroleum Council (2019), explains this by stating that the absorption of CO_2 occurs in a packed column. The diameter of this packed column is proportionally larger for dilute gas streams because more gas must move through the column for the same amount of CO_2. Additionally, they mention that the ducts and fans which are required to transport the gas to the packed column must be larger for more diluted streams. Due to the increase in equipment size (the packed column, ducts and fans), the unit capital costs for point sources with more diluted streams are higher. Based on the increasing equipment size, it could be expected that more electrical energy would be consumed. This difference is reflected between the high- and low-purity streams, however, within these categories there only exist small differences. This should be considered during calculations based on the numbers that have been provided.

Table 9 Capital and operating costs (non-energy and energy-related) for PCC at different types of point sources. Adapted from (National Petroleum Council, 2019).

Point Source of CO_2 Emission	**Unit Capital Costs 20-Year Life (low-high) (€/tonneCO_2)**	**Unit OPEX (non-energy) 20-Year Life (low-high) (€/tonneCO_2)**	**Unit Energy Operating Costs (€/tonneCO_2) (based on US$ 50/MWh)**	**Average Unit Total Cost 20-Year Life (€/tonneCO_2)**
Ammonia production plants	5.3 – 9.7	5.3 – 8.9	8.0	22.6
Natural gas processing plants	6.2 – 10.6	7.1 – 11.5	8.0	25.7
(Bio)Ethanol production plants	5.3 – 8.9	7.1 – 11.5	9.7	24.4
Steel and iron manufacturing plants	23.0 – 39.0	19.5 – 32.8	25.7	65.9
Hydrogen production plants	16.8 – 29.2	13.3 – 23.0	24.8	65.9
Cement production plants	15.1 – 25.7	19.5 – 32.8	24.8	71.4
Large coal power plants (>500 MW)	29.2 – 48.7	19.5 – 32.8	26.7	91.8
Large gas power plants (>500 MW)	30.1 – 51.4	25.7 – 43.4	27.5	102.8
Medium coal power plants (<360 MW)	47.8 – 80.6	31.0 – 52.3	23.0	128.9
Medium gas power plants (<360 MW)	50.5 – 84.1	41.6 – 70.0	23.0	146.1

Small coal power plants (<230 MW)	78.8 – 132.0	50.5 – 84.1	20.4	193.1
Small gas power plants (<230 MW)	81.5 – 137.3	66.4 – 111.6	20.4	218.8

Based on the average unit costs to capture a tonne of CO_2, that has been provided in Table 9, ideally, all CO_2 that is used in the CO_2ER supply chain originates from high-concentration point sources such as ammonia production plants, natural gas processing plants and ethanol production plants. However, industrial processes with high CO_2 concentrations in their exhaust gases commonly capture the CO_2 themselves and sell it to commercial markets. An example is provided by Haugen et al. (2017), who state that Yara International ASA, which is a company that produces ammonia, has been selling purified CO_2 to commercial markets for over 3 decades. Consequently, the more diluted CO_2 streams need to be considered as possible CO_2 feedstocks for the CO_2ER supply chain. Apart from the fact that the concentrated CO_2 streams are commonly captured by the emitter itself, the other point sources also contribute significantly more to the total CO_2 emissions. To address the contribution of the various point sources to the total amount of CO_2 that is being emitted, Figure 5 provides a combination of the average unit total cost to capture that has been provided in Table 9 and their respective quantity. The latter is based on data provided by the research of Badgett et al. (2022).

It must be noted that the total annual emissions that have been provided in Figure 5 are based on U.S. data, and according to Statista (2020), the total CO_2 emissions in the U.S. alone were 5.676 Mtpa in the year 2020. The sum of the individual CO_2 emissions by each point source that has been provided in Figure 5 is 2126 Mtpa. Based on these quantifications, approximately 37% of the total CO_2 emissions in the U.S. is emitted by the combined total of the point sources that have been depicted in Figure 5. For the EU (including the UK and Iceland) the total CO_2 emissions were estimated at 2.547 Mtpa in 2020 (Tiseo, 2022). Based on the assumption of a similar ratio of CO_2 emissions of point sources to the total CO_2 emission in the EU and the U.S., the total CO_2 emissions by point sources in the EU is estimated at 942 Mtpa in 2020. Additionally, state-of-the-art PCC technology has an average CO_2 capture efficiency of 90% (Yuan Wang et al., 2017). Based on this capture efficiency, “only” 1913 Mt-CO_2 can be captured per year based on the U.S. figures, and 848 Mt-CO_2 per year based on the EU figures.

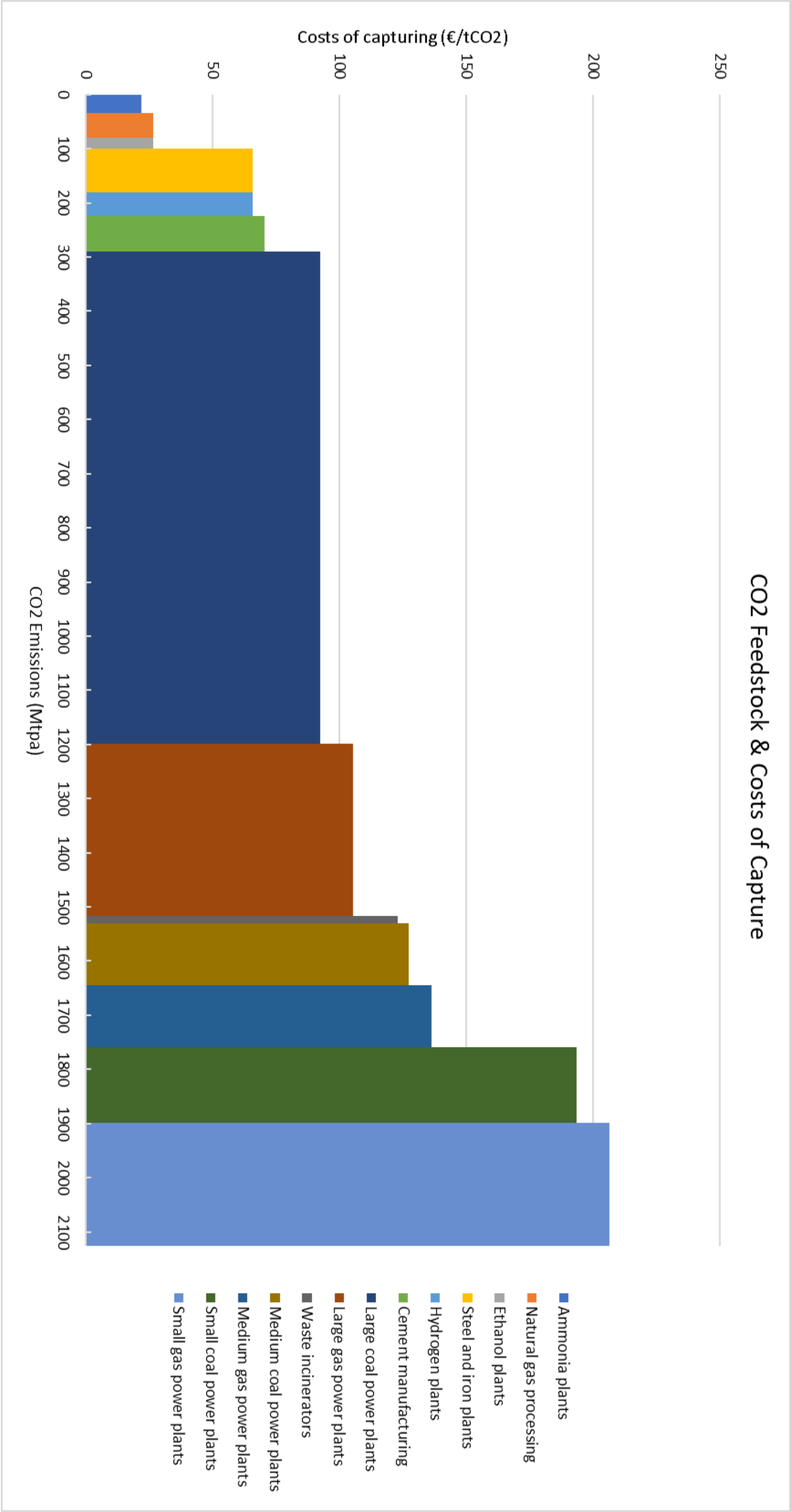

Figure 5 An overview of the costs to capture CO_2 from the various point sources that have been provided in Tables 7 and 8, and the quantification of their contribution to the total CO_2 emissions (CO_2 emissions quantity based on (Badgett et al., 2022)).

4.2.1.3 Theoretical and Practical Limitations of CO_2 Capture Processes

To provide a partial answer to the first sub-research question, this section aims to delineate the theoretical limitations associated with the CO_2 capture processes that could be used to provide the CO_2 feedstock within the CO_2ER supply chain. Firstly, the sizes (in terms of capturable CO_2) that have been found in the literature vary from 15 ktpa - 1 Mtpa for HT-DAC technology, and 24 ktpa – 3.329 Mtpa for PCC technology. However, the sizes for HT-DAC technology are based on technology by Carbon Engineering which is not commercially available yet, and the largest practical implementation size that has been identified in the literature is 900 tonnes per anum (based on solid DAC of Climeworks) (W. A. Smith et al., 2019). Additionally, according to Larson (2017), the largest CO_2 capture capacity at a single location (a 240-MW coal power plant) that utilises PCC technology is 1.4 Mtpa. Consequently, the theoretical limitations are not the state-of-the-art practical limitations for HT-DAC and PCC technology.

If HT-DAC is used as CO_2 capture technology, theoretically, the performance of an HT-DAC system with a capture capacity of 1 ktpa, varies little from the performance of a DAC system up to 1 Mtpa, with a capital cost per unit capacity that is nearly constant from 1 ktpa up to 100 ktpa, and decreases in per unit costs in a capacity range of 100 ktpa – 1 Mtpa (Keith et al., 2018). Consequently, DAC units follow the economies of scale function. Nevertheless, the calciner design (which is responsible for $CaCO_3$ formation and subsequently CO_2 release) is appropriate to an internal diameter of about 1 m, which corresponds to a 15 ktpa system, thus, a theoretically lower limit for annual capacity would be 15 ktpa. However, Carbon Engineering (2018) states that, given cost scaling, the smallest economically practical size for a complete DAC process unit is about 100 ktpa. Another important practical limitation of HT-DAC technology is that it requires high-temperature heat of around 900 ˚C. These heat requirements cannot be met by excess heat from industrial processes, consequently HT-DAC systems require an external heating source.

If PCC is used as a capture technology, its total annual capacity is mainly limited by the size and type of point source. From Figure 5 it can be concluded that the largest share of CO2 is emitted by coal plants, distantly followed by gas plants. For these point sources, CAPEX and OPEX decrease with increasing size. Consequently, it can be concluded that they benefit from economies of scale. As such, it is beneficial to primarily focus on capturing CO_2 via PCC, in large quantities from large point sources. Furthermore, according to Bui et al. (2018), the required surface for PCC units is approximately 600 times smaller than DAC units. Which leads to a required surface area for a 1 Mtpa PCC process of approximately 73 m^2. The required energy input of PCC processes is also dependent on the point source, nevertheless, when comparing the energy requirements of Table 7 and Table 9, it can be concluded that the energy requirements for PCC are indeed smaller than the energy requirements for DAC, with a factor in the range of 1.5-2.5, which corresponds to the findings of Ebbehøj (2015). Furthermore, the location of HT-DAC technology is theoretically not limited by any factor, whereas the usage of PCC technology creates an additional limitation in the sense that it must be located at a CO_2 point source.

4.2.2 The Conceptualisation of the Syngas Production Facility

To conceptualise the syngas production facility several aspects need to be considered. Moreover, in the CO_2ER supply chain, the location of the production facility is the location where the H_2O and CO_2 feedstocks are delivered at specific temperatures and pressures depending on the transportation means that have been used. Additionally, due to the limitations associated with syngas transportation that have been identified in Chapter 2, it is also the location of the syngas demand. Before the H_2O and CO_2 can be fed into the SOEC system, the temperature and pressure of the respective feedstocks must be adjusted. At the appropriate operating conditions, H_2O (g) and CO_2 (g) are electrochemically reduced to H_2 and CO. As already explained in previous sections, the ratio of H_2:CO plays an important role in the further usage of syngas. To this end, the syngas properties (such as HHV and density) and several calculations based on the ideal gas law have been provided in Appendix B.9. In this following section, the available sizes for HT-SOECs, their respective operating requirements, and their costs will be treated, resulting in the quantification of the production facility.

4.2.2.2 Conceptualisation of High-Temperature Solid Oxide Electrolyser

A single HT-SOEC is composed of a solid electrolyte, an anode and a cathode and between these two electrodes with catalytic active sites, ion species migrate (this migration results in the reduction of CO_2 to CO and the reduction of H_2O to H_2). To obtain a larger overall output, single cells are connected in series forming either planar or (flat) tubular stacks (Elder et al., 2015) (Bianchi & Bosio, 2021). Single cells are combined into stacks, since increasing the area of a single cell endlessly is not possible, mainly due to the difficulties associated with controlling the temperature over larger areas (Ebbehøj, 2015). Early HT-SOEC systems generally used tubular cells and stacks, since their geometry results in higher mechanical and thermal stability, and they are easier to seal than planar designs. However, as research on the topic continued, planar designs have been used more frequently, since they have much higher volumetric density and the current collection path is shorter than that of tubular designs, resulting in improved electrolysis performance (Elder et al., 2015).

The size of single cells and the size of stacks that are mentioned in the literature differ widely. Moreover, the research by Schreiber et al. (2020), uses an individual cell size of 10x10 cm, with an active area of 80 cm^2. Additionally, they specify that a system of 150 kW consists of two stacks with 120 levels each, with 8 cells per level which corresponds to a total of 960 single cells. Alternatively, Elder et al. (2015) mention a 15 kW integrated laboratory scale system, consisting of three modules, each module consists of four stacks and each stack consists of 60 cells with a single cell active area of 64 cm^2. Yet other research by Hauch et al. (2020), mention that the largest HT-SOEC demonstration plant is located in Salzgitter, Germany, and has a capacity of 40 Nm^3-H_2/hr (which is approximately 140 kW). This plant consists of six modules, each module containing 48 stacks and each stack consisting of 30 cells. Furthermore, a project that is being run by the EU has developed a 10 kW system with an associated energy consumption of 3.37 kWh/Nm^3 (Bianchi & Bosio, 2021). Unfortunately, they do not specify the single-cell area, nor the number of cells that constitute the entire system. From the literature, it can be concluded that both cell and stack sizes differ throughout the available research. According to Hauch et al. (2020), single cells often have an active area in the range of ~100 cm^2, however, cells with active areas of up to 550 cm^2 have been produced and demonstrated. Furthermore, they state that stacks typically contain between 30 and 100 cells, however, designs for stacks with 350 cells have been proposed. Increasing the active area, the number of cells in a stack and the number of stacks in a system all contribute to an increase in the possible output of HT-SOEC systems.

Having explained the possible configurations of HT-SOEC systems in terms of single cells and stacks, from now on forth, this section focuses on the size of the system, since this is directly related to the amount of syngas that can be produced and consequently also to the required quantity of feedstocks. Moreover, according to Bianchi & Bosio (2021), state-of-the-art HT-SOECs have a power capacity between 1 kW and 200 kW (the highest tested size). The average energy consumption that they report is 3.70 kWh Nm^{-3} (H2) and 3.44 kWh Nm^{-3} (CO), with a global process efficiency of 80-90%. However, much effort is dedicated to developing HT-SOECs on an industrial scale. An example of an industrial-scale HT-SOEC system that is currently being developed by the German company Sunfire, which produces electrolysers, is SYNLINK. The SYNLINK system is a 2890 kW HT-SOEC system for the co-electrolysis of CO_2 and steam (Sunfire, 2022). The operating parameters for the SYNLINK system and a 150 kW SOEC developed by Linde AG, which is described in the research by Schreiber et al. (2020), are shown in Table 10. Apart from the operating parameters in Table 10, estimations of the stack lifetime of the SYNLINK system have been provided, which is 40000 h in 2020 and 75000 h in 2030

(Posdziech, 2021). Additionally, the system requires an area of approximately 300 m^2. Schreiber et al. (2020), also provide an estimation of the lifetime of the 150 kW Linde AG system, which requires total cell replacement after 10 years (=87600 hours based on full load hours), which is based on the assumption of a degradation rate of 1%/1000hr (Schreiber et al., 2020).

Table 10 A comparison between the operating parameters of the SYNLINK system that has been developed by Sunfire, (2022), but is not yet in operation, and the system developed by Linde AG which is used by (Schreiber et al., 2020). The syngas density is based on the calculations provided in Appendix B.9.

	Sunfire (SYNLINK)	**Sunfire (SYNLINK) (at a molar ratio of 2 H_2:CO) (based on the ρ_{syngas} = 0.473 kg/m^3)**	**Linde AG**
Syngas production			
Net production rate	750 Nm^3/h	354.8 kg/h	16.8 kg/h
Production capacity dynamic range	5% - 100%	5% - 100%	-
Hot idle ramp time	<10 min	<10 min	-
Operating temperature	850 ˚C	850 ˚C	800 ˚C
Delivery pressure	1 bar	1 bar	20 bar
Available H_2:CO ratios	1.5 – 3.5	2	2
Power input & electrical efficiency			
System power rating (AC)	2890 kW	2890 kW	150 kW
Specific power consumption at stack level (DC)	3.4 kWh/Nm^3	7.19 kWh/kg	-
Specific power consumption at the system level (AC)	3.85 kWh/Nm^3	8.14 kWh/kg	8.82 kWh/kg
System electrical efficiency	82%	82 %	75%
Steam/H_2O input			
Consumption	560 kg/h (steam)	560 kg/h (steam)	19 kg/h (H_2O (l))
Temperature	150 ˚C – 200 ˚C	150 ˚C – 200 ˚C	-
Pressure	3.5 bar – 5.5 bar (gas)	3.5 bar – 5.5 bar (gas)	-
CO_2 input			
Consumption	730 kg/h	730 kg/h	23,2 kg/h
Temperature	0 ˚C – 40 ˚C	0 ˚C – 40 ˚C	-
Pressure	6 bar (g) – 8 bar (g)	6 bar (g) – 8 bar (g)	-

When comparing the operating parameters of the SYNLINK 2890 kW system, based on a ratio of 2 H_2:CO, with the operating parameters of the Linde AG 150 kW system, it can be concluded that the specific power consumption of the Linde AG system is slightly larger (approximately 8%) than the specific power consumption of the SYNLINK system. The SYNLINK system has a syngas delivery pressure of 1 atmp, whereas the Linde AG system has a delivery pressure of 20 bar. Additionally, the Linde AG system has a lower electrical efficiency than the SYNLINK system, the combination of higher delivery pressure and the lower electrical efficiency could explain the difference in power consumption. Additionally, it can be seen that the SYNLINK system has a higher operating temperature compared to the Linde AG system, consequently, it is expected that this would result in larger power consumption per kg of syngas produced. Another aspect that should be taken into consideration to explain the difference, is that Schreiber et al. (2020), mention that "*a complex fully heat integrated HT-co-electrolysis process at commercial scale, however, has not been built so far*", consequently, they do not consider heat integration, whereas a presentation of Sunfire on their electrolyser systems, states that the overall system efficiency is based on industrial off-heat integration via steam provision (Posdziech, 2021). Although some possible explanations have been provided for the differences, there remains a high degree of uncertainty which should be considered whilst interpreting results that are based on these quantifications.

Apart from the operating parameters and conditions, this section aims to quantify the costs of HT-SOEC systems in terms of their non-energy OPEX and CAPEX. Based on the literature that has been reviewed it can be concluded that there is no commonly agreed-upon quantification of the operating parameters of HT-SOEC systems nor of the CAPEX and OPEX of such systems. Nevertheless, a quantification must be provided. The most practical estimation for the system CAPEX is provided by Reytier et al. (2015), as they link system output to the CAPEX. Unfortunately, their estimations are based on an H_2 output and a system that operates at 700 ˚C, and therefore not suitable for this work. Alternatively, the research by Yao Wang et al. (2017) provides the CAPEX for HT-SOEC stacks, however, based on the varying number of stacks within HT-SOEC systems (e.g. 2 stacks in 150 kW system described by Schreiber et al. (2020) and 12 stacks in 15 kW system described by Elder et al. (2015)), such an estimation for CAPEX seems inappropriate. Consequently, this work will use the CAPEX estimation of € 2000/kW installed capacity, which has been provided by Hauch et al. (2020), which allows for the comparison of alternative HT-SOEC system sizes, based on the amount of installed capacity in kW. The non-energy OPEX of the HT-SOEC system can also be based on the information that has been provided by Hauch et al. (2020), who states that the OPEX consists of 70% of the electricity costs, consequently, the non-energy OPEX can be calculated based on the energy OPEX. This metric is selected since it allows the differentiation between non-energy OPEX and energy OPEX, which is in line with previous sections.

4.2.2.3 Theoretical and Practical Limitations of the Syngas Production Facility

To provide a partial answer to the first sub-research question, this section aims to delineate the theoretical limitations associated with the syngas production facility that is part of the CO_2ER supply chain. The output of the syngas production facility is limited by the size of the HT-SOEC system of which it consists. In turn, the size of the HT-SOEC system is determined by the number of single cells, stacks and modules. The literature does not mention any specific theoretical limitations, however, the largest active single-cell active area that has been produced and demonstrated is 550 cm^2, and stacks that consist of up to 350 single cells have been proposed. There is much effort dedicated to increasing the size of HT-SOEC systems, by researchers but more importantly also by commercial players. Nevertheless, the largest demonstration plant that is currently running utilises an HT-SOEC system of approximately 140 kW, designed for the production of H_2 (Hauch et al., 2020), and the highest tested size has a capacity of 200 kW (Bianchi & Bosio, 2021). For the lifetime of HT-SOEC systems, there is no specific limitation mentioned either. The literature indicates lifetimes of 40.000 hours up to almost 90.000 hours, however, state-of-the-art electrolyser technology is rather proximate to the lower limit than to the higher limit (Song et al., 2019).

4.2.3 The Conceptualisation of the Syngas Market

The conceptualisation of the syngas market will be based on two main aspects: the size of the market and the customers that constitute the market. The size of the market allows for determining the total possible demand for syngas, which can be used to assess the growth potential opportunities for syngas production via HT-SOEC systems. The customers identify the amount of syngas demand for a specific location, this can be used to assess the alternative configurations of decentralised and centralised supply chains. To this end, the available literature should be reviewed such that the market – size, growth, trends and forecast can be determined. Thereafter, it is important to further delineate the potential customers for syngas in terms of the quantity they require and the locations from which they operate.

4.2.3.1 The Syngas Market – Size, Growth, Trends and Forecast

According to Choe et al. (2022) (based on Inkwood Research, (2017)), the global syngas market shows a steady growth trend at a compound annual growth rate (CAGR) between 2017 and 2026 of 9.52%. In 2016, the global syngas market was estimated to be worth approximately US$ 140 billion, which corresponds to 133 GW of syngas (Inkwood Research, 2017). The stated CAGR leads to an expected market value of US$ 320 billion in 2026 (Choe et al., 2022), which corresponds to 330 GW of syngas (Inkwood Research, 2017). Moreover, in 2020 the global syngas market was estimated at a valuation of US$ 180 billion, and the European syngas market contributed approximately US$ 40 billion to the global market, which is approximately 22%. Taking into account the 2020 Euro-Dollar exchange rate, these numbers correspond to € 158 billion and € 35 billion respectively. The market research by Inkwood Research (2017), does not specify the market size in terms of GW of syngas for the year 2020, however, a rough estimation can be made by dividing the amount of syngas in 2016 (in GW) by its market value (in US$) and multiplying this number by the 2020 market value. Via this estimation the global market size of syngas in 2020, is estimated to be in the order of 191 GW of syngas, of which approximately 42 GW is devoted to Europe. Alternatively, another market research company, IMARC, also provide an estimation of the global syngas market. They state that the global volume for syngas demand was 308.8 GW in 2021 and they mention an expected market growth with a CAGR of 10.3% between 2022 and 2027, up to 574.5 GW in 2027 (IMARC, 2021). If it is assumed that the market also grew at a CAGR of 10.3% from 2020 to 2021, the market in 2020 would have an approximate size of 279 GW.

The market research company ReportLinker, also provide a report on the market – growth, trends, and forecast. They expect the market to grow at a CAGR of over 11% during the forecast period of 2022-2027 (ReportLinker, 2022). However, as opposed to the market research that has been done by IMARC and Inkwood Research, ReportLinker provides the market size in Millon metric normal cubic meters of syngas per hour (MM Nm^3-syngas/hr). They quantify the market in 2022 at 210 MM Nm^3-syngas/h. If it is assumed that the market also grew at a CAGR of 11% between 2020 and 2022, the market in 2020 would have an approximate size of 170 MM Nm^3-syngas/h. Although the market estimations and the associated CAGRs that have been mentioned in the other research provide valuable insights into the size of the market and its expected growth rate, they are complex to use in calculations since it is not clear how GW should be converted to quantification of syngas without assuming a specific production unit. Consequently, the metric that is provided by ReportLinker (2022) will be used for further calculations and based on their quantification, a visual representation of the market and its expected growth rate is provided in Figure 6. Nevertheless, to provide an overview of the various estimations, the specific market sizes have been provided in Figure A. 7 (in Appendix B.10).

Since the report by Inkwood Research (2017), is the only report that provides a quantification of the European market size compared to the global market size, the stated 22% is used to provide estimates of the European market size for the other research, including the research by ReportLinker (2022). This estimation for the European market is also provided in Figure 6.

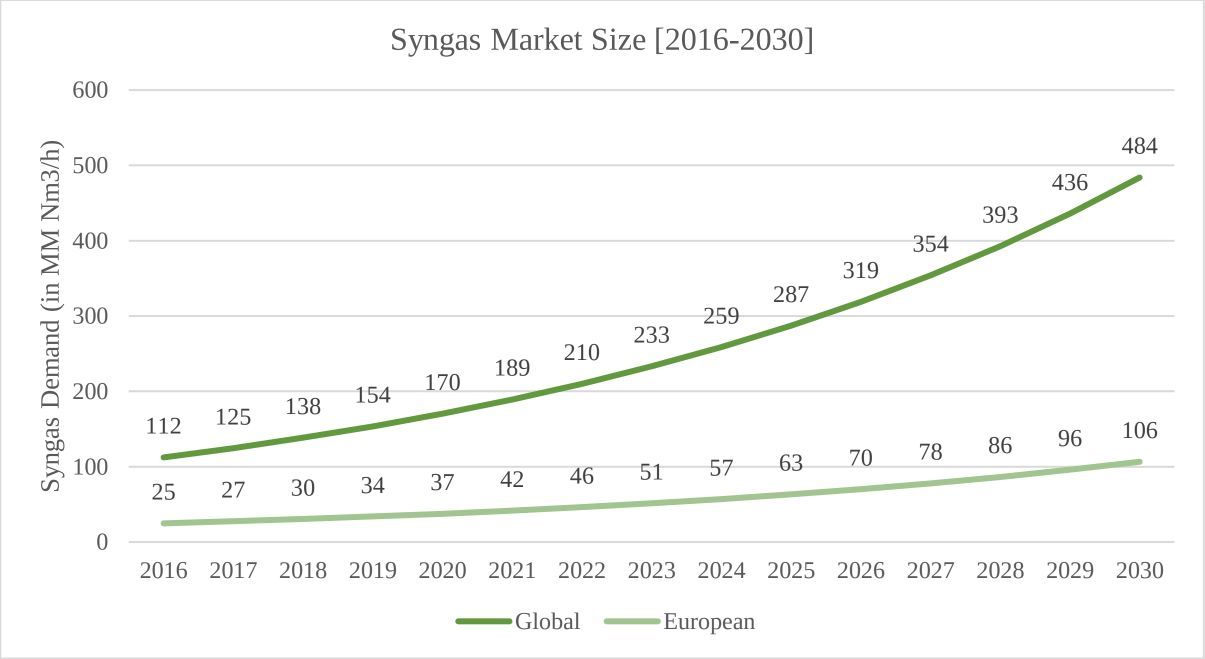

Figure 6 Estimated global/European syngas market size (in MM Nm^3-syngas/hr) based on the quantity and CAGR that is provided by ReportLinker (2022).

According to IMARC (2021), one of the key factors that drive market growth is the growing demand for syngas from the chemical industry. ReportLinker (2022), identify the growing demand for syngas from the power generation and chemical industries, the increasing awareness of consumers and government regulations on renewable fuel use, and the increasing demand of H_2 for the production of fertilizers as the key drivers of the expected market growth. This aligns with the research by Stratas Advisors, who identify that fertilizer production is expected to be the main factor that causes a steady growth rate in syngas demand in the coming few years (up to 2024), whereas methanol, SNG/gaseous fuels and liquid fuels will cause a steep increase in syngas demand in the years after 2024 (Posdziech, 2021).

4.2.3.2 The Syngas Market – Consumers, Quantity and Locations

The previous section already identified some of the key industrial players that contribute to the syngas market growth, this section will focus on the specific industrial consumers that constitute the syngas market. Both Inkwood Research (2017) and IMARC (2021) provide specifications on the capacity share based on the type of product that is being produced with syngas. The respective capacity shares have been provided in Figure 7.

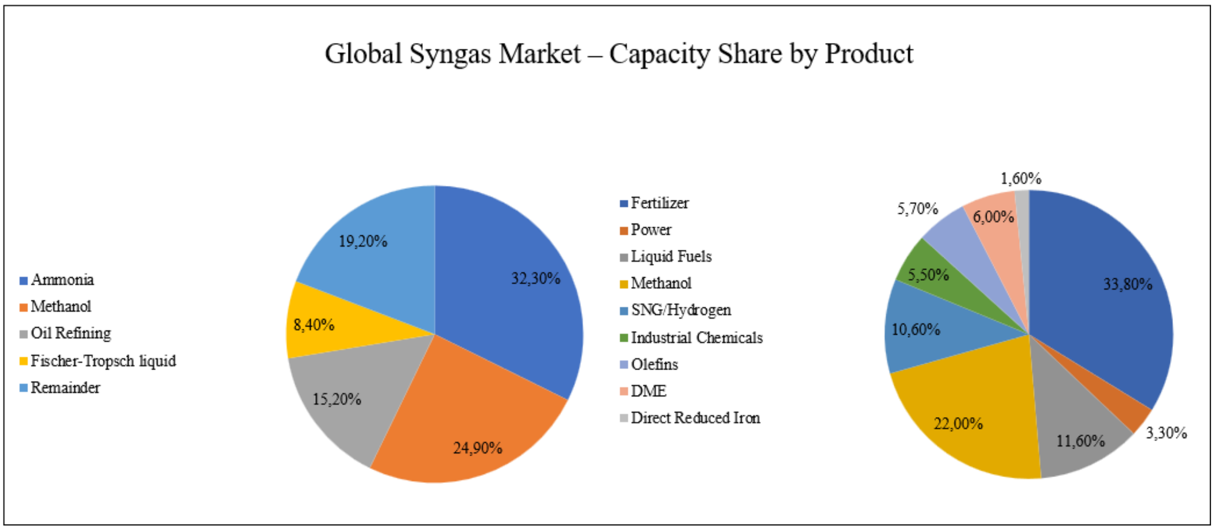

Figure 7 An overview of the capacity share of the products that are being produced with syngas. Based on Inkwood Research (2017) (left) and IMARC (2021) (right).

By combining the specific capacity share of a product, that has been provided in Figure 7, with the size of the global syngas market/the European syngas market, that has been provided in Figure 6, the total syngas demand for each specific product within a specific market can be calculated. This information could be used to determine whether the total demand for one specific product can be met by syngas produced by HT-SOECs.

However, instead of the syngas demand for a specific category of products, this work rather focuses on the estimation of the syngas demand of one specific location, since this determines the required size of the syngas production facility. An example of the demand of one specific location can be provided based on a methanol production facility that utilises syngas. A common production scale for a MeOH plant is 400 ktMeOH per year (Ebbehøj, 2015). Moreover, the production of methanol from syngas with a ratio of 2 H_2:CO has an efficiency of approximately 83%, which is determined by the exothermicity of the MeOH synthesis from syngas (W. A. Smith et al., 2019). Consequently, methanol production plants with a size of 400 ktpa require approximately 482 kt-syngas pa. Apart from the specific methanol example, the European Commission (2019a), indicates the required net output of a production facility, which should be at least 80 kg pure (2 H_2:CO) syngas/hr, to successfully substitute fossil-based syngas. Another important aspect of the syngas market that should be considered is that the production of syngas is commonly done by using fossil fuels, consequently, the price of syngas is highly dependent on the price of these fossil fuels (such as NG and coal). Nevertheless, Jouny et al. (2018), state that the market price for syngas is *US$ 0.06/kg-syngas*, which can be used as a reference price throughout this work.

4.2.3.3 Theoretical and Practical Limitations of the Syngas Market

To provide a partial answer to the first sub-research question, this section aims to delineate the theoretical and practical limitations associated with the syngas market that is part of the CO_2ER supply chain. By comparing the various market size estimations, it can be concluded that there is no commonly agreed-upon size of the current (2020) and future (2030) syngas market. Furthermore, although it has been identified that a syngas ratio of 2 H_2:CO is deemed optimal for various industrial applications, the various products that have been provided in Figure 7 might require alternative ratios. Consequently, the theoretical assumption that the size of the syngas market is based on a 2 H_2:CO ratio, is not a real practical limitation. Furthermore, since this work excludes the possibility of syngas transportation, another limitation is that the syngas demand locations must be at the same location as the syngas production facility. Additionally, only one price indication for syngas, of US$ 0.06/kg-syngas has been provided by Jouny et al. (2018).

4.3 Matching Scales of the CO_2ER Supply Chain Units

This section aims to provide an answer to the first sub-research question by combining the theoretical and practical limitations that have been found in the previous sections and investigating whether their combination opposes any additional limitations for the supply chain as a whole via *back-of-the-envelope calculations*. To this end, an overview of the limitations opposed by the various supply chain units is provided in Appendix B.11. To investigate whether the combinations of limitations that have been delineated oppose any additional limitations or constraints to the CO_2ER supply chain from a system perspective, both the supply chain requirements for the smallest (single location) and largest (global market) syngas demand are calculated. As such, the scales of the individual supply chain units are matched and compared with the theoretical and practical limitations.

4.3.1 Global Scale-Match

To assess whether the various supply chain units can be matched to meet the syngas demand on a global scale, the quantification of the global syngas market in 2020 that has been provided in Figure 6 will be used. The quantification of the global syngas market corresponds to an annual demand of 1489 Billion Nm^3-syngas. In this work, a syngas ratio of $2H_2$:CO is used and based on the calculations in Appendix B.9, the produced syngas has a density of ρ_{syngas} = 0.473 kg/m^3 (at STP). By multiplying the global annual demand by the calculated ρ_{syngas}, the annual syngas demand (in tonnes) is calculated at 704 Mtpa. To quantify the requirements to meet this demand, the SYNLINK (2890 kW) and Linde AG (150 kW) systems that have been specified in Table 10 (section 4.2.2.2) will be used. Based on the syngas demand and the specific operating parameters of these systems, the feedstock requirements, the required DAC surface area, the required RE input for conversion, and the required number of HT-SOEC systems can be calculated. To calculate the stated requirements several assumptions have to be made. The assumptions and calculations are provided in detail in Appendix B.12 and the quantified requirements are provided in Table 11.

Table 11 Comparison of the requirements of two SOEC systems for global syngas demand.

Requirements	SYNLINK	Linde AG
Global Syngas Demand	704 Mtpa	704 Mtpa
Required CO_2 Feedstock	1450 Mtpa	972 Mtpa
Required H_2O Feedstock	1111 Mtpa (g)	796 (l) Mtpa
DAC surface area	64 km^2	43 km^2
# of DAC units required	1.6 million	1.1 million
RE input for annual conversion	5.73 PWh	6.21 PWh
# HT-SOEC systems required	226509	4783649

By comparing the CO_2 requirements with the total amount of capturable CO_2 in the U.S. alone (1913 Mtpa based on capture efficiency of 90%) that has been provided in section 4.2.1.2, it can be concluded that the global syngas demand can be easily met by the total amount of capturable CO_2 from point sources in the *U.S. alone*.

To provide a context for the water requirements; the annual requirement of 1111 Mt is approximately 5.4% of the annual water requirement for the global green hydrogen economy that was calculated by Beswick et al. (2021); 20.5 Gt-freshwater per year, and they claimed that there was abundant water availability to meet these requirements. Furthermore, if the CO_2 feedstock is to be delivered by DAC technology, 1.6 million DAC units are required to deliver the required CO_2 feedstock for the SYNLINK system. According to Budinis (2022), there are currently 18 DAC units (of small scale) in operation. Consequently, the mismatch can easily be identified.

Furthermore, Keith et al. (2018), identified the operation of HT-DAC units (by Carbon Engineering) requires 4.7 tonnes of H_2O per tonne of captured CO_2. As such, the usage of HT-DAC technology in combination with SYNLINK systems to meet the global syngas demand would result in an additional water requirement of approximately 6.82 Gtpa. Combining this quantification with the water requirement for the conversion process results in approximately 39% of the water requirement for the green hydrogen economy, which is significant.

To deliver global syngas demand, Table 11 identifies that for conversion alone, an electrical energy input of 5.73 PWh is required. To meet these requirements a continuous power source with a capacity of approximately 654 GW is required. Comparing this with the global installed capacity of RESs, which was 3068 GW in 2021 (Statista, 2022), it can be concluded that, for conversion alone, almost 22% of the globally installed RES capacity is required to meet global syngas demand. Additionally, this requires 226509 SYNLINK systems, whereas there are currently 0 in operation.

4.3.2 Local Scale-Match

To assess whether the various supply chain units can be matched on a local scale, the minimum syngas production requirement of 80 kg/hr will be used. This requirement has been provided by the EC and was mentioned in section 4.2.3.2. The production of 80 kg syngas/hr corresponds to an annual production of 701 tonnes of syngas. The requirements to meet this demand (based on the systems that have been specified in Table 10) have been provided in Table 12.

Table 12 Comparison of the requirements of two SOEC systems for local syngas demand.

Requirements	SYNLINK	Linde AG
Local Syngas Demand	701 tpa	701 tpa
Required CO_2 Feedstock	1441 tpa	968 tpa
Required H_2O Feedstock	1106 tpa (g)	793 tpa (l)
DAC surface area	63.5 m^2	42.6 m^2
# of DAC units required (calculated value)	2 (1.59)	2 (1.07)
RE input for annual conversion	5.71 GWh	6.18 GWh
# SOEC systems required (calculated value)	1 (0.23)	5 (4.76)

By comparing the CO_2 requirements with the specific quantity of CO_2 that can be captured from the smallest and largest point sources that have been provided in Table 7 (24 ktpa/3.324 Mtpa), it can be concluded that for the smallest point source (an NG processing plant) only 2.9% of the capturable CO_2 is required to meet the local demand, whereas for the largest point source (a steel and iron manufacturing plant) only 0.02% of the capturable CO_2 is required to meet the local demand. As such, these requirements can easily be met, however, there is a mismatch in scales. Alternatively, when considering HT-DAC technology, an approximate capture surface area of 43 m^2 is needed if Linde AG systems are used. Which is almost equal to the 40 m^2 DAC unit that has been used as a reference size.

In the previous section, it has been identified that the usage of HT-DAC technology does impose additional H_2O requirements. Based on the required quantity of CO_2 for the Linde AG system, these additional H_2O requirements are approximately 3727 tonnes (or m^3) per year, resulting in a total water requirement of 4520 tonnes per year. To provide a context for these water requirements; households of 3 up to 4 people living in Amsterdam use between 145.000 and 191.000 litres of H_2O per year, which corresponds to approximately 145 – 191 tonnes per year (Waternet, 2022). Consequently, a syngas production facility that produces 80 kg of syngas per hour and uses HT-DAC capture technology, consumes approximately 27 times more than an average household of 3-4 people in Amsterdam.

To deliver the local yearly syngas demand, Table 12 identifies that for conversion alone, an annual energy input of 6.18 GWh is required. To place this number into context; households of 3 up to 4 people living in the Netherlands have an average annual electric energy consumption of 3655 kWh in 2022 (Nibud, 2022). Consequently, a small-scale syngas production facility requires approximately 1691 times more electrical energy (for conversion alone) than a single household.

4.3.3 Delineating the Theoretical and Practical Limitations

This section concludes Chapter 4 by synthesizing the most important information that has been found to formulate a concrete answer to the first sub-research question; "*What are the theoretical and practical limitations of a HT-SOEC CO_2ER supply chain focused on producing syngas?*".

Based on the global scale-match that has been provided in section 4.3.1 it can be concluded that the amount of CO_2 that is available from point sources in the U.S. alone is sufficient to meet the CO_2 feedstock that is required to produce the global syngas demand via HT-SOEC technology. As such, if the CO_2 feedstock is to be delivered by PCC technology, it does not oppose any additional limitations apart from the required purity and quantity demanded by a specific location. Nevertheless, in section 4.3.2 which focuses on the local scale-match, it has been identified there exists a mismatch between the quantity of CO_2 that can be captured from point sources and the CO_2 demand of a local-scale syngas production facility. Consequently, a practical limitation that can be identified, is that the combination of PCC as technology for CO_2 feedstock and small-scale syngas production is not a good match. Furthermore, the consideration of HT-DAC as a technology to deliver the required CO_2 feedstock to meet global syngas demand delineated several practical limitations, the most prominent can be identified as the lack of capacity (i.e. quantity and scale of systems), the massive increase in H_2O requirements, and the high-temperature heat requirements. Based on these limitations it can be argued that the usage of HT-DAC, as a technology to deliver the CO_2 feedstock required for global syngas demand, is a mismatch. However, the almost perfect match between CO_2 requirements for local syngas production and the required quantity of HT-DAC units to meet these requirements delineates the potential for the technology at smaller scales. However, also at smaller scales, the opposed H_2O requirements and high-temperature heat requirements remain significant. Consequently, a practical limitation that arises when HT-DAC technology is used, is the need for abundant availability of an H_2O feedstock and an additional high-temperature heat supply. Additionally, the electrical energy requirements delineate the need for the availability of abundant RES.

The lack of syngas infrastructure and the lack of literature that is available on the topic make it both a prominent practical and theoretical limitation of the HT-SOEC CO_2ER production process that produces syngas. Moreover, some of the research on the topic does identify that the transportation of syngas is possible with an H_2:CO_2 ratio of at least 3 (Ridjan et al., 2013). Such a ratio would require additional purification processes at the demand location. Nevertheless, no further information exists on this topic. The consequences of this limitation are significant since it requires the production facility to be close to the demand location. Additionally, there is also a lack of information available on the storage of syngas. Consequently, a practical limitation is that the syngas should be used directly. Whereas the transportation of syngas opposes significant limitations, sections 4.1.1 and 4.1.2 (on CO_2 and H_2O quantification) rather delineated several opportunities. Moreover, the literature identified that, in theory, HT-SOECs do not require the processing of seawater due to their characteristic high operating temperatures (>800˚C). Additionally, the various CO_2 transportation means and the economic preference associated with the quantity and distance of CO_2 transportation identify the potential for matching scales on both local and global scales for CO_2ER supply chains.

Chapter 5

Analysis of the Horizontal Supply Chain

This Chapter aims to answer the second sub-research question of this work; "*How do different supply chain units influence the performance of decentralised and centralised supply chain configurations and which supply chain units have the highest impact when comparing these configurations?*". The methodology that will be used to answer this question has been identified in Chapter 3, and consists of two core elements; (i) calculating and comparing the simple payback period of alternative configurations and (ii) determining the influences of individual supply chain units. Additionally, the vast amounts of cost quantifications that have been found in Chapter 4 require some categorization. Consequently, section 5.1 will focus on delineating quantifications of the supply chain units. Thereafter, section 5.2 addresses the first element and section 5.3 addresses the second element and concludes by providing an answer to the second sub-research question.

5.1 Selection of Parameters for Analysis

To estimate the simple payback period for alternative supply chain configurations and assess the influence of individual supply chain units on the total costs of the supply chain, several assumptions have to be made. The set of parameters that will be considered in the economic analysis of this work, and their quantification, are provided in Table 13. The selection of these parameters and several additional assumptions that are required are further explained below.

Table 13 The assumptions that will be used to calculate the simple payback period for alternative supply chain configurations.

Parameters	Quantification	References
Electricity price	€ 0.068/kWh	(Statista, 2022b)
Syngas selling price	€ 0.053/kg	(Jouny et al., 2018)
Production facility operating time	350 days/year	(Jouny et al., 2018)
Electrolyser operating parameters	SYNLINK (Table 10)	(Sunfire, 2022)
CO_2 price: HT-DAC	Carbon Engineering (Table 7)	(Keith et al., 2018)
CO_2 price: PCC	Steel & iron manufacturing plant (Table 8 & Table 9)	(National Petroleum Council, 2019)
CO_2 price: transportation	Onshore transportation (Table 4)	(Psarras et al., 2020)
H_2O price	Dutch water supply network (Figure 4)	(Waternet, 2022)

It is assumed that the *electricity price* that has been provided in Table 13 corresponds to electricity that originates from RES. Moreover, according to Jouny et al. (2018), who use an electricity price of 0.05 US$/kWh, the price of renewable electricity could become as low as 0.02 US$/kW (~0.018 €/kW). Based on their research, the assumed electricity price is rather high. However, the stated price of 0.068 €/kWh corresponds to another geographic location and another year (the Netherlands (2020) versus the U.S. (2018)), which explains the differences. Nevertheless, based on research by Jouny et al. (2018) lower electricity prices could be taken into consideration. Apart from the price of electricity, it is assumed that there is abundant continuous RE available, and varying load hours will not be taken into consideration. The *syngas selling price* that has been provided in Table 13 is provided by Jouny et al. (2018) and was first mentioned in section 4.2.3.2. It must be noted that no other syngas reference prices were found. Most likely because, at the current stage, syngas is being produced by fossil-based production processes, such as NG reforming, and consequently, the price of syngas is highly related to the price of NG (Pei et al., 2016). Additionally, section 4.2.1.2 identifies that point sources with a high exhaust outlet concentration of CO_2, generally capture and utilise this CO_2 themselves. Consequently, if the CO_2 is used for syngas production which is used by the emitter itself, no selling prices for syngas will be provided. The *production facility operating time* of 350 days per year is based on the research by Jouny et al. (2018), who validate this operating time based on an annually required 2 weeks of downtime for maintenance of the electrolyser. Furthermore, it is assumed that the production facility operates 24 hours per day. The *electrolyser operating parameters* are based on the SYNLINK system. The reason for selecting the SYNLINK system primarily relates to the fact that it requires less energy during operation, due to its higher system efficiency (82% versus 75% for Linde AG). The literature that has been reviewed in section 2.1.4 identified that electricity costs are frequently mentioned as the biggest cost contributor for a CO_2ER process that relies on HT-SOEC technology (M. Li et al., 2021) (M. Y. Lee et al., 2020). Quantification of the electricity requirements to meet global syngas demand, which has been provided in section 4.3.1 endorse these claims. Consequently, selecting the electrolyser system with the “smallest” electricity requirements makes sense. Nevertheless, it must be noted that the SYNLINK system operating parameters are based on heat integration for the provision of steam. This should be taken into consideration whilst interpreting the results that are based on calculations with the SYNLINK system. Apart from the operating parameters, the CAPEX and OPEX estimations that have been provided by Hauch et al. (2020) will be used. The *CO_2 price* is dependent on the type of capture technology that is being used for the provision of CO_2 feedstock and the transportation mean, distance and quantity of CO_2 that must be transported. Section 4.2.1 identified two possible technologies that can be used for the provision of CO_2 feedstock. If this feedstock is captured by *HT-DAC technology*, the costs of capturing will be based on Carbon Engineering HT-DAC technology that has been quantified by Keith et al. (2018), since their quantification allows for the differentiation of CAPEX for alternative system sizes. If the feedstock is captured by *PCC technology*, it is assumed that the point source is a steel & iron manufacturing plant. Based on the information that has been provided in section 4.2.1.2, which identifies steel & iron manufacturing plants are the cheapest “low concentration” point source (apart from hydrogen production plants that use syngas to produce hydrogen) to which PCC technology can be applied, the costs for CO_2 capture and processing will be based on the cost quantifications for steel and iron manufacturing plants that have been provided in Table 9. The cost of *CO_2 transportation* will be based on land transportation (i.e. no ships or offshore pipelines will be included) and the economic preferences that have been provided in section 4.1.1.2 (trucks for quantities < 300 ktpa, onshore pipelines for quantities > 300 ktpa (Psarras et al., 2020)). Finally, the *H_2O* price that will be used is based on the information provided by Waternet (2022). This price is selected since it allows for the differentiation of costs related to the quantity of consumption, and the price is validated in section 4.1.2.1 as a representative price for a larger geographic region (the EU).

5.2 Economic Analysis of Simple Payback Period

The previous section provided the argumentation for the selection of the parameters that are required to calculate and compare the *simple payback period* for alternative supply chain configurations. However, a specification of these alternative supply chain configurations also needs to be provided. Consequently, section 5.2.1 aims to delineate the specific centralised and decentralised supply chain configurations that will be analysed. Hereafter, the simple payback period of these alternative configurations will be calculated and analysed in section 5.2.2.

5.2.1 Delineating Supply Chain Configurations

Although further processing of syngas is outside the boundaries of this work, a somewhat realistic case for the analysis is desirable. To this end, a common production scale for a MeOH production process will be used as a reference point. According to the information that has been provided in section 4.2.3.2, a common scale for such a production process is 400 kt-MeOH per year (Elder et al., 2015). Moreover, based on the efficiency of MeOH production from syngas (which is 83%), a syngas feedstock of 482 ktpa is required. This capacity will be used as a reference for the centralised supply chain configuration. To assess the trade-offs and limitations between centralised and decentralised supply chains, for the decentralised supply chain configuration, it is assumed that there are 5 smaller sized MeOH production processes, each with an annual capacity of 80 ktpa, resulting in a demand of 96.4 kt-syngas per year. A schematic representation of the alternative configurations has been provided in Figure 8.

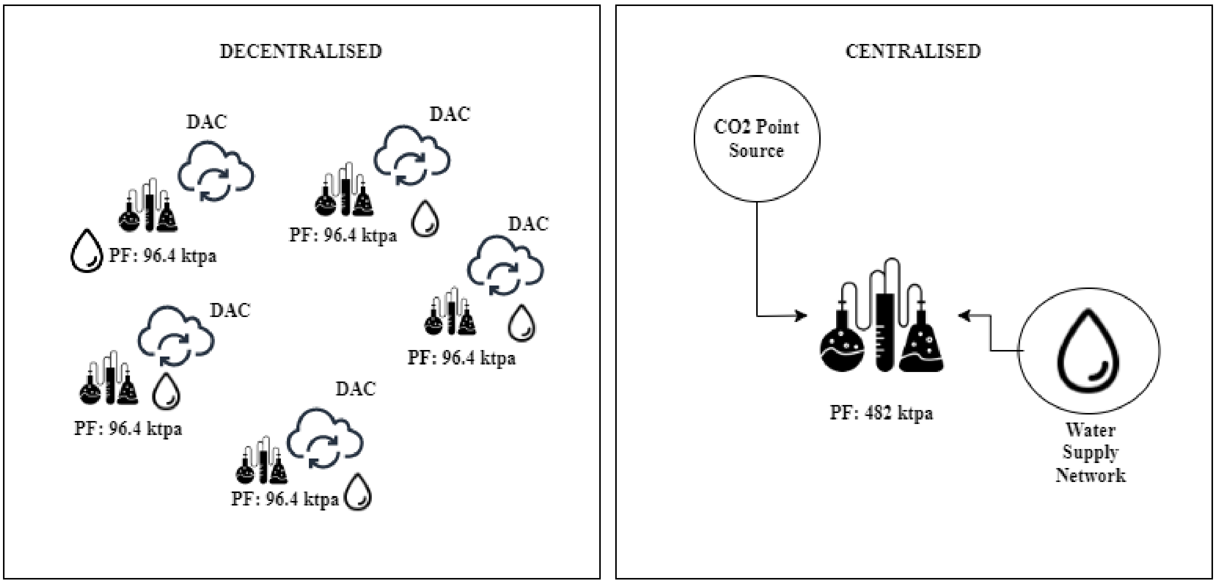

Figure 8 The centralised and decentralised supply chain configurations that will be analysed.

Due to the modular nature of DAC technology, in a decentralised configuration, the CO_2 feedstock is assumed to be supplied by HT-DAC technology, which is close to the production plant, eliminating the need for CO_2 transportation. Additionally, since both electrolyser technology and HT-DAC technology are portable, it is assumed that there are *free-of-charge* H_2O feedstocks at the production facilities. For the centralised configuration, the CO_2 feedstock is captured at a steel and iron manufacturing plant (as has been identified in the previous section), and according to the information that has been provided in Table 8, up to 3324 kt-CO_2 per year can be captured at the provided reference size steel and iron manufacturing plants. This quantity is sufficient to provide the required CO_2 feedstock[8] for the centralised production facility, however, in section 5.3 this work also aims to identify the influence of individual supply chain units, including the transportation of CO_2. To address this aspect, a supply chain in which CO_2 is captured and transported from a point source to the production facility will be taken into consideration. If the transportation of CO_2 is taken into consideration, a transportation distance of 160 km will be used, since this allows the comparison of the transportation means that have been quantified by Psarras et al. (2020).

5.2.2 Comparing Alternative Supply Chain Configurations

To provide an estimation of the *simple payback period*, an Excel spreadsheet was developed and the most important calculations have been provided in Appendix C.1 and C.2. The simple payback period can be calculated based on Equation (i) which was described in Chapter 3, and provided again below.

---

[8] The required CO_2 feedstock for the centralised configuration is calculated using SYNLINK operating parameters: 482 kt-syngas pa * (730 kg-CO_2/h [CO_2 feedstock for SYNLINK system] / 354.8 kg-syngas/h [production capacity of SYNLINK system] = 992 kt-CO_2 pa.

(i) Simple Payback Time $= \frac{Total\ Investment}{Average\ Annual\ Cashflow}$

According to Towler & Sinnott (2022), the total investment is the sum of fixed CAPEX (i.e. investments in plants), and the average annual cash flow is the annual net income from the operation. The latter can be calculated by subtracting the OPEX from the revenue of selling the produced syngas (as can be seen in Equation (viii)). To calculate the simple payback period, the *point of view of the production facility* is considered. From the production facility perspective, the costs for the CO_2 feedstock and H_2O feedstock are considered non-energy OPEX for the centralised configuration (as can be seen in Equation (ix)). However, for the decentralised configuration, the CAPEX for HT-DAC units are attributed to the total investment (as can be seen in Equation (x)). Based on the explanation that has been provided for the various cost-attributes that need to be considered for the calculation of the simple payback time, Appendix C.1 and C.2 provide the calculations for the electrolyser CAPEX, the HT-DAC CAPEX, non-energy OPEX, the energy OPEX and the revenue for selling syngas based on the alternative configurations.

(viii) Average Annual Cashflow $= Revenue - Total\ OPEX$

(ix) Total Investment (C) $= CAPEX\ Electrolyser$

(x) Total Investment (D) $= CAPEX\ Electrolyser + CAPEX\ DAC$

The results of the calculations for the average annual cash flow and the total investment have been provided in Figure 9, in which D1 represents the quantification for a single production facility within the decentralised supply chain, D2 represents the quantification for the combination of the five production facilities in the decentralised configuration, C1 represents the quantification of the centralised supply chain in which CO_2 transportation costs are excluded, and C2 represents the quantification of the centralised supply chain in which CO_2 transportation costs (via onshore pipelines) are included. The calculations and assumptions for these calculations have been provided in detail in Appendix C.1 for the decentralised configuration and C.2 for the centralised configuration.

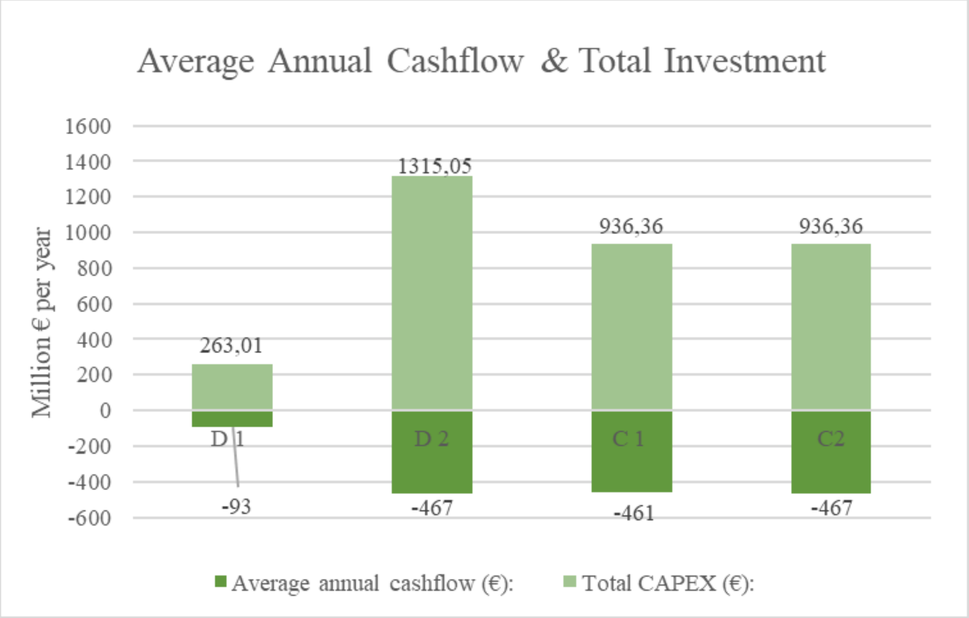

Figure 9 The calculated average annual cash flow and the total investment of D1, D2, C1 and C2.

From Figure 9, it can be concluded that the average annual cash flow is highly negative. Consequently, there will not be a payback time. Nevertheless, Figure 9 does provide some valuable insights into the possibilities of alternative configurations. Moreover, based on the possible advantages of centralised and decentralised supply chains that have been provided in Table 1 and Table 2 respectively, and the quantifications that have been provided in Figure 9, it can be concluded that in a decentralised configuration production facilities can be added gradually, resulting in smaller initial CAPEX (~ 28% of centralised) requirements, even considering the investment in two HT-DAC plants (of 98 ktpa and 100 ktpa respectively) for the provision of the CO_2 feedstock. When comparing the two configurations based on an equal capacity of 482 kt-syngas per year, it can be concluded that the total CAPEX for the decentralised configuration is approximately 40% higher, whilst the average annual cashflow is only 1% higher than in a centralised supply chain that does not include CO_2 transportation and equal in a centralised configuration that does include CO_2 transportation costs. Additionally, an interesting finding is that there are 162 SYNLINK systems required for the centralised configuration, whereas the total SYNLINK units required for five decentralised production facilities are 165. Consequently, given the specified production capacity and the assumption of using SYNLINK systems, it can be concluded that in the centralised configuration the demand can be met with lesser systems. This emphasizes the need for varying electrolyser system sizes for the operation of decentralised configurations, as alternative sizes allow them to meet the demand more precisely. Furthermore, In section 5.1 it has been identified that the selected electricity price is rather high. Consequently, similar calculations were made based on an electricity price of 0.018 €/kWh (which was provided by Jouny et al. (2018)), the results of these calculations have been provided in Figure A. 8 (in Appendix C.3). From Figure A. 8, it can be concluded that, given an optimistic electricity price, all of the specified supply chain configurations are not capable of generating a positive net income. This emphasizes the need to investigate the influence of individual supply chain units on the total costs of the supply chain, which will be done in the next section.

5.3 Economic Analysis of Influence of Supply Chain Units

To determine the influence of each supply chain unit on the total costs of the supply chains, the annual costs for each of the units are calculated and compared. Section 5.3.1 focuses on analysing the influence of the individual supply chain units in a decentralised configuration and section 5.3.2 focuses on a centralised configuration. Finally, based on the information that has been found, section 5.3.3 aims to provide a concrete answer to the third sub-research question.

5.3.1 Influence of Supply Chain Units in Decentralised Configuration

To analyse the influence of the individual supply chain units in a decentralised configuration, Figure 10 depicts the calculated CAPEX and OPEX of a single production facility.

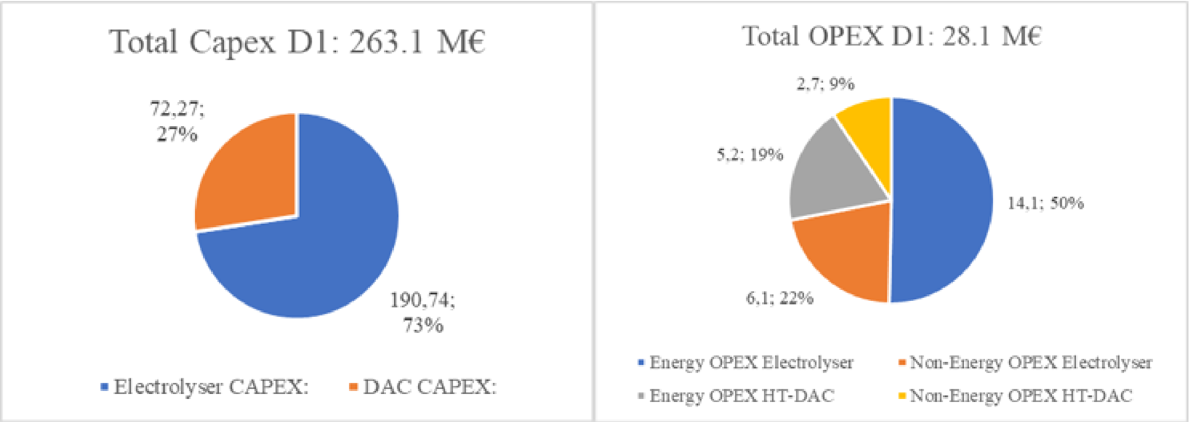

Figure 10 The total CAPEX and OPEX and the percentage shares of the individual supply chain units of a single decentralised production facility.

From Figure 10, it can be concluded that 73% of the total CAPEX is related to HT-SOEC investment and the remaining 27% is related to the HT-DAC investment. Based on the literature that has been reviewed, at the current stage, HT-SOECs only display a lifetime of 4.5 years (Posdziech, 2021). Consequently, if the total CAPEX is depreciated over the system lifetime, HT-SOECs cost roughly 42.4 Million €/year. Even taking into account the expected lifetime in 2030, which was estimated at 8.5 years (Posdziech, 2021), HT-SOECs would still cost 22.4 Million €/year. These substantial costs indicate the need for improving system lifetime, but also reducing the overall costs of the technology. Alternatively, HT-DACs have an estimated lifetime of 25 years, and if the total CAPEX is depreciated over the system lifetime, the costs would be “only” 2.9 Million €/year.

By analysing the total OPEX and the percentage shares of the individual supply chain units, it can be concluded that the combined energy OPEX account for approximately 70% of the total OPEX, with an annual cost of approximately 19.3 Million €. Given that the annual revenue for the quantity of syngas that is being produced at a single decentralised location is approximately 5.1 Million €/year, the need for substantially lower electricity prices is endorsed. Nevertheless, even if the electricity price would drop to zero, a single decentralised production facility would still not be able to generate a net income, since the non-energy OPEX, which accounts for a total of approximately 8.8 Million €/year, are higher than the annual revenue. The latter stresses the need for a higher market price for syngas or investigating the economics for further processing into products with higher market prices.

5.3.2 Influence of Supply Chain Units in Centralised Configuration

In the centralised supply chain, the CAPEX solely consists of the investment in HT-SOECs, which accounts for a total of roughly 936 Million €. Since there is not much to investigate in terms of CAPEX, this section will look into the influence of each of the OPEX cost-attributes, which have been provided in Figure 11.

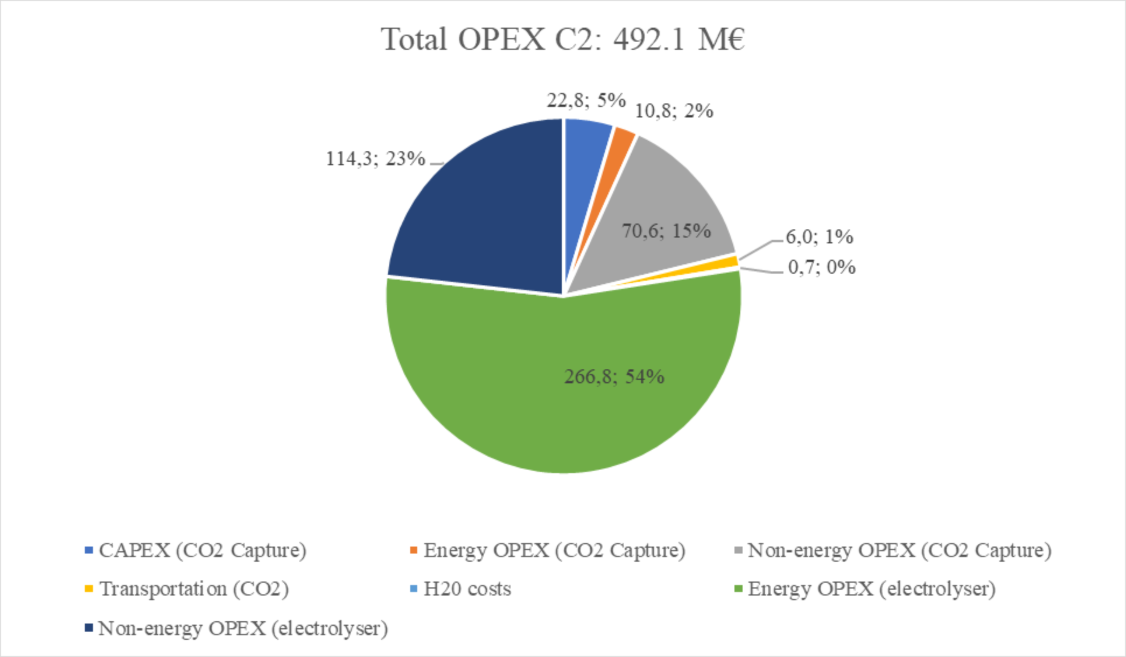

Figure 11 The total OPEX and the percentage shares of the individual supply chain units in a centralised supply chain configuration.

From Figure 11, it can be concluded that the combined energy OPEX account for approximately 56% of the total OPEX, the combined OPEX for feedstock acquisition (total costs for CO_2 feedstock plus the costs for the H_2O feedstock) accounts for approximately 21% of the total OPEX, and the non-energy

OPEX of the electrolyser account for 23% of the total OPEX. Based on these percentage shares it can be concluded that compared to the decentralised configuration, in the centralised configuration the energy OPEX is also responsible for the majority share of the operating cost. Furthermore, the total annual revenue that can be made by selling the produced syngas is calculated at 25.5 Million € and based on Figure 11, it can be concluded that the annual non-energy OPEX is 208.4 Million € per year. Consequently, even if electricity costs would be zero, the investigated supply chain would not be able to generate a net income. Additionally, it can be concluded that the transportation cost of CO_2 accounts for 1% of the total OPEX. The selected transportation means is an onshore pipeline, if trucks would be used these costs would be approximately double, nevertheless, compared to the cost contribution of other supply chain units, the costs for transportation of CO_2 do not have a prominent role in the supply chain that has been investigated.

5.3.3 Delineating the Influence and Performance of Alternative Supply Chain Configurations

After having explored the economic performance of alternative supply chain configurations and the influence of the individual supply chain units that constitute these supply chains, a concrete answer to the third sub-research question; "*How do different supply chain units influence the performance of decentralised and centralised supply chain configurations and which supply chain units have the highest impact when comparing these configurations?*" can now be provided.

It must be noted that this work only considered a specific supply chain, hence the results that have been found are not representative of all CO_2ER supply chains, and are merely an indication of the costs, based on back-of-the-envelope calculations. Nevertheless, some valuable insights have been obtained, which allow answering the third sub-research question. It can be concluded that the HT-SOEC has the largest influence on both a decentralised and centralised supply chain configuration. The CAPEX for HT-SOEC constitutes the majority share of the CAPEX in the decentralised configuration and is considered the sole contributor to CAPEX in the centralised configuration. Additionally, in both configurations, the energy OPEX for HT-SOEC operation constitute over 50% of the total OPEX. However, when comparing both configurations it can be seen that the energy OPEX is substantially lower in centralised configurations. This can be explained by the fact that the energy OPEX of HT-DAC technology is almost twice the energy OPEX of PCC technology, identifying the impact of HT-DAC systems on the total supply chain.

Chapter 6

Exploring and Analysing the Vertical Supply Chain

This Chapter aims to answer the third sub-research question of this work; "*What are the implications of increased syngas demand scenarios for the vertical supply chain and the usage of critical materials?*" The methodology that will be used to answer this question has been identified in Chapter 3 and consists of four core elements; (i) a list of critical materials (2020) based on the EU perspective, (ii) the identification of materials that can be used in SOECs, (iii) the quantification of material requirements (in g/kW) in SOEC technology, and (iv) delineating whether SOEC material requirements might oppose any limitations for the increased adoption of CO_2ER supply chains that use SOEC technology to produce syngas. Section 6.1 will address the first two elements, section 6.2 mainly focuses on the third element and section 6.3 addresses the fourth and final element, and concludes by providing an answer to the third sub-research question.

6.1 Identification of EU Critical Materials and HT-SOEC Materials

This section first focuses on the delineation of a list of critical materials from the EU perspective, thereafter it aims to identify the specific materials that can be used in SOECs. By combining the findings of these individual aspects, an indication of theoretical critical material usage in SOECs from the EU perspective can be provided.

6.1.1 Delineating Critical Materials from the EU's Perspective

In Chapter 3, the research of Blengini et al. (2020) has been introduced. In their report for the EC, titled "*Study on the EU's list of Critical Raw Materials (2020)*", they identify that 30 materials should be listed as critical (for the EU) based on ratings for economic importance and supply risk. These materials have been provided in Table 14 and their corresponding criticality ratings (based on economic importance and supply risk) have been provided in Figure A. 9 (in Appendix D.1). Apart from the individual materials, Table 14 includes three material groups; Heavy Rare Earth Elements (HREEs), Light Rare Earth Elements (LREEs), and Platinum Group Metals (PGMs). The individual materials that constitute these groups have been provided in Table 15. It must be noted that the materials that have been listed in Table 18 are provided individually in Figure A. 9, whilst the HREEs, LREEs and PGMs that have been listed in Table 19 are provided as a group. The reason to treat HREEs and LREEs as a group originates from the fact that they share the same physical and chemical properties and the various materials are found in the same ore deposits and share great parts of the same value chain (European Commission, 2020a). Furthermore, the EU is entirely dependent on imports of both HREEs and LREEs for its consumption, the majority of which (around 70-90%) is being produced in, and supplied by China. To this end, these groups are prone to high supply risks (Bobba et al., 2020). The reason to treat PGMs as a group originates from the fact that these metals show very similar chemical properties, however, unlike HREEs and LREEs, they have varying physical properties (European Commission, 2020a).

Table 14 List of critical raw materials, based on the assessment of Blengini et al. (2020), executed for the EC. *The materials for each of these categories are further delineated in Table 15.

Critical Raw Materials in 2020			
Antimony (Sb)	Fluorspar (CaF_2)	Magnesium (Mg)	Silicon metal
Baryte ($BaSO_4$)	Gallium (Ga)	Natural Graphite	Tantalum (Ta)
Bauxite	Germanium (Ge)	Natural Rubber	Titanium (Ti)
Beryllium (Be)	Hafnium (Hf)	Niobium (Nb)	Vanadium (V)
Bismuth (Bi)	HREEs*	PGMs*	Tungsten (W)
Borates (B + O)	Indium (In)	Phosphate rock	Strontium (Sr)
Cobalt (Co)	Lithium (Li)	Phosphorus (P)	
Coking Coal	LREEs*	Scandium (Sc)	

Table 15 List of the critical materials of which the LREE, HREE and PGM groups consist based on Blengini et al., (2020).

Light Rare Earth Elements	Heavy Rare Earth Elements	Platinum Group Metals
Cerium (Ce)	Dysprosium (Dy)	Iridium (Ir)
Lanthanum (La)	Yttrium (Y)	Palladium (Pd)
Praseodymium (Pr)	Terbium (Tb)	Platinum (Pt)
Neodymium (Nd)	Holmium (Ho)	Rhodium (Rh)
Samarium (Sm)	Erbium (Er)	Ruthenium (Ru)
	Thulium (Tm)	
	Ytterbium (Yb)	
	Lutetium (Lu)	
	Gadolinium (Gd)	
	Europium (Eu)	

6.1.2 HT-SOEC Materials for Co-electrolysis

According to Elder et al. (2015), many of the electrode compositions and structures used in SOFCs (i.e. in fuel cell mode, generating electricity) have shown equally good performance compared to electrolysis operation (i.e. in SOEC mode). Bianchi & Bosio (2021) support this claim, however, they do mention that there are still some aspects, such as the differences in thermal behaviour during fuel cell and electrolysis modes, which might favour the usage of different materials for the different applications. Alternatively, the research by Kiemel et al. (2021) states that assuming an equality of structure, the different power densities of HT-SOFCs and HT-SOECs (~0.3-0.4 W/cm^2 and ~1.2 W/cm^2 respectively), result in smaller material requirements for HT-SOECs (a factor ~3.43 smaller). Yet other research by Mahmood et al. (2019), identifies that cathode thickness greatly affects the mass transport of CO_2 to the electrode/electrolyte interface and therefore the performance of HT-SOECs in co-electrolysis mode, underlining the lack of knowledge on the usage of the same materials for alternative operating modes. Since there exist discrepancies in the literature on whether material usage influences the performance in fuel cell and electrolysis mode, this section will focus on materials that have been mentioned in the literature on HT-SOECs that operate in co-electrolysis mode. Nevertheless, to provide future researchers with a comprehensive overview of the possible materials, all materials that have been mentioned in the literature that has been used in this work (in both SOFC and SOEC modes), have been provided in Appendix D.2. Based on the reviewed literature it can be concluded that it is common practice to provide the specific material composition of single SOECs according to the following notation; *Cathode|Electrolyte|Anode*, consequently, a similar notation has been provided in Table 16. Apart from the cathode, electrolyte and anode of a single cell, HT-SOEC systems also consist of other elements such as the interconnects between single cells, the cell sealant, and the housing of the stack (Schreiber et al., 2020), nevertheless, this section focuses on the single cell composition.

Table 16 An overview of SOEC material compositions based on the literature that identifies and validates their usage for co-electrolysis applications.

Raw Materials	Cell Composition	Reference(s)
Nickel (Ni), Yttrium (Y), Zirconium (Zr), Lanthanum (La), Strontium (Sr), Manganese (Mn)	*Ni-YSZ|YSZ|YSZ-LSM* **YSZ**: Yttria Stabilised Zirconia **LSM**: Lanthanum Strontium Manganite **Yttria**: Y_2O_3 **Zirconia**: ZrO_2 **Manganite**: MnO	(Lu et al., 2020) (Yun Zheng et al., 2017) (Choe et al., 2022) (Andika et al., 2018) (Redissi & Bouallou, 2013) (W. Li et al., 2013)
Lanthanum, Strontium, Vanadium, Yttrium, Zirconium, Platinum	*LSV|YSZ|Pt* **LSV**: Lanthanum-doped Strontium Vanadate **Vanadate**: VO_4	(Yun Zheng et al., 2017) (Zhang et al., 2019)
Palladium, Cerium, Zirconium, Yttrium, Lanthanum, Strontium, Manganese, Ferrite	*Pd,CZY,LSCM-YSZ|YSZ|LSF-YSZ* **CZY**: Ceria Zirconia Yttria **LSCM**: Lanthanum Strontium Ceria Manganite **LSF**: Lanthanum Strontium Ferrite **Ceria**: CeO_2	(Yun Zheng et al., 2017)
Strontium, Ferrite, Manganese, Samarium, Cerium, Lanthanum, Gadolinium	*SFM-SDC|LSGM|SFM-SDC* **SFM**: Strontium Ferrite Manganite **SDC**: Strontium Doped Ceria **LSGM**: Strontium Doped Lanthanum Gadolinium	(Yao Wang et al., 2017)
Nickel, Yttrium, Strontium, Zirconium, Scandium, Lanthanum, Manganese	*Ni-YSZ|ScSZ|LSM-ScSZ* **ScSZ**: Scandia Stabilised Zirconia **Scandia**: Sc_2O_3	(Yao Wang et al., 2017)
Nickel, Yttrium, Strontium, Zirconium, Lanthanum, Cobalt, Ferrite, Gadolinium	*Ni-YSZ|YSZ|LSCF-CGO* **LSCF**: Strontium Iron Doped Lanthanum Cobalt **CGO**: Ceria Doped Gadolinium	(Yun Zheng et al., 2017) (X. Chen et al., 2015)
Nickel, Scandium, Cerium, Zirconium, Gadolinium, Lanthanum, Strontium, Cobalt, Ferrite	*Ni-ScSZ|ScSZ-CGO|LSCF-CGO*	(D. Y. Lee et al., 2020)
New: 8YSZ – 8mol% yttria-doped stabilized zirconia, Nickel, Yttrium, Zirconium	*Ni-8YSZ|8YSZ|LSCF-CGO*	(Schreiber et al., 2020) (Nechache & Hody, 2021) (Reytier et al., 2015) (Ebbehøj, 2015)
Nickel, Yttrium, Strontium, Zirconium, Lanthanum, Ferrite, Gadolinium, Cerium	*Ni-YSZ|YSZ|(Sr,Co)(La,Fe)-GCO*	(L. Wang et al., 2019)

Based on the cell compositions and the associated raw materials that have been provided in Table 16, it can be concluded that the most common configuration of SOECs for co-electrolysis is Ni-YSZ|YSZ|YSZ-LSM. This is validated by various pieces of research, including Yun Zheng et al. (2017), Hauch et al. (2020), Nechache & Hody (2021) and Y. Jiang et al. (2021). Another frequently mentioned composition is Ni-8YSZ|8YSZ|LSCF-CGO, which consists of a similar cathode and electrolyte (with a specific molar percentage of yttria) but an alternative anode composition. Based on the frequency of occurrence of these two cell compositions, the individual raw materials Nickel, Yttrium, Zirconium, Lanthanum, Gadolinium, Cerium, Strontium and Manganese, are identified as important raw materials for HT-SOECs in co-electrolysis mode. To this end, these materials will be considered in the remainder of this chapter. However, although these compositions have been mentioned frequently, the literature also identifies that they are prone to some limitations, including the oxidation of Ni to NiO and sulfur poisoning, both resulting in stability issues (Yun Zheng et al., 2017). Although this work further focuses on the eight individual raw materials that have been specified, these limitations emphasize the importance of considering alternative cell compositions in future research on the topic.

6.1.3 Critical Materials for HT-SOEC Applications from EU's Perspective

To provide a preliminary indication of the potential critical material usage in HT-SOECs that produce syngas via co-electrolysis, the materials that have been provided in Table 14 and Table 15 can be compared with the materials that have been found in the literature and are depicted in Table 16. This comparison is provided in Figure 12, which consists of red and green plots. In Figure 12, red corresponds to a "*critical material*" from the EU perspective, and green corresponds to a "*non-critical material*" from the EU perspective.

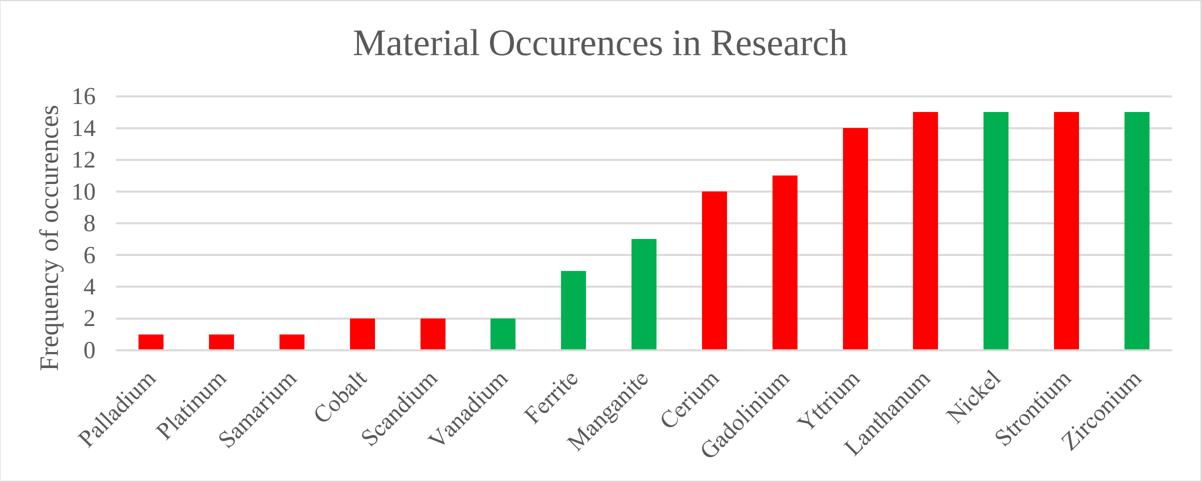

Figure 12 List of raw materials, the frequency of its occurrences in the 15 papers that provide information on materials for SOECs in co-electrolysis operating mode, and classification as critical material (red) or non-critical material (green) based on Tables 18 and 19 (total research papers: 15).

Based on Figure 12 it can be concluded that 66% of the materials, that have been mentioned in the literature on materials suitable for SOECs in co-electrolysis mode, are categorised as critical materials according to the list of critical materials for the EU that has been provided by Blengini et al. (2020). Additionally, Figure A. 10 (in Appendix D.3) depicts the same materials, however, based on occurrences in cell composition. Based on the information that has been provided in Figure A. 10 it can be concluded that every SOEC composition which has been provided in Table 16 requires at least three different materials that have been listed as critical. Also, five of the eight materials, that are deemed important for SOECs in co-electrolysis mode, are listed as critical. The identification of the usage of critical materials emphasizes the importance of the search for risk-reducing measures, such as the possibilities for alternatives and increasing research into recycling possibilities (Lotrič et al., 2021).

6.2 Material Usage in HT-SOECs

Ideally, the material requirements for each component of a SOEC system are obtained from direct information provided by the top manufacturers of SOEC systems that produce syngas (e.g. Sunfire).

However, such information is not publicly available. Consequently, an alternative approach for estimating material usage in HT-SOECs must be used. To this end, various research papers including the research by Häfele et al. (2016), Bachmann et al. (2019), Schreiber et al. (2020), Kiemel et al. (2021), and Choe et al. (2022), that provide material requirements for SOECs or SOFCs, have been reviewed and a complete overview of the material requirements that have been mentioned is provided in Appendix D.4.

The research by Häfele et al. (2016), Bachmann et al. (2019), and Choe et al. (2022) provide the material requirements of HT-SOEC in terms of cathodes, anodes and electrolytes, whereas the research by Schreiber et al. (2020), and Kiemel et al. (2021) (which is based on work by Marscheider-Weidermann et al., (2016)), provide the individual material requirements or the material requirements in oxidised-form. Furthermore, all of the research that has been reviewed, except for the research by Choe et al. (2022), provides additional material requirements for stack and/or system construction. Since this work focuses on the eight materials that have been identified as important (Nickel, Yttrium, Zirconium, Lanthanum, Gadolinium, Cerium, Strontium and Manganese), and solely on the materials that are used in the cells and not for the construction of the stacks or system, Table 17 depicts the converted material requirements (in g/kW) of the eight important materials, that have been mentioned in the research by Schreiber et al. (2020), and Kiemel et al. (2021).

Table 17 The specifications of material usage by different researchers and the efficiency that is stated in the respective literature. The last column delineates the suggested quantity of the specific material required per kW (based on cell and stack information).

Ref.	Single-cell size	System size	Efficiency	Materials	Requirements
(Schreiber et al., 2020)	10 x 10 x 0,05 (active cell area of 80 cm^2)	2 Stacks, 120 levels each, 960 cells in total, 150 kW	Approx.. 75%	Ceria	1,2864 g/kW
				Lanthanum oxide	12,672 g/kW
				Gadolinium oxide	0,3392 g/kW
				Yttria	15,488 g/kW
				Strontium carbonate	2,0736 g/kW
				Nickel cermet	114,56 g/kW
				Zirconia	95,36 g/kW
				Manganese	18,93 g/kW
				Nickel	132 g/kW
				Lanthanum	3,22 g/kW
(Kiemel et al., 2021) based on (Marscheider-Weidermann et al., 2016)	n.a.	n.a.	n.a.	**Cerium**	14,88 g/kW
				Lanthanum	62,14 g/kW
				Zirconium	116,69 g/kW
				Gadolinium	3,79 g/kW
				Yttrium	4,08 g/kW

From Table 17 (and Appendix D.4), it can be concluded that the research by Schreiber et al. (2020) and Kiemel et al. (2021), use different units and state the materials in alternative forms (e.g. yttrium versus yttria and cerium versus ceria). These alternative material forms have a significant impact on the material requirements, for example, Marscheider-Weidermann et al. (2016), identify that HT-SOFCs require 14 g/kW capacity of yttrium, according to their research this is equal to 17.7 g of yttria, additionally they provide the requirements for scandium (23 g/kW) and scandia (35 g/kW). Consequently, if the material requirements are stated in g/kW of yttria (or any oxidized form), they will be significantly larger than when they are stated in g/kW of yttrium (or any individual raw material form). Additionally, another important difference between these research papers is that Kiemel et al. (2021), provide requirements for cells with a Ni-YSZ|YSZ|YSZ-LSM composition, and Schreiber et al. (2020) provide requirements for cells with a Ni-8YSZ|YSZ|LSCF composition. To this end, a detailed comparison of their respective material requirements would not be valid. Furthermore, the research by Choe et al. (2022), Häfele et al. (2016) and Bachmann et al. (2019) provide the material requirements based on the composition of the cathode, electrolyte and anode, which consists of various alternative forms of raw materials. Hence it can be concluded that there exist significant differences between the material requirements that have been provided in the various research. These differences should be taken into account during the assessment and interpretation of the results, stressing the importance of the availability of direct information from HT-SOEC manufacturers. Nevertheless, the material requirements in g/kW can now be used in the following section.

6.3 Criticality Assessment

To provide an answer to the third sub-research question, this section aims to establish a relationship between the material requirements (in g/kW) and their implications for the increased adoption of HT-SOEC technology for the production of syngas. To this end, section 6.3.1 quantifies the global annual production of these materials and their global availability. Additionally, it provides a quantification of the average European annual material demand, which can be used for comparison purposes. Thereafter, section 6.3.2 uses the quantification of the syngas market that has been provided in Chapter 4 (section 4.3.2) to determine the required amount of installed SOEC capacity (in GW). Finally, section 6.3.3 uses the material requirements (in g/kW) and the required installed capacity, which has been provided in Table 17, to calculate the total material requirements. Thereafter, the total material requirements are compared with the global annual production and availability of these materials to indicate whether the vertical supply chain opposes any limitations to the increased adoption of SOEC technology for syngas production.

6.3.1 Material Availability

The quantification of the global annual production, the European annual demand, and the global availability of the eight materials that have been identified as important have been provided in Table 18. Besides the eight materials, several other materials have been mentioned, their quantification has been provided in Appendix D.5 These quantifications are based on the Critical Material Factsheet (European Commission, 2020a) and the Non-Critical Material Factsheet (European Commission, 2020b). Additionally, some supporting information on these materials, such as the products in which they are commonly used and the countries that supply them, is provided in Appendix D.6.

Table 18 The global annual production, European annual demand and global availability of the 15 materials have been identified in Table 20. All information is based on the work of the European Commission (2020a) and the European Commission (2020c). For the REEs it is difficult to obtain global availability in tonnes, consequently, this is provided in ppm in the upper crust of the Earth.

Material	Global Annual Production	European Annual Demand	Global Availability
Manganese	17.5 Mtonnes	481 tonnes	>17 Gtonnes
Cerium	51.2 ktonnes	4000 tonnes	63 ppm
Gadolinium	1596 tonnes	11.3 tonnes	4 ppm
Yttrium	8-10 ktonnes	520 tonnes	21 ppm
Lanthanum	29 ktonnes	645 tonnes	31 ppm
Nickel	>2 Mtonnes	440 ktonnes	300 Mtonnes
Strontium	160 ktonnes	49 ktonnes	> 1 Gtonnes
Zirconium	1423 ktonnes	231 ktonnes	>148 Mtonnes

6.3.2 Material Requirements to Meet Global/European Syngas Demand

In Chapter 4 (section 4.2.3), a conceptualisation of the global and European syngas market in 2020, and an extrapolation of these numbers to 2030, has been provided. This data, which is based on the market research of ReportLinker (2022), will be used to assess the total material requirements assuming that all syngas is produced by HT-SOEC technology. The global syngas market was quantified in Million Nm^3-syngas per hour, and the material requirements in Table 17 are provided in grams per kW. Consequently, the syngas demand must be provided in Watts as well. To this end, the market size is calculated by multiplying the density of syngas (calculated in Appendix B.9) by the market size that has been provided by ReportLinker (2022), resulting in the market size (or syngas demand) provided in kg-syngas per hour as can be seen in the second column of Table 19. Furthermore, in Chapter 4, two HT-SOEC systems (SYNLINK and Linde AG) have been identified and used for calculation purposes. These systems will be used in this section as well. The grounds for providing calculations, in this section, based on two systems instead of a single system, mainly revolve around the potential to identify the possible role that improved performance of HT-SOEC systems can play in decreasing the raw material requirements, but also the stated lifetime of the respective systems (40000 hours up to almost 90000 hours). Based on the size and production capacity of the two systems (SYNLINK (2890 kW) with a production capacity of 354.8 kg-syngas/hr and Linde AG (150 kW) 16.8 kg-syngas/hr), the total number of required systems is calculated and provided in the third column of Table 19. Finally, the total number of systems is multiplied by the respective size (in kW) of a single system, resulting in the required installed HT-SOEC system capacity, depicted in the last column of Table 19.

Table 19 An overview of the syngas demand in 2020 and 2030 and quantification of the required installed SOE system capacity to meet this demand. In the first column, GD stands for Global Demand and ED stands for European Demand.

System & Year	Demand (in kg-syngas/hr)	Number of Systems Required	Required Installed Capacity (in GW)
SYNLINK GD (2020)	80410000	226635	655
Linde AG GD (2020)	80410000	4786310	718
SYNLINK ED (2020)	17501000	49326	143
Linde AG ED (2020)	17501000	1041726	156
SYNLINK GD (2030)	227040000	639910	1849
Linde AG GD (2030)	227040000	13514286	2027
SYNLINK ED (2030)	47300000	133315	385
Linde AG ED (2030)	47300000	2815476	422

The required installed capacity (in GW) which has been provided in the last column of Table 19, can be used to quantify the material requirements, based on the requirements in g/kW that have been found and provided in the last column of Table 17. The material requirements based on the production capacity and size of the two systems are provided in Table 20.

Table 20 The material requirements for the eight important materials to meet global/European syngas demand based on the SYNLINK and Linde AG systems.

		SYNLINK		**Linde AG**	
Year	**Material**	**Global Demand (in tonnes)**	**European Demand (in tonnes)**	**Global Demand (in tonnes)**	**European Demand (in tonnes)**
2020	Manganese	12401	2699	13593	2959
	Cerium	9743	2120	10679	2324
	Gadolinium	2483	541	2722	592
	Yttrium	2674	582	2932	638
	Lanthanum	2109	459	2312	503
	Nickel	86457	18817	94769	20626
	Strontium (Carbonate)	1358	296	1489	324

	Zirconium	76414	16631	83760	18230
2030	Manganese	35014	7295	38381	7996
	Cerium	27509	5731	30154	6282
	Gadolinium	7012	1461	7686	1601
	Yttrium	7551	1573	8278	1724
	Lanthanum	5955	1241	6527	1360
	Nickel	244113	50857	267583	55746
	Strontium	3835	799	4203	876
	Zirconium	215756	44949	236500	49271

6.3.3 Implications of Syngas Demand on Critical Material Usage

To delineate the implications of increased syngas demand on the usage of critical materials, this section differentiates between the material requirements based on the global perspective, which compares the global annual production with the material requirements, and the European perspective, which compares the European annual consumption with the material requirements for the respective materials. The global perspective will be treated in section 6.3.3.1 and the European perspective will be treated in section 6.3.3.2.

6.3.3.1 Global Perspective

The Global Annual Production (GAP) that has been provided in Table 18, is provided in Figure 11. Additionally, Figure 11 depicts the Global Demand in 2020 and 2030, based on SYNLINK system operating parameters (SL-GD (2020) and SL-GD (2030)), and based on Linde AG system operating parameters (LA-GD (2020) and LA-GD (2030)). The material production and material requirements can be compared to assess whether the vertical supply chain opposes any additional limitations to syngas production via HT-SOEC technology.

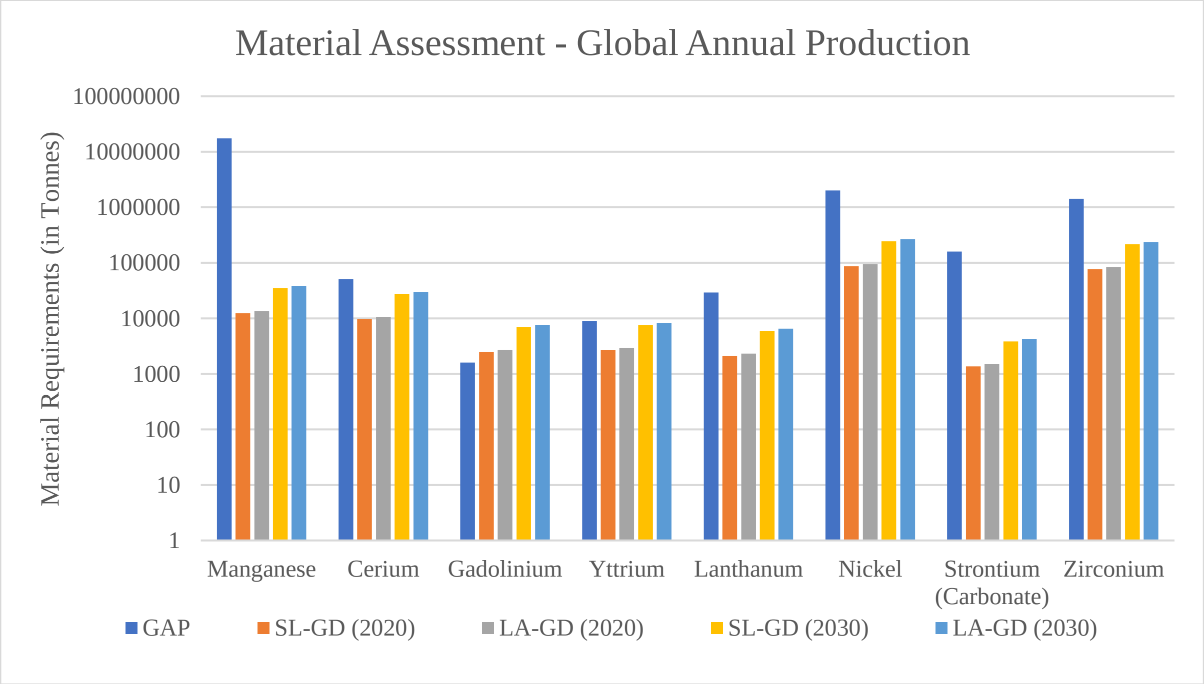

Figure 13 A comparison between the global annual production and the material requirements to meet the global syngas demand through syngas production via HT-SOEC technology.

Based on the comparison of global annual production and the material requirements to meet the syngas demand in 2020 and 2030, via either SYNLINK systems or Linde AG systems, it can be concluded that the global annual production of Gadolinium needs to be increased to meet the material requirements in any of the four global demand quantifications that have been provided in Figure 13. However, when taking into account the global availability of Gadolinium (provided in Table 18), which has an upper Earth crust concentration of approximately 4 ppm, and comparing this with the concentration of the other REEs, it can be concluded that Gadolinium is rare. Consequently, the search for alternatives for Gadolinium and increasing the recycling possibilities of the material is essential.

Apart from the material requirements for Gadolinium, all of the material requirements can be met. Nevertheless, the material requirements as a percentage share of the global annual production have been calculated and provided in Appendix D.8. These calculations identify that almost all of the materials require a significant share of the global annual production. Moreover, based on the 2020 global demand, the materials with percentage shares lower than 10% of the global annual production are Lanthanum (7%), Nickel (4%), Strontium (0.85%), Zirconium (5%) and Manganese (0.07%), whereas Yttrium (30%), Cerium (19%) and Gadolinium (156%) have percentage shares larger than 10% of the global annual production. Additionally, Appendix D.8 also provides the percentage shares for the material requirements based on 2030 demand quantifications. From these percentage shares, it can be concluded that only Manganese and Strontium remain below 10% of the global annual production.

However, since HT-SOEC systems have lifetimes larger than 1 year, the material requirements do not have to be met in a single year. To this end, Appendix D.7 provides similar figures as Figure 13 but based on a multiplication of the global annual production by 4.5, 8.5 and 10 years (Figure A. 11, Figure A. 12, and Figure A. 13) respectively. These years are based on the HT-SOEC system lifetimes that have been specified by Schreiber et al. (2020), and Posdziech (2021). Additionally, Appendix D.8 provides the percentage shares associated with these alternations. From these results, it can be concluded that for 4.5 years of global annual production, all the material requirements, including that for gadolinium, can be met. The material requirements for Gadolinium are still above a 10% share of the global 4.5 years of production, however, all the other material requirements are below the 10% percentage share. Consequently, from a global perspective, taking into account the lifetime of HT-SOEC systems, the vertical supply chain does not oppose any additional limitations. However, the search for alternatives or recycling possibilities for Gadolinium is deemed important due to its high percentage share and relatively small global availability.

6.3.3.2 European Perspective

Figure 14 depicts the European Demand for 2020 and 2030 respectively, based on SYNLINK system operating parameters (SL-ED (2020) and SL-ED (2030)), and based on Linde AG system operating parameters (LA-ED (2020) and LA-ED (2030)). Like the previous section, this section will compare the material requirements with their availability, however, now from a European perspective. Moreover, in section 6.1 it has been identified that the materials; *Yttrium, Lanthanum, Cerium, Gadolinium and Strontium*, are listed as critical materials for the EU. A similar conclusion can be drawn from the data that has been provided in Figure 14, however, it also identifies Manganese as a material whose requirements cannot be met by the current annual demand of the EU, whereas the Strontium requirements can easily be met. Additionally, similar to the previous section, the percentage shares of these material requirements based on the annual demand, have been calculated and provided in Appendix D.8. From this data, it can be concluded that all the material requirements, except for Nickel (12%), Strontium (2%), and Zirconium (19%), require at least two times the current European annual demand. Additionally, an interesting finding is that the material requirements for Nickel, a material that previously has been identified as non-critical, account for approximately 12% of the total European annual demand, which is significant.

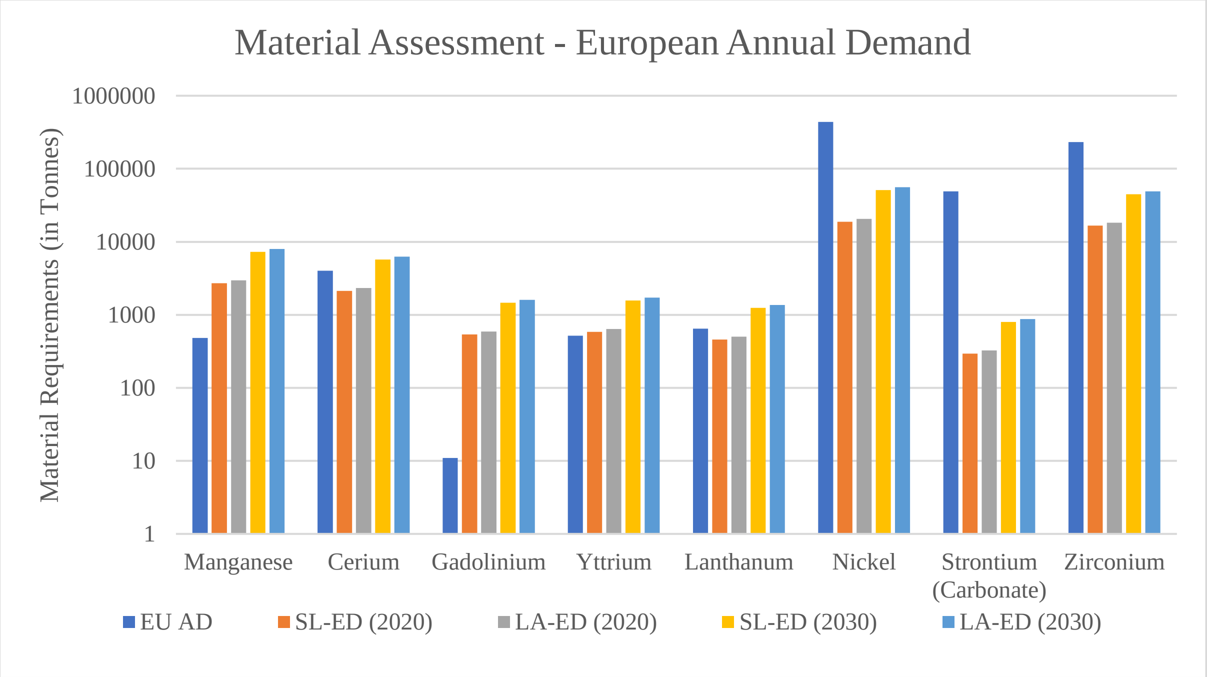

Figure 14 A comparison between the European annual demand and the material requirements to meet the European syngas demand through syngas production via HT-SOEC technology.

Like the previous section, the stated system lifetimes are also considered from the European perspective, and the comparison of material requirements and 4.5, 8.5 respectively 10 years of European annual demand have been provided in Appendix D.7 (Figure A. 14, Figure A. 15 and Figure A. 16) and the respective percentage shares have been provided in Appendix D.8. From these figures, it can be concluded that for 4.5 years of European annual demand, the material requirements for Manganese (125%) and Gadolinium (1093%) can still not be met. The other material requirements can be met, however, Lanthanum (16%), Yttrium (25%) and Cerium (12%) still require a significant share of the European 4.5-year demand. For 8.5 years and 10 years, similar conclusions can be drawn. Consequently, from the European perspective, the vertical supply chain does oppose additional limitations for the HT-SOEC supply chain that produces syngas. The search for alternative materials for Manganese and Gadolinium is a necessity since these material requirements cannot be met. Additionally, Lanthanum, Yttrium and Cerium also require a significant share of the European annual demand, consequently, diversification in HT-SOEC compositions (i.e. search for alternatives) and increased research into recycling possibilities of these materials is an important consideration for the EU.

Chapter 7

Conclusion

The urgent need for fighting global warming has resulted in increased research towards technological innovations and processes with the potential to contribute to this fight. A process with a high potential to decrease the amount of CO_2 that is emitted into the atmosphere is the electrochemical reduction of carbon dioxide, which utilises CO_2 and renewable energy for the production of value-added chemicals and fuels. There exist multiple configurations of the process in terms of the type of electrolyser that is being used and the specific product that is being produced, but also aspects related to its potential supply chains, such as the capturing and transportation of feedstocks and products. There exist many possible technological implementation possibilities, however, at the current stage, favourable technology implementation conditions remain unknown. To this end, this work has applied an exploratory research approach to delineate the limits and opportunities of the process and its supply chain.

This work focuses specifically on a supply chain that uses high-temperature solid oxide cells for the co-electrolysis of H_2O and CO_2 to produce syngas. This specific technological configuration is selected due to the combination of the potential higher conversion efficiency of solid oxide electrolysers compared to other electrolyser technologies, its ability to co-electrolyse CO_2 and H_2O resulting in the direct production of syngas, and the already established syngas market which is expected to grow rapidly. Additionally, various processes have been considered for the deliverance and transportation of the CO_2 and H_2O feedstocks that are required to produce syngas, mainly to investigate the opportunities for alternative supply chain configurations. As such, this work aims to investigate the feasibility and opportunities for the production of syngas via solid oxide electrolysers, resulting in the formulation of the following main research question:

> **"How do alternative supply chain configurations impact the technical feasibility and economic performance of carbon dioxide electrochemical reduction plants that produce syngas?"**

To provide an answer to this research question, this work was structured based on three sub-research questions. The first sub-research question revolved around the theoretical and practical limitations of a carbon dioxide electrochemical reduction process that utilises high-temperature solid oxide electrolyser cells to produce syngas. Adequate system assessments allow for determining whether the proposed solution can be scaled to the physical sizes which are deemed necessary to accomplish the envisioned end goal of the technology, consequently, these physical sizes were the main focus of the investigation, and the following sub-research question was formulated:

> "*What are the theoretical and practical limitations of a HT-SOEC CO_2ER supply chain focused on producing syngas?*"

During the exploration of the theoretical and practical limitations, a local perspective and a global perspective were considered. The global perspective entails producing the global syngas demand by high-temperature solid oxide electrolyser technology, and the local perspective entails producing syngas on the smallest scale that is deemed commercial. A prominent practical limitation that has been identified early in the research, is the lack of syngas transportation (or storage) infrastructure. Theoretically, the transportation of syngas is feasible, however, the current infrastructure is not deemed suitable, mainly due to the high hydrogen content and the toxicity of carbon monoxide, the two primary gasses of which syngas consists. Consequently, a practical limitation for the supply chain revolves around the issue that syngas must be produced in proximity to the demand location. Furthermore, it was found that the global syngas demand can be met by CO_2 captured from point sources in the U.S. alone. Consequently, the CO_2 feedstock does not oppose any theoretical limitations to meet global or local syngas demand. However, it was found that there exists a mismatch between the quantity of CO_2 that can be captured from point sources and the CO_2 demand of a local-scale syngas production facility. Consequently, a practical limitation was identified, which is that the combination of post-combustion capture for CO_2 feedstock and local syngas production is not a good match. Another technology that was considered for the provision of CO_2 feedstock was high-temperature direct air capture. The scale of high-temperature direct air capture systems and local syngas demand matched almost perfectly, however, the CO_2 capture technology results in significant water and high-temperature heat requirements, opposing prominent practical geographical limitations. It must be noted that the water requirements for the conversion process alone do not impose any substantial limitations. Apart from the feedstock requirements, a prominent practical limitation is the current status and size of high-temperature solid oxide electrolyser systems. To meet the global syngas demand, almost five million of the largest state-of-the-art high-temperature solid oxide electrolyser systems are required, whilst only one of such systems is currently operating as a demonstration plant.

Due to the modular nature of electrolyser technology, the distributed nature of renewable energy and water sources, and the possibility to capture CO_2 via direct air capture technology which is also portable by nature, a possible opportunity for the considered supply chain is its configuration in a decentralised manner. Such a supply chain configuration generally reduces transportation costs and consequently, might result in improved economic performance. It can be identified as a possible opportunity, and to quantify this opportunity the second sub-research question was formulated as follows:

“*How do different supply chain units influence the performance of decentralised and centralised supply chain configurations and which supply chain units have the highest impact when comparing these configurations?*”

To answer this question, the literature that has been reviewed to answer the first sub-research question was used to quantify the costs of specific centralised and decentralised supply chains. To measure economic performance, simple payback time was selected as a key performance indicator. However, the calculations resulted in a negative average annual cash flow. Consequently, the specific centralised and decentralised supply chain configurations that were investigated did not have a payback time. Hence, the influence of the individual supply chain units on the costs of the supply chain was further investigated. It was concluded that the high-temperature solid oxide electrolyser has the largest influence on the costs of both supply chain configurations, both in terms of operating expenses and capital expenses. Throughout the supply chain, the majority of the operating expenses are primarily related to energy consumption, with the electrolyser being the biggest cost contributor. Consequently, it has been investigated whether the supply chain configurations could have a positive average annual cash flow if the electricity costs were set to zero, however, the non-energy operating expenses were also too high. A comparison of the decentralised and centralised supply chain configurations did identify that decentralised configurations allow for the possibility to start at a relatively smaller scale, lowering the negative annual cash flow and requiring lesser capital expenses, however, if the production capacity was equal, centralised configurations require lesser capital expenses in total.

Although the answer to the previous sub-research question identifies that at the current technological status, supply chains that utilise high-temperature solid oxide electrolyser technology to produce syngas are not economically viable, increased performance might result in future increased adoption. To this end, the first sub-research question identified the feasibility in terms of scale, however, another important aspect of feasibility is related to the material requirements. To address this aspect of feasibility, the third sub-research question was formulated as follows:

“*What are the implications of increased syngas demand scenarios for the vertical supply chain and the usage of critical materials?*“

To provide an answer to this question, global and European perspectives were considered. Based on a literature review, eight materials were considered important materials for high-temperature solid oxide electrolyser systems for the production of syngas; Nickel, Yttrium, Zirconium, Lanthanum, Gadolinium, Cerium, Strontium and Manganese. From the global perspective, it was found that based on the annual global production of these materials, the required amount of Gadolinium exceeds the global annual production significantly and consequently limits the feasibility of the supply chain. Additionally, the required amount of Yttrium and Cerium required high percentage shares of the global annual production and consequently might hinder the feasibility to deliver global syngas demand via high-temperature solid oxide electrolyser technology. The lifetime of solid oxide electrolyser systems was also considered and based on the global production based on lifetime, only Gadolinium hinders the technical feasibility of the supply chain to meet global syngas demand. From the European perspective, it was found that based on the European annual demand for the eight materials, Manganese, Cerium, Gadolinium, Yttrium and Lanthanum exceed the current annual European demand. Additionally, the lifetime of the electrolysers was also considered and unlike the global perspective, Manganese and Gadolinium still exceeded the current annual demand and Lanthanum, Yttrium and Cerium required high percentage shares and consequently might hinder the feasibility to deliver European syngas demand via high-temperature solid oxide electrolyser technology.

“How do alternative supply chain configurations impact the technical feasibility and economic performance of carbon dioxide electrochemical reduction plants that produce syngas?”

By synthesizing all the information that has been found, a concrete answer to the main research question can be formulated. At the current technological stage, the technical feasibility of carbon dioxide electrochemical reduction plants is mainly limited by the size and economic performance of electrolyser systems. The capital investments that need to be made for a supply chain that produces syngas on a large scale are high, additionally, the operating expenses currently hinder the generation of a positive income. Consequently, such supply chains cannot exist without subsidies or investments from third parties that are not interested in making a profit anytime soon. Furthermore, one of the main advantages of decentralised supply chains, especially from an economic perspective, is the decrease in transportation costs with which it is generally associated. In this work, it has been identified that at the current stage, the transportation of feedstocks only has a small impact on operating expenses. Additionally, there is no existing infrastructure for the transportation of the product, highly limiting the supply chain possibilities. Nevertheless, decentralised supply chain configurations allow for the opportunity to gradually built out capacity, and based on the specific supply chain configurations that were investigated in this work, smaller decentralised syngas production facilities require less capital investment and the average annual cashflow is less negative. Furthermore, although the material requirements are not different in alternative supply chain configurations, gradually increasing capacity (as in a decentralised configuration) allows for a larger period to extract or acquire the required materials. In conclusion, although the production of syngas to meet global demand is feasible based on its feedstock requirements, it is not expected that high-temperature solid oxide electrolysers and their corresponding supply chains will be used at such scales. Especially due to the importance of the geographic location (i.e. low electricity prices, high availability of renewable electricity, high availability of water).

Chapter 8

Discussion

The overarching goal of this work was to provide insights into the limits of alternative supply chain configurations for CO_2ER processes that utilise SOEC technology. As such, it aimed to identify the *feasibility and boundaries* of an industrial-scale CO_2ER supply chain by comparing the requirements of its supply chain with the potential to meet *global* and *European* syngas production. Additionally, the aim was to identify the *opportunities* associated with potential alternative configurations that might result in the improved economic performance of CO_2ER supply chains. Moreover, the goal was not to find a specific quantification of a single optimal supply chain configuration (either centralised or decentralised), rather it is to map the supply chain requirements. To this end, it aims to find the trade-offs and limitations of the possible alternative configurations by exploring the solution space of CO_2ER supply chains implemented at an industrial scale. The results and discussions presented along the way indicated several uncertainties and limitations, the most important aspects will be highlighted in this chapter.

8.1 Reflection on the Research Findings

Due to a large amount of research that is available on the various individual supply chain units, and the attention that several of its units receive nowadays, this work does not include every single study on the technical and economic aspects of the various supply chain units that were considered in this work. However, no specific research or author was excluded intentionally. On the contrary, this work aimed to include as much research as possible, including that from various geographic locations since this provides a thorough overview of the aspects that could influence the economic performance and technical feasibility of the supply units. Moreover, it must be noted that various of the research that has been reviewed, indicate that the costs they calculated are merely indications and that, for example, the CO_2 transportation costs constitute only one of the multiple cost components of supply chains. To this end, the overall accuracy should ideally be determined based on the aggregated transportation infrastructure in terms of distance and quantity within a specific context (i.e. case study). To address this limitation, the various appendices that have been provided as supporting information provide detailed conversions of both units and costs.

Apart from the unintended exclusion of scientific studies, this work did not include several aspects that should be considered in a realistic CO_2ER supply chain. Moreover, the storage of commodities is not taken into consideration. Consequently, this work relies on the assumption of a continuous flow of feedstocks and products. A realistic supply chain would have storage facilities for H_2O, CO_2 and syngas. The consequences of exclusion are primarily related to the costs for the overall supply chain. However, the exclusion of syngas storage (and transportation) has severe implications. The storage and transportation of syngas are not well reported in the available literature. However, storing syngas has some advantages when compared to its immediate use. Moreover, if syngas can be stored and transported, it can be produced during periods of low demand and high electricity supply, and consequently, could be sold during periods of high demand and low supply. This would not only result in providing a resource upon demand but also creates economic benefits to producers (and consumers). Since it has been identified that the price for syngas is too low to create a positive income, investigating specific cases in which the selling price for syngas would be higher seems a valuable research direction.

Additionally, although these aspects have been mentioned in this work, no detailed exploration of purification and or compression of H_2O and CO_2 has been treated. Furthermore, the supply chain is commonly assessed from today's point of view whereas HT-SOEC is often mentioned as a technology of the future. Chapter 5 includes an assessment of a decreasing electricity price, however, other potential learning rates and improvements were not specifically assessed. Since learning rates improve efficiencies and possibly reduce the cost of the technologies in other ways, which might sketch a more promising outlook for the future of the technologies that have been treated. This work has identified the importance of improving the overall efficiency of several supply chain units, the quantification of targets, such as a syngas price or electrolyser OPEX is however lacking.

For the economic analysis that was done in Chapter 5, the selected approach was not a good fit. Moreover, the aim was to identify trade-offs, consequently, it would be most beneficial if various configurations were compared, instead of only two. Consequently, this can be identified as one of the limitations of this research. Nevertheless, the results that have been found provide some valuable information, especially considering the exploratory nature of this work. Nevertheless, more accurate research, via for example mathematical modelling approaches, could provide valuable insights on the centralisation versus decentralisation topic.

8.2 Reflection on the Methodological Contribution

The methodology to assess the vertical supply chain was selected to address the potential implications of increased syngas demand on the usage of critical materials, and consequently, provide a prior indication of the feasibility based on the material requirements of HT-SOEC technology for the production of syngas on a global scale. To provide these insights, several generalisations and assumptions were made which are worthwhile discussing.

The literature that has been reviewed was prone to several discrepancies. Moreover, it has been identified that solid oxide cells have shown equally good performance in fuel cell mode and electrolysis mode. However, it was also identified that several aspects, such as the differences in thermal behaviour during the alternative operating modes, might result in alternating material preferences. Due to these contradictory claims, this work only focused on the materials that have been mentioned in the literature as good performing in co-electrolysis mode. Hence, many possible electrolyser cell configurations were not considered during the assessment. To address this limitation, a complete overview of the materials that have been mentioned was provided in the Appendix. Nevertheless, they have not been considered as possible critical materials. Having said that, the research indicates that, for an HT-SOEC which is solely composed of the materials that have been researched, the global syngas demand can be met with only Gadolinium opposing technical feasibility limitations. Consequently, even though other materials would be listed as critical, the researched compositions do not hinder technical feasibility on a global scale.

From the European perspective, additional material assessments would be an important research topic, since the materials that have been assessed hinder the technical feasibility of meeting European syngas demand. However, it must be noted that this work does not take into account current recycling rates. The results are based on raw material supply. Since there already exist recycling possibilities for almost all of the materials that have been reviewed, the stated material requirements will be less critical than indicated, creating a more promising outlook from a vertical supply chain perspective.

8.4 Recommendations for Future Research

Many technologies fail in the transition from benchtop to industrial scale. To overcome failure, the development of a deeper understanding of the physical and energetic relationships of HT SOEC CO_2ER processes is deemed essential. Effective identification of such relationships allows the design of optimized CO_2ER supply chains at an industrial scale. To develop such a deeper understanding, an efficient bidirectional feedback loop between early adopters and experimental (scientific) research will be necessary, as it will provide critical data for complete system engineering and individual technical component improvement and design. The assessment of the vertical supply chain in this work was based on scarcely available data. The provision of the exact material requirements for a single SOEC would greatly enhance the possibilities for research on the topic. Consequently, such feedback loops should include the interaction between HT-SOEC manufacturers and researchers on the topic.

Apart from the more general recommendation for cooperation between researchers and manufacturers, several knowledge gaps have been identified. Moreover, there exists only a handful of research on the topic of syngas transportation and storage, and no literature focuses on the actual design of syngas transportation pipelines, most likely because it is difficult and dangerous to transport at certain compositions. However, the literature does identify that, with higher concentrations of CO2 remaining in the syngas, this danger decreases. Consequently, an alternative to consider, and an interesting topic for future research is to use a downstream purification unit. An interesting trade-off to research would be to compare supply chains that produce syngas with properties that make it transportable in existing NG pipelines by solely increasing the operating pressure, however, does require additional purification processes at the demand side versus a supply chain of which the syngas infrastructure is constructed to transport syngas with a molar ratio of 2 H2:CO.

Appendices

Appendix A: Introduction, State-of-the-art and Methodology

A.1 Schematic Overview of Alternative CCUS Pathways

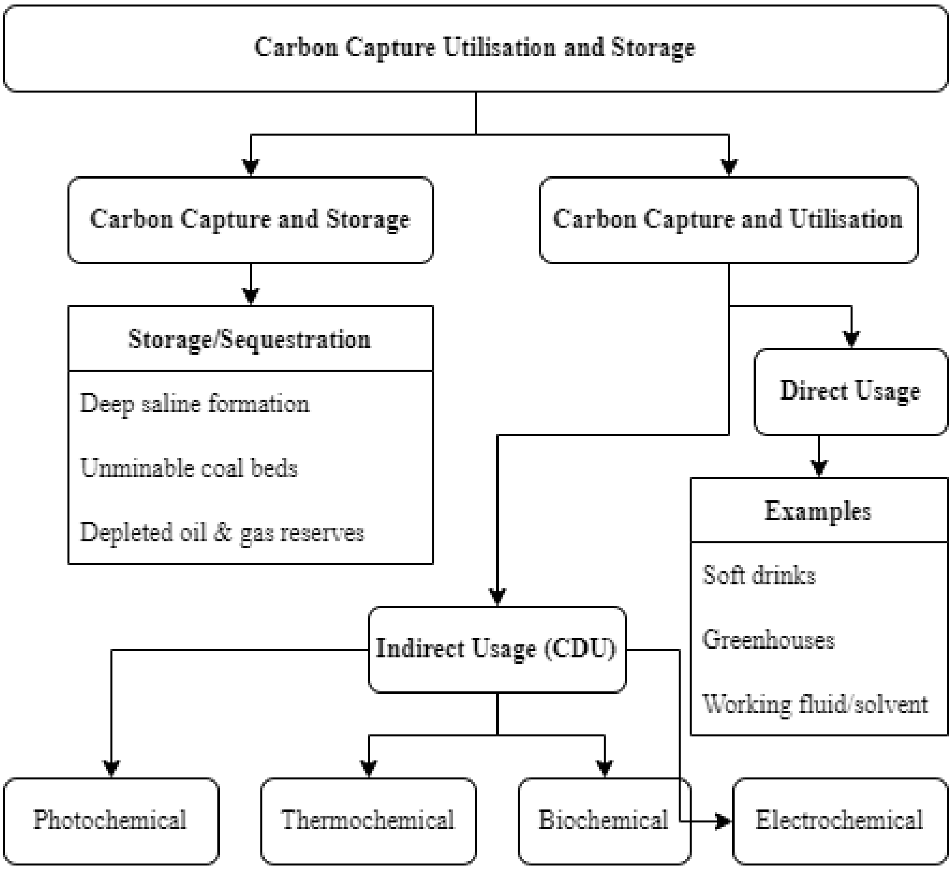

Figure A. 1 A schematic representation of the various categories and sub-categories that are within the boundaries of the concept CCUS.

Photochemical (photosynthetic and photo-catalytic): Reduction of the CO_2 molecule to more reduced chemical species (i.e. reducing oxidation state) by using light irradiation.

Thermochemical: Reduction of the CO_2 molecule, by breaking down the bonds between adjacent molecules via increasing the temperature of the molecules.

Biochemical: Reduction of the CO_2 molecule through the use of living organisms, examples of which are algae.

Electrochemical: Reduction of the CO_2 molecule via electrolysis (i.e. using electricity to generate more reduced chemical species).

A.2 Comparison of Energy Needs of DAC Technology

The comparison of the energy needs that has been provided below is copied from Budinis (2022). The largest difference in energy requirements is opposed by the heat requirements. However, in an ideal scenario, these requirements can be met by using excess heat from industrial processes. Nevertheless, the electricity requirement for solid sorbent DAC is approximately three times higher than the electricity requirement for liquid DAC. Consequently, liquid DAC or HT-DAC is the preferred technology. Additionally, since it has high operating temperatures (between 300-900˚C), there exist potential synergies between HT-SOEC and HT-DAC.

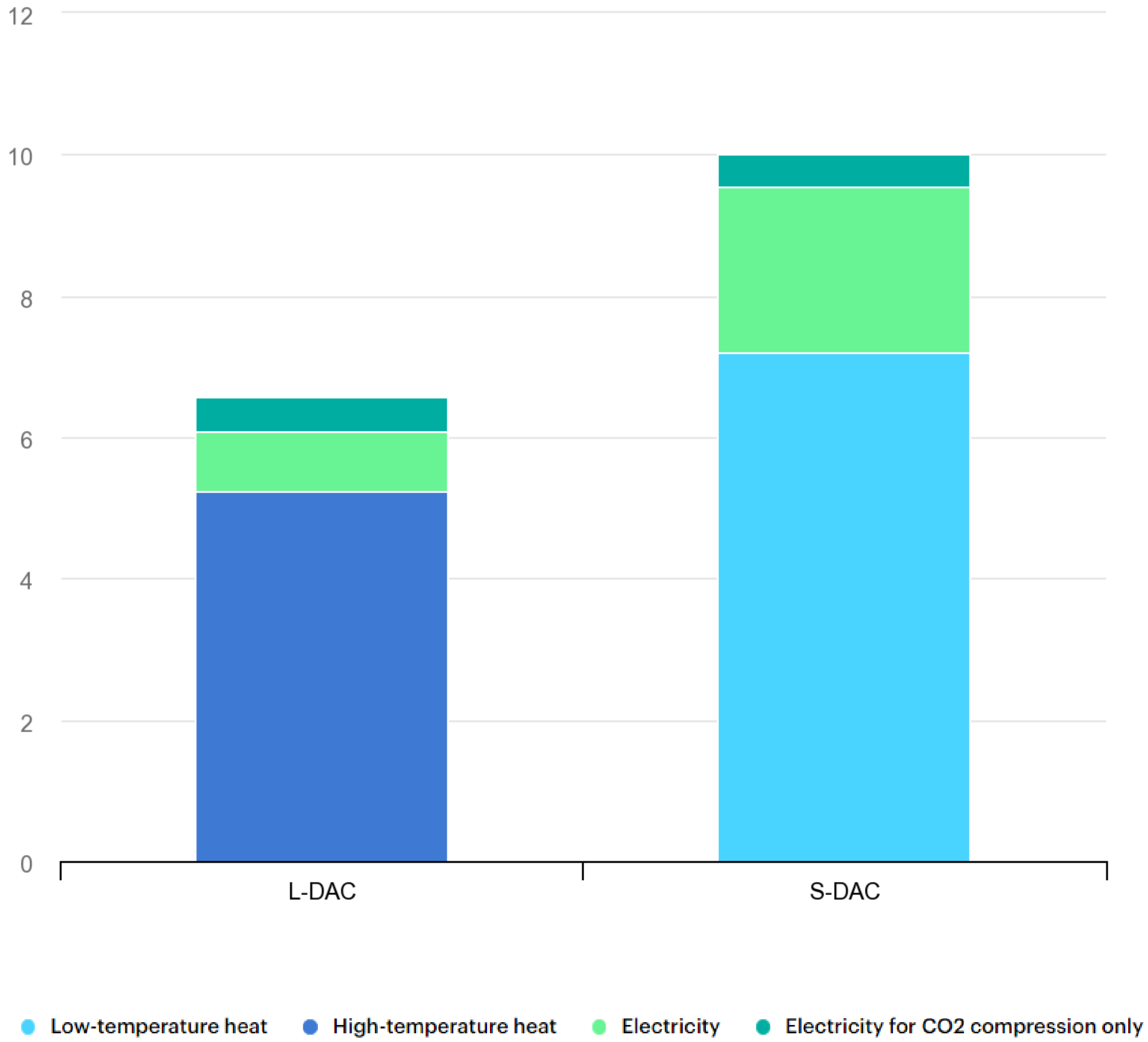

Figure A. 2 A comparison of the various energy requirements, including heat, electricity and electricity for compression, for Liquid DAC (HT-DAC) and Solid DAC (Low-temperature DAC).

A.3 The phase diagram of pure CO_2 based on the temperature and pressure

The phase diagram for pure CO_2 is based on temperature (T) and pressure (P). For the transportation of CO_2, the aim is to have a single state. For transportation via pipeline, this is the supercritical phase, and for transportation by ship, truck and train this is the liquid state. For the liquid state, the size of the vessel in which the CO_2 is transported determines the temperature and pressure.

Transportation Mean	Typical Operating Temperature	Typical Operating Pressure	Transport Phase of CO_2
Onshore Pipeline	10 ˚C – 44 ˚C	85 bar – 150 bar	Dense phase (Supercritical)
Offshore Pipeline	12 ˚C – 44 ˚C	Min of 78 bar	Dense phase (Supercritical)
Ship	-60 ˚C – -40 ˚C	5.2 bar - 17 bar	Liquid phase
Train (rail tankers)	-20 ˚C	26 bar	Liquid phase
Truck	-30 ˚C – -20 ˚C	17 - 26 bar	Liquid phase

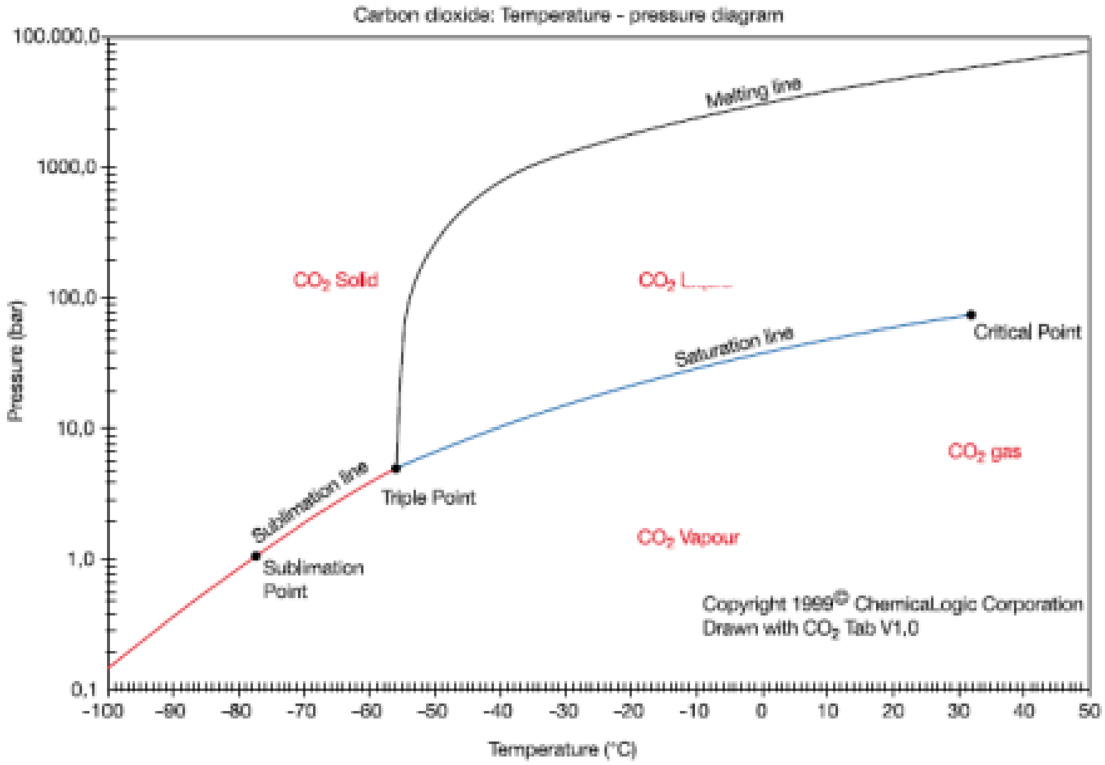

Figure A. 3 The phase diagram for CO_2 based on alternating temperatures and pressures

Appendix B: Exploring and Quantifying the Horizontal Supply Chain

B.1 The Assumptions of the Various Research on CO_2 Transportation

Psarras et al. (2020)

Assumptions Truck and Pipeline Transport:

(i) The CO_2 is transported at 1.7 MPa and -30 ˚C, however, the liquefaction costs associated with the desired conditions, primarily related to the energy consumption of approximately 111 kWh/tonne CO_2, are part of the costs associated with the CO_2 capture process (in their research a DAC plant).

(ii) the maximum hauling payload per delivery truck is set at 20 tonnes of CO_2 and the trucks can drive a maximum of 100.000 miles per anum.

(iii) The costs for fuel consumption are $0.3166 per mile for a full truck (during delivery) and $0.2468 per mile for post-delivery transit (return after delivery).

(iv) The labour costs are $ 20/hr assuming an average speed of 38 mph and accounting for an additional waiting hour during load transfer.

(v) General maintenance of the truck and the replacement of tires are calculated at $0.886 and $0.0477 per mile travelled.

(vi) The purchase price of one truck is $175.000 and is serviceable for 5 years (additional trucks must be added when the earlier stated constraint of 100.000 miles per year is exceeded).

(vii) The plant lifetime (and consequently also the transportation system) is set to 30 years.

(viii) Apart from assumptions i-vii, it must be noted that the study does not take into account escalation factors such as labour, elevation, and material costs and that it uses prices/values based on the U.S. economy.

(ix) The costs for transporting CO_2 via onshore pipelines are based on a compression requirement of 100 bar, which is reached using five stages of interstage cooling, a compression ratio of 1.76, and isentropic efficiency of 0.75 (a measure of the degradation of energy).

(x) The total energy required for this process is calculated to be 140 kWh/tonne of CO_2.

Additional Conclusions:

(i) When a delivery closes in on the maximum capacity, both in terms of distance (100.000 miles total travel per year) and maximum capacity (20 tonnes of CO_2) for each trip, economies of scale are optimized.

(ii) Their cost estimate for the transportation of CO_2 via trucks is claimed to be reliable within 19%.

(iii) Their cost estimate for the transportation of CO_2 via onshore pipelines is claimed to be reliable within 12%.

Zero Emissions Platform (2010)

Assumptions for Pipeline and Ship Transport:

(i) A capacity of 2.5 Mtpa is used based on the scale of CCS demonstration projects and a capacity of 20 Mtpa is used based on the expected size of future commercially-driven CCS networks.

(ii) Both capacities are assumed to have a lifetime of 40 years.

(iii) The costs are based on the assumption of point-to-point connections, as such, costs of capturing are attributed to the capturing process and not to transportation, however, liquefaction costs are included for ships at both the 2.5 and 20 Mtpa capacity.

(iv) The assumed electricity costs throughout the study are set at €0.11/kWh.

(v) The ships are fueled by either LNG or conventional marine diesel oil and for both fuels, a cost assumption of 514 USD/tonne was used.

(vi) The CO_2 is assumed to be delivered (at the CCS / EOR site) at 110 bar and ambient temperature.

(vii) For all transportation means it is assumed that the CO_2 is delivered, before transport, at 60 bar and a temperature of 10 C.

(viii) The ship size is optimized for each transport assignment, with a minimum and maximum cargo capacity of 10.000 m^3 respectively 40.000 m^3 CO_2 per ship.

(ix) The calculated costs are based on the assumption of full capacity utilisation from day one,

(x) In ships, the CO_2 is transported at approximately 8 bar and -55 ˚C.

(xi) The annual operation and maintenance (O&M) costs for all transportation means are set equal to 6% of the total capital costs.

Dursut & Joos (2018)

Assumptions for Ship Transport:

(i) An electricity price (for compression and liquefaction) of £ 0.08/kWh is used

(ii) Ships with a capacity of 10 ktCO_2 are used (they also specify the CAPEX associated with ships with a capacity in the range of 2 – 50 ktonnes of CO_2)

(iii) A fuel price of £ 279/tonne of LNG is used

(iv) The lifetime of a ship is 20 years which is used as the lifetime of the system.

Kujanpää et al. (2011)

Assumptions for Ship Transport:

(i) The transportation distance is set to 1950 km (one way) based on off-shore CCS storage.

(ii) An average cruising speed of 30 km/h is used, and to this end, the journey would take over 9 days.

(iii) On- and off-loading rates of 1000 tonnes of CO_2/h are used.

(iv) A tanker with 40.000 tonnes of CO_2 capacity is used

(v) The system lifetime is 30 years however the ship investment is depreciated over 15 years.

(vi) The CO_2 is transported at 10 ˚C and 8 – 11 MPa.

L. Gao et al. (2011)

Assumptions for Train, Pipeline and Ship Transport:

(i) For CO_2 transportation by rail, they use already existing rail infrastructure with a distance of 598 km from point A to B.

(ii) For the usage of onshore pipelines, they assume a direct pipeline of 300 km from point A to B.

(iii) For the usage of ships, they also use a distance of 300 km.

(iv) 4.000 tonnes of CO_2 need to be handled every day (from CO_2 source to sink), which corresponds to a required capacity of 1.46 Mtpa.

(v) The onshore pipeline operates at an average temperature of 14 ˚C and with in- and outlet pressures of 15.2 and 10.3 MPa respectively

(vi) Ship transport is done in semi-pressurised vessels at pressures near the triple point (0.65 MPa and -52 ˚C).

(vii) Based on the 4000 tonnes of CO_2 that need to be handled per day and the density of CO_2 at the stated operating conditions ($\rho = 1162$ kg/m^3), ships with vessels of 3600 m^3 are used.

(viii) A tanker speed of 33 km/h and a loading time of 25.1 hours are assumed and based on these assumptions there are 3 ships needed to match the daily demand.

(ix) The rail costs are based on Chinese tariffs but are not further specified in their research.

B.2 Cost conversions for CO_2 Transportation Means

Cost provided in the literature	**Metric provided in the literature (year of literature)**	**Conversion**	**The Metric used in this work: € per tonne CO_2 (2020) for specific distances in km**	**Reference(s) in which costs are specified**
Various costs for transporting CO_2 by truck and onshore pipeline based on the quantity and distance of transport	US$ per tonne CO_2 (2020) for specific distances in miles	Miles to km: 1.609 US$ in 2020 to € in 2020: 0.877	Given costs multiplied by 0.877 Given miles divided by 1.609	(Psarras et al., 2020)
Various costs for transporting CO_2 by onshore pipeline, offshore pipeline and ships based on the quantity and distance of transport	€ per tonne CO_2 (2010) for specific distance in kilometres	€ in 2010 to € in 2020: 1.130	Given costs multiplied by 1.13	(Zero Emissions Platform, 2010)
Various costs for transporting CO_2 by ship, rail and onshore pipeline based on the quantity and distance of transport	Chinese Renminbi (¥) per tonne CO_2 for a specific distance in kilometres	¥ in 2011 to ¥ in 2020: 1.21 ¥ in 2020 to € in 2020: 0.127	Given costs multiplied by 1.21 and 0.127	(L. Gao et al., 2011)
Generalised cost for transporting CO_2 by ship over 200 km and 500 km with a quantity of 0.5 Mtpa and 5 Mtpa	British pounds (£) per tonne of CO_2 (2018) for specified distances	£ in 2018 to £ in 2020: 1.03 £ in 2020 to € in 2020: 1.125	Given costs multiplied by 1.03 and 1.125	(Durusut & Joos, 2018)
Costs for transporting 5 – 40 Mtpa of CO_2 by truck over 60 and 250 km	€ per tonne CO_2 (2010) for specific distance in kilometres	€ in 2010 to € in 2020: 1.130	Given costs multiplied by 1.13	(Fu et al., 2010)
Costs for transporting a range of (small) capacities over distances larger than 100 km	€ per tonne CO_2 (2019) for specific distance in kilometres	€ in 2019 to € in 2020: 1.130	Given costs multiplied by 1 (inflation not significant)	(Fasihi et al., 2019)
Costs for transporting 0.73 and 7.3 Mtpa of CO_2 by onshore pipelines over 100 and 500 km	US$ per tonne CO_2 (2005) for specific distance in kilometres	US$ in 2005 to US$ in 2020: 1.33 US$ in 2020 to € in 2020: 0.877	Given costs multiplied by 1.33 and 0.877	(McCollum & Ogden, 2006)
Costs for transporting 3 Mtpa of CO2 by ship over 1950 km	€ per tonne CO_2 (2011) for specific distance in kilometres	€ in 2011 to € in 2020: 1.10	Given costs multiplied by 1.10	(Kujanpää et al., 2011)

B.3 Calculations to Determine Economies of Scale for CO_2 Transportation Means

Based on Table 4, the research by McCollum & Ogden (2006), Psarras et al. (2020) and the Zero Emissions Platform (2010), provide cost estimations for alternating distances and quantities. Consequently, a comparison can be made between the costs of transporting CO_2 over the same distance but with increased capacity, and as such, determine whether and to what extent these transportation means could benefit from economies of scale advantages. This assessment of economies of scale is done by equations (i) and (ii).

(i) $\Delta Q_{capacity} = \frac{(Q_{high} - Q_{low})}{Q_{low}} * 100$ = Percentual **increase** in transportation capacity (%)

(ii) $\Delta C = \frac{(C_{lowQ} - C_{highQ})}{C_{lowQ}} * 100$ = Percentual **decrease** in per unit costs (%)

To calculate whether, and to what degree, the possible CO_2 transportation means follow the economies of scale function, the following equations are used; Q_{high} is the increased capacity of a network (in Mtpa), Q_{low} is the small capacity of a network (in Mtpa), C_{lowQ} are the costs to transport the lower capacity over a specific distance (in €/tonneCO_2), and C_{highQ} are the costs associated with transportation of the higher capacity over the same distance as C_{lowQ} (in €/tonneCO_2). Both the quantity and costs are obtained from Table 4.

$\Delta Q_{capacity} = \frac{(Q_{high} - Q_{low})}{Q_{low}} * 100$ = Percentual **increase** in transportation capacity (%)

$\Delta C = \frac{(C_{lowQ} - C_{highQ})}{C_{lowQ}} * 100$ = Percentual **decrease** in per unit costs (%)

For ships:

- The values that include liquefaction costs at 2.5 Mtpa capacity are used since these are also included in the costs at 20 Mtpa capacity
- $\Delta Q_{capacity}$ = (20 – 2.5) / 2.5 * 100% = 700%
- ΔC (180 km): (15.3 – 12.5) / 15.3 * 100% = 18.3%
- ΔC (500 km): (16.7 – 13.8) / 16.7 * 100% = 17.4%
- ΔC (750 km): (18.0 – 14.9) / 18.0 * 100% = 17.2%
- ΔC (1500 km): (22.4 – 18.2) / 22.4 * 100% = 18.8%

For offshore pipelines:

- $\Delta Q_{capacity}$ = (20 – 2.5) / 2.5 * 100% = 700%
- ΔC (180 km): (10.5 – 3.8) / 10.5 * 100% = 63.8%
- ΔC (500 km): (23.1 – 6.8) / 23.1 * 100% = 70.6%
- ΔC (750 km): (32.4 – 9.3) / 32.4 * 100% = 71.3%
- ΔC (1500 km): (58.4 – 18.4) / 58.4 * 100% = 68.5%

For onshore pipelines:

- $\Delta Q_{capacity}$ = (20 – 2.5) / 2.5 * 100% = 700%
- ΔC (180 km): (6.1 – 1.7) / 6.1 * 100% = 72.1%
- $\Delta Q_{capacity}$ = (7.3 – 0.73) / 0.73 * 100% = 900%
- ΔC (100 km): (7.9 – 1.7) / 7.9 * 100% = 78.5%
- ΔC (500 km): (50.9 – 11.4) / 50.9 * 100% = 77.6%

For trucks:

- $\Delta Q_{capacity}$ = (0.01 – 0.001) / 0.001 * 100% = 900%
- ΔC (32.2 km): (47.4 – 7.0) / 47.4 * 100% = 85.2%
- ΔC (80.5 km): (50.0 – 9.6) / 50.0 * 100% = 80.8%
- ΔC (160.9 km): (53.5 – 14.0) / 14.0 * 100% = 73.8%
- $\Delta Q_{capacity}$ = (0.1 – 0.01) / 0.01 * 100% = 900%
- ΔC (32.2 km): (7.0 – 3.5) / 7.0 * 100% = 50.0%
- ΔC (80.5 km): (9.6 – 7.5) / 9.6 * 100% = 21.9%
- ΔC (160.9 km): (14.0 – 14.0) / 14.0 * 100% = 0.0%

B.4 Cost- and Unit Conversions for H_2O Consumption

Cost provided in the literature	Metric provided in the literature (year of literature)	Conversion	The Metric used in this work	Reference(s) in which costs are specified
The generalized cost price of desalinized seawater (and its flowrate) that can be used for syngas production by co-electrolysis using HT-SOEC technology	€ (2011) per m^3 of desalinized water Inlet flowrate of H_2O in kg/hr	€ in 2011 to € in 2020: 1.10 Kg/hr to m^3/hr: 997 kg/m^3 (atmp & 20 ˚C)	Given costs multiplied by 1.1 Given quantity divided by 997	(Redissi & Bouallou, 2013) based on (Graves et al., 2011)
A generalized cost price of deionised H_2O that can be used for the production of syngas by HT-SOEC technology	€ (2010) per tonne of deionised water Inlet flowrate of H_2O in kg/day	€ in 2010 to € in 2020: 1.13 and tonnes to m^3: 0.997 Kg/day to m^3/hr: 997 kg/m^3 (atmp & 20 ˚C) – day to hr: 24	Given costs multiplied by 1.13 and multiplied by 0.997 Given quantity divided by 997 and divided by 24	(Fu et al., 2010)
A generalized cost price of water from a water supply network to produce syngas via a zinc/zinc-oxide cycle in a desert area	US$ (2014) per litre of water The output of syngas in kg/hr (no ratio so not possible to convert)	US$ in 2014 to US$ in 2020: 1.09 US$ in 2020 to € in 2020: 0.877 Litre water to m^3 water: multiply by 1000	Given costs multiplied by 1.09 and 0.877 to have € (2020)/L And multiplied by 1000 to obtain € (2020)/m^3	(Nicodemus et al., 2014)
A specification of the water requirements of an HT-SOEC co-electrolysis unit that produces syngas with a molar ratio of 2 H_2:CO	147 tonnes of syngas per year and 1.13 kg of H_2O per kg of syngas	Tonnes of syngas per year to m^3 of syngas per hour m^3 of syngas per hour to m^3 of water per hour	Given quantity divided by 365 and 24 (and multiplied by 1000) Multiply by 1.13 to obtain the required amount of kg H_2O per hour, and divide by the density of H_2O to obtain m^3/hr	(Schreiber et al., 2020)

B.5 Cost- and Unit Conversions for H_2O Consumption

The fixed and variable costs of water consumption. The costs are based on four ranges of consumption for the Netherlands specifically (based on Waternet (2022)).

Consumption (m^3)	**Year**	**Fixed Costs (€)**	**Flexible Costs (€/m^3)**
0-1.000	2020	75,28	0,79
	2021	76,42	0,83
	2022	82,82	0,87
1.000-10.000	2020	605,00	0,79
	2021	610,00	0,83
	2022	660,27	0,87
10.000-100.000	2020	4.865,00	0,79
	2021	4.940,00	0,83
	2022	5.350,37	0,87
>100.000	2020	39.500,00	0,79
	2021	40.010,00	0,83
	2022	43.355,58	0,87

These costs are based on a point-to-point connection and are divided into fixed costs and flexible costs. They do not include a 9% tax rate yet, which should be paid over the total costs. Furthermore, there is an additional cost, of 0.359 €/m^3, for the first 300 m^3 of water that is used (Waternet, 2022).

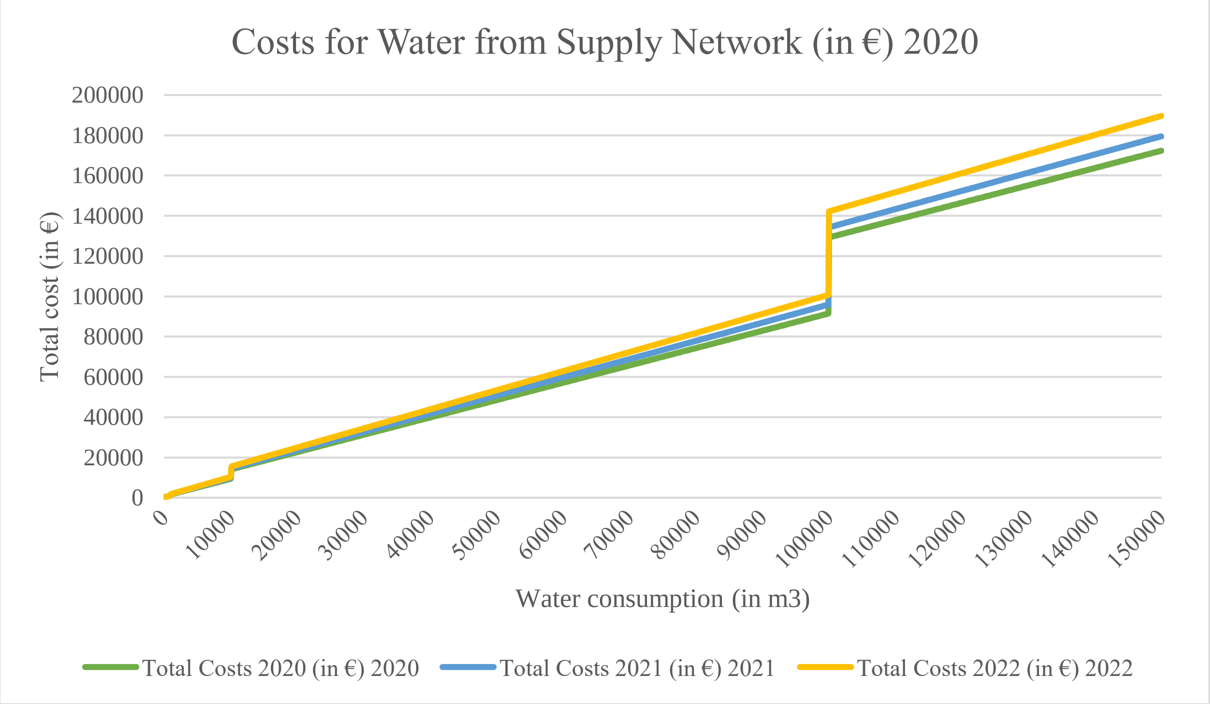

Figure A. 4 The calculated costs for water supplied by the Dutch water supply network in the years 2020, 2021 and 2022, based on the information provided by (Waternet, 2022).

B.6 Comparison of The Average Price per m3 of Water for European Countries

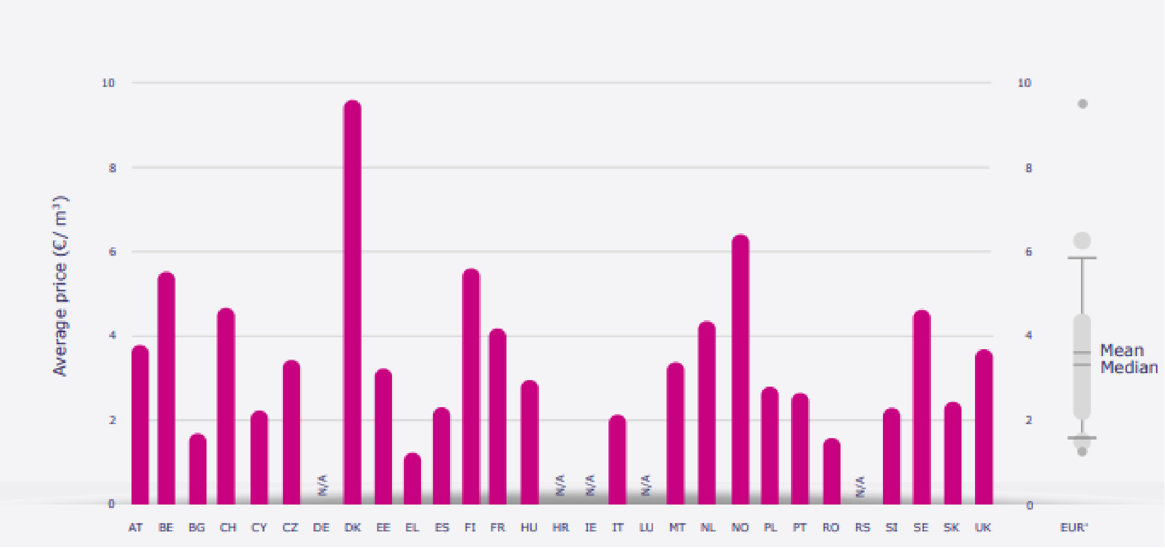

Figure A. 5 The average price of water in various European countries, based on an average consumption per household of 105 m^3/year.

Figure A. 6 The composition (in %) of the water tariffs in various European countries, categorised into water services (delivery), wastewater services, environment & resource fees, value-added tax (VAT), and others (such as additional taxes, fees or rainwater charges).

The combination of these two figures is used to validate the water prices that have been provided by Waternet (2022).

B.7 Cost and unit conversions for DAC

The conversion of the energy requirements for DAC processes. In the third column, T stands for Total, Th stands for thermal, E stands for electric, and C stands for compression.

Provided Operating Requirements	**Conversion**	**Converted Operating requirements (kWh/tCO$_2$)**	**Ref.**
1786-3014 (T), 1420-2250 (Th), 366-764 (E) in kWh/tCO$_2$	n.a.	1786-3014 (T), 1420-2250 (Th), 366-764 (E)	(Fasihi et al., 2019)
6.6 (T), 5.3 (Th), 0.8 (E), 0.5 (C) in GJ/tCO$_2$	Multiply by 277.8	1833 (T), 1472 (Th), 222 (E), 139 (C)	(Budinis, 2022)
2000 (T), 1500 (Th), 500 (E)	n.a.	2000 (T), 1500 (Th), 500 (E)	(Schreiber et al., 2020)

The conversion of the CAPEX and OPEX of the HT-DAC processes, which have been provided in the literature.

Costs and operating parameters provided in the literature	**The Metric provided in the literature**	**Conversion**	**The Metric used in this work**	**Ref.**
The CAPEX and OPEX of an HT-DAC unit that can capture 1-3 Mtpa based on a 25-year lifetime, an electricity price of 50 €/MWh$_{el}$, an inlet concentration of 400 ppm, ambient absorption temperature, 900 ˚C desorption temperature, the outlet pressure of 1 bar, outlet concentration of >97% purity	€ (2020) per tonne of CO$_2$ & OPEX is a percentage of CAPEX	n.a.	€ (2020) per tonne of CO$_2$ & OPEX is a percentage of CAPEX	(Fasihi et al., 2019)
The CAPEX and OPEX of an HT-DAC unit that can capture 1 Mtpa based on a 25-year lifetime, an electricity price of 27-54 €/MWh, an inlet concentration of 400 ppm, ambient absorption temperature, 900 ˚C desorption temperature, the outlet pressure of 10 or 150 bar, outlet concentration of 97.1 % purity	US$ (2016) per tonne of CO$_2$ & OPEX is a percentage of CAPEX GJ/tCO$_2$	S$ (2016) to US$ (2020): 1.08 US$ (2020) to in € (2020): 0.877 GJ/tCO$_2$ to kWh$_{th}$/tCO$_2$: 277.8	Provide costs multiplied by 1.08 and multiplied by 0.877 Provided energy requirement multiplied by 277.8	(Keith et al., 2018)
The CAPEX and OPEX of an HT-DAC unit that can capture 0.1 Mtpa are based on the information provided by Keith et al. (2018), who state that the energy intensity is approximately equal, whilst the CAPEX is 80% higher for a 1 Mtpa HT-DAC unit	€ (2020) per tonne of CO$_2$ & OPEX is a percentage of CAPEX	CAPEX for 1 Mtpa to CAPEX for 0.1 Mtpa: 1.80	Converted costs from Keith et al. (2018) divided by 1.80	Calculated based on (Keith et al., 2018)

B.8 Cost and unit conversions for PCC

The conversion of the energy consumption, the CAPEX, the OPEX (non-energy), and energy costs associated with the various point sources for which PCC technology can be used to provide a CO_2 feedstock.

Costs and units provided in the literature	The Metric provided in the literature	Conversion	The Metric used in this work
Energy consumption for the separation process	Provided in MMBTU	MMBTU to MWh: 0.29	MWh. Provided quantity multiplied by 0.29
CAPEX of PCC technology for the various types of point sources. Costs are based on amine absorption as a separation technique, compression to the supercritical phase (i.e. ready for pipeline transport), a 90% capture efficiency, electricity prices of 50 US$/MWh,	CAPEX in US$ (2019) per tonne of CO_2 captured OPEX in US$ (2019) per tonne of CO_2 captured	US$ (2019) to US$ (2020): 1.01 US$ (2020) to € (2020): 0.877	€ (2020) per tonne CO_2 captured Provided cost multiplied by 1.01 and multiplied by 0.877
(Non-energy) OPEX of PCC technology for the various types of point sources. Costs consist of annual fixed costs (taxes, insurance, overhead, salaries), semi-variable costs (repairs, maintenance, overhauls), variable non-energy costs (replacement of process chemicals, water, water treatment), variable energy costs	OPEX in US$ (2019) per tonne of CO_2 captured	US$ (2019) to US$ (2020): 1.01 US$ (2020) to € (2020): 0.877	€ (2020) per tonne CO_2 captured Provided cost multiplied by 1.01 and multiplied by 0.877

B.9 Delineating Syngas Properties

The table below identifies several properties of NG[9], H_2 and CO (obtained from The Engineering ToolBox (2022a) and The Engineering ToolBox (2022b)) and the properties of syngas that have been calculated, respectively that have been provided by other research. The properties of NG are included in the table for comparison purposes. Moreover, the research by Schreiber et al. (2020), provides the properties of syngas with a molar ratio of 2 H_2:CO at a temperature of 40 ˚C and a pressure of 20 bar. The syngas in their research consists of 66.4 mol% of H_2, and 33.2 mol% of CO and the remaining 0.4 mol% is composed of a combination of CO_2, nitrogen, H_2O and hydrocarbons. They report a density (ρ) of 0.481 kg/m^3 (at a given temperature and pressure) and a lower heating value (LHV) of 23.59 MJ/kg, which corresponds to an LHV of 11.35 MJ/m^3. Since these properties are based on a temperature and pressure that are different from the standard temperature and pressure (STP = 1 atmospheric pressure (= 1.01325 bar) and a temperature of 0 ˚C), a comparison between syngas compositions at different pressures and temperatures would not be valid. Consequently, these properties are calculated for "pure" syngas, solely consisting of H_2 and CO, with a ratio of 2 H_2:CO. Based on this ratio, the molar mass of "pure" syngas (M_{syngas}) can be calculated via Equation (i). It must be noted that syngas is a mixture of gases, consequently, the ideal gas law for a gas mixture, provided by The Engineering ToolBox (2022c), and represented as Equation (ii), should be used for further calculations. To calculate the density for the "pure" syngas, Equation (iii) is used, resulting in a density of 0.473 kg/m^3 which is close to the density of 0.52 kg/m^3 which was calculated for an "unpure" syngas mixture containing traces of H_2O and CO_2. Furthermore, the HHV (=12.18 MJ/m^3) and LHV (=12.01 MJ/m^3) of syngas can be calculated via Equations (iv) and (v), in which wt%H_2 (=12.48%) and wt%CO (=87.52%) are the weight percentages of H_2 and CO in syngas, which can be obtained via equation (xiv).

(i) $M_{syngas} = 2 * M_{H_2} + M_{CO}$

(ii) $p * V = m_m * R_m * T$

(iii) $\rho_m = \frac{\rho_1 v_1 + \rho_2 v_2 + \cdots + \rho_n v_n}{v_1 + v_2 + \cdots + v_n}$

(iv) $HHV_{syngas} = wt\%H_2 * HHV_{H_2} + wt\%CO * HHV_{CO}$

(v) $LHV_{syngas} = wt\%H_2 * LHV_{H_2} + wt\%CO * LHV_{CO}$

(vi) $wt\%_x = \frac{M_x}{M_{syngas}} * 100\%$

With p = absolute pressure in the mixture (N/m^2), V = volume of the mixture (m^3), m_m = mass of the mixture (kg), R_m = the individual gas constant for the mixture (J/kg K), T = absolute temperature in the mixture (°K), $m_1 + m_2 + \ldots + m_n$ = the mass of each gas component in the mixture (kg), ρ_m = density of the gas mixture (kg/m^3), $\rho_1 \ldots \rho_n$ = density of each of the components (kg/m^3), $v_1 \ldots v_n$ = volume share of each of the components (m^3) (v = 22.04 dm^3 per mol at STP).

Properties/Gas to be transported	**NG (STP)**	**H_2 (STP)**	**CO (STP)**	**Syngas 2H_2:CO (STP) (calculated)**	**Syngas 2H_2:CO (1 bar, 25 ˚C) (Aspen Plus)**	**Syngas 2H_2:CO (20 bar, 40˚C) (literature)**
Molar mass (M)	-	2.016 g/mol	28.01 g/mol	32.04 g/mol	-	n.a.
Density	0.777 kg/m^3	0.090 kg/m^3	1.24 kg/m^3	0.473 kg/m^3	0.52 kg/m^3	0.481 kg/m^3

---

[9] The values for NG are obtained from The Engineering ToolBox (2022b), who base these numbers on NG in the U.S. market. Which, according to their web page, consists of a mixture of several different compounds which may vary in quality between seasons and markets. This varying quality may give heating values within a range of 5-10% higher and lower than the given value. may vary in quality between seasons and markets.

Individual gas constant (R)	518.28 J/kg K	4124.2 J/kg K	296.48 J/kg K	-	-	-
The individual gas constant of a mixture (R_m)	-	-	-	774.18 J/kg K		
HHV	40.6 MJ/m^3 14.5 kWh/kg 52.2 MJ/kg	12.7 MJ/m^3 39.4 kWh/kg 141.7 MJ/kg	12.035 MJ/m^3 - -	12.18 MJ/m^3 - 25.75 MJ/kg	-	12.21 MJ/m^3 - -
LHV	36.6 MJ/m^3	10.8 MJ/m^3	12.035 MJ/m^3	12.01 MJ/m^3	-	11.35 MJ/m^3

When comparing the calculated values for syngas with the values that are provided by Schreiber et al. (2020), it can be seen that there is a small difference in the HHV values and a larger difference in the LHV value and the respective densities. The small difference in the HHV values can be explained by the 0.4 mol% that partially consists of carbon-containing molecules (CO_2 and hydrocarbons which contribute to the HHV) and the larger difference in LHV can also be explained by the 0.4mol% that partially consists of H_2O, since LHV accounts for the heat that is not recovered from water vapour (The Engineering ToolBox, 2022b), but also by comparing the values for the HHV and LHV that have been provided. Moreover, according to The Engineering ToolBox (2022a), the HHV and LHV of CO are equal. Since CO has a wt% of 87.52% which is significantly more than the wt% of H_2, the difference between the HHV and LHV will also be smaller. The temperature and pressure that have been used in the research by Schreiber et al. (2020) differ from the STP, in combination with the 0.4mol% that consists of a combination of other molecules, this could explain the differences in density. However, when the alternating temperature and pressure, in combination with $M_{syngass} = 32.04$, are used in Equation (ii), the resulting ρ_{syngas} is 24.6 kg/m^3. This is much higher than the density that is provided by Schreiber et al. (2020). Consequently, calculations are strictly related to the ratio and composition of syngas, in this work $\rho_{syngas} = 0.473$, is used for calculations.

B.10 Quantification of the Syngas Market

The quantifications of the syngas market in GW, which have been provided in section 4.2.3.1 (and provided in the table below), are extrapolated to provide an estimate of the global syngas market size in GW. This estimation is provided in Figure A. 7 below.

Research by (Year of publication)	**Global Market Size (2020)**	**European Market Size (2020)**	**Compound Annual Growth Rate in % [period]**
Inkwood research (2018)	Billion € 158 171 GW	Billion € 35 38 GW	9.52 [2017-2026]
IMARC (2021)	280 GW	62 GW	10.3 [2022-2027]
ReportLinker (2022)	170 MM Nm^3-syngas/h	37 MM Nm^3-syngas/h	>11 [2022-2027]
Stratas Advisors (2018)	750 GW	165 GW	8.25 [2018-2024], 13 [2024-xxxx]

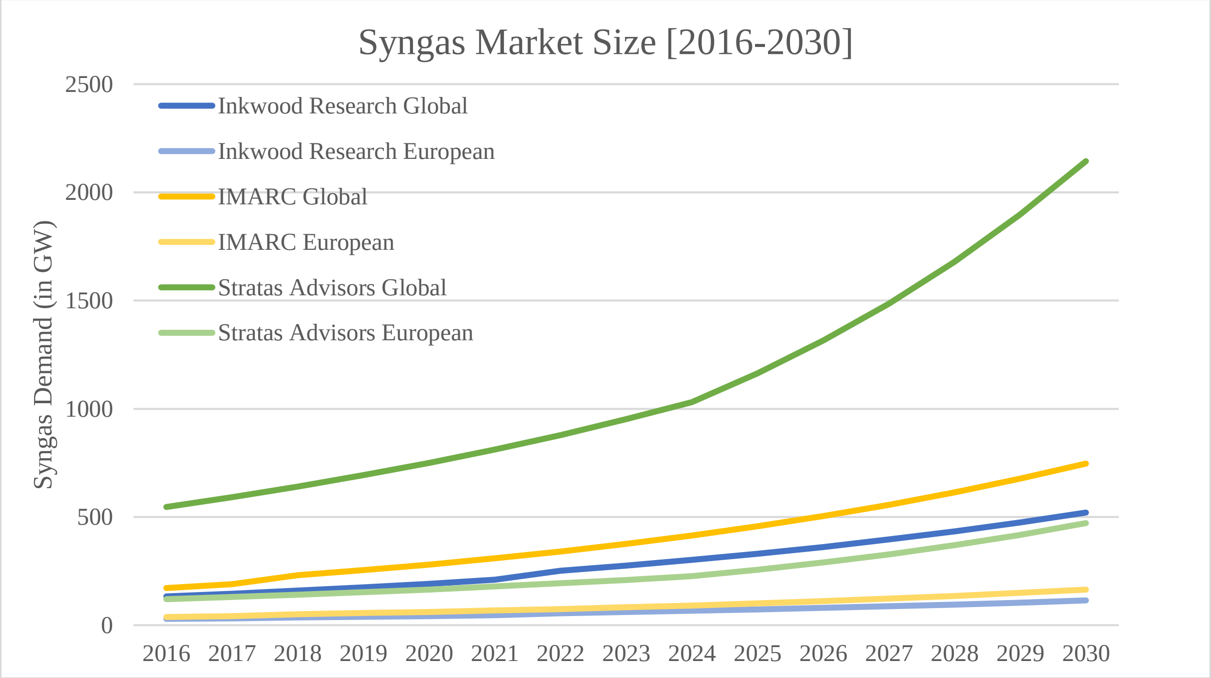

Figure A. 7 The estimated global/European market size (in GW) that has been provided below, is based on the quantities and compound annual growth rates that have been provided in the various market reports.

B.11 Overview of Theoretical and Practical Limitations

An overview of the limitations of the individual supply chain units that have been found and calculated.

	CO_2ER supply chain	
	Theoretical Limitations	**Practical Limitations**
Feedstock Availability	• CO_2 qty. available at point sources (& purity) • CO_2 qty. available in atmospheric air (at 400 ppm) • Global H_2O availability	• Geographic locations • Lifetime of units • Available qty. at point source multiplied by 90% capture efficiency (U.S.: 1.913 Mtpa, EU: 848 Mtpa) • Surface area required for DAC capture unit – largest currently available 40 m^2 • Water requirements for DAC capture unit • CAPEX & Non-energy OPEX • Energy consumption for the capture process is limited by RE availability • Type of water that is being used
Feedstock and Product Transportation	• CO_2 transport means limited by pressure & temperature • Transportation of H_2O is not limited • Transportation of syngas in existing infrastructure is limited to the specific composition	• Geographic locations (population density, height, close to sea/river) • Availability of existing water supply network • Lifetime of infrastructure • TRL of infrastructure components • Syngas cannot be transported (at a ratio of 2 H_2:CO) • CAPEX & Non-energy OPEX • Energy consumption for transportation processes
Demand	• Upper-limit opposed by the usage of syngas • Lower-limit opposed by the smallest size of SOEC system – production rate • Syngas ratio required by downstream process(es) • Lack of transportation at certain compositions requires the demand location to be close to the production location	• Practical upper-limit opposed by current & future market size (170 MM Nm^3-syngas/h for the global market (2020) and 37 MM Nm^3-syngas/h for the European market (2020)) • Practical lower limit: quantity required for specific downstream processes – EC: 80 kg-syngas/hr (2 H_2:CO) • Syngas price
Production Facility	• SOEC system size: no theoretical limit since modules can be added endlessly • Stack & cell size: theoretically limited but no quantification • Limited to cell degradation – requires replacing	• The largest size currently available: is 140 kW (for H_2) • CAPEX & Non-energy OPEX • Energy consumption for processes limited by RE availability • Low TRL

B.12 Calculations for Global and Local Scale Match

Global Scale Match:

1. 170 MM Nm^3-syngas/hour – multiply by 8760 = **1489 GM Nm^3-syngas/year**
2. Syngas ratio (ass.) 2 H_2:CO – $\rho_{syngas} = 0.473$ kg/Nm^3
3. 1489 GM Nm^3-syngas/year – multiply by $\rho_{syngas} = 704 * 10^9$ kg-syngas/year
4. 1 tonne is 1000 kg – **704 Mtpa**
5. Required CO_2 feedstock (SYNLINK): (730 kg-CO_2/hr / 355 kg-syngas/hr) * 704 Mtpa = **1448 Mt-CO_2 pa**.
6. Required H_2O feedstock (SYNLINK): (560 kg-CO_2/hr / 355 kg-syngas/hr) * 704 Mtpa = **1111 Mt-H_2O pa**.
7. Required CO_2 feedstock (Linde AG): (23.2 kg-CO_2/hr / 16.8 kg-syngas/hr) * 704 Mtpa = **972 Mt-CO_2 pa**.
8. Required H_2O feedstock (Linde AG): (19 kg-CO_2/hr / 16.8 kg-syngas/hr) * 704 Mtpa = **796 Mt-H_2O pa**.
9. Required DAC surface area (SYNLINK) (based on assumptions below): $V_{air,req} / v_{wind} = (1.10 * 10^{13} / 86400) / 2 =$ **64 km^2**
10. Required DAC surface area (Linde AG): $V_{air,req} / v_{wind} = (7.40 * 10^{12} / 86400) / 2 =$ **43 km^2**
11. # of units (of 40 m^2) required (SYNLINK): $64 * 10^6 / 40 =$ **1.6 million units**
12. # of units (of 40 m^2) required (Linde AG): $43 * 10^6 / 40 =$ **1.1 million units**
13. RE input for annual conversion (only HT-SOEC systems) (SYNLINK): 8.14 kWh/kg * (704 * 10^9 kg-syngas) = **5.73 PWh**
14. RE input for annual conversion (only HT-SOEC systems) (Linde AG): 8.82 kWh/kg * (704 * 10^9 kg-syngas) = **6.21 PWh**
15. # HT-SOEC systems required (SYNLINK): (704 * 10^9 kg-syngas/year / (365 * 24)) / 354.8 kg-syngas/hr = **226509 SYNLINK systems of 2890 kW**
16. # HT-SOEC systems required (Linde AG): (704 * 10^9 kg-syngas/year / (365 * 24)) / 16.8 kg-syngas/hr = **4783649 Linde AG systems of 150 kW**

Assumptions DAC Calculations:

(i) A capture area of 40 m^2 is assumed (based on the largest operating DAC unit by Climeworks – it must be noted that this is not HT-DAC technology, however, the size is merely used for comparison purposes)
(ii) An average air speed of 2 m/s is assumed
(iii) The density of air is assumed at $\rho_{air} = 1.184$ kg/m^3 (STP)
(iv) It is assumed that the air has a CO_2 concentration of 400 ppm, which corresponds to 0,608 g-CO_2/kg-air
(v) The capture efficiency is 50%.

Equations DAC calculations (provided in section 4.2.1.1):

(vi) $$V_{\text{air,req}} = \frac{1}{\rho_{air}} * \frac{m_{air}}{m_{CO2,air}} * \frac{m_{CO2,req}}{\eta_{cap}}$$

(vii) $$A_{\text{capture}} = \frac{Volume\ of\ air\ required\ per\ day}{V_{wind}} [m^2]$$

Local Scale Match:

Similar calculations as for the global scale match, however, a production requirement of 80 kg-syngas/hr is used.

1. 80 kg-syngas/hr * 8760 = **700.8 tonnes-syngas/year**

2. Required CO_2 feedstock (SYNLINK): (730 kg-CO_2/hr / 355 kg-syngas/hr) * 701 tpa = **1441 t-CO_2 pa**.
3. Required H_2O feedstock (SYNLINK): (560 kg-CO_2/hr / 355 kg-syngas/hr) * 701 tpa = **1106 t-H_2O pa**.
4. Required CO_2 feedstock (Linde AG): (23.2 kg-CO_2/hr / 16.8 kg-syngas/hr) * 701 tpa = **968 t-CO_2 pa**.
5. Required H_2O feedstock (Linde AG): (19 kg-CO_2/hr / 16.8 kg-syngas/hr) * 701 tpa = **793 t-H_2O pa**.
6. Required DAC surface area (SYNLINK) (based on assumptions below): $V_{air,req}$ / v_{wind} = ($11*10^6$ / 86400) / 2 = **63.5 m^2**
7. Required DAC surface area (Linde AG): $V_{air,req}$ / v_{wind} = ($7.4*10^6$ / 86400) / 2 = **42.6 m^2**
8. # of units (of 40 m^2) required (SYNLINK): 63.5 / 40 = **1.59** (**thus 2 units)**
9. # of units (of 40 m^2) required (Linde AG): 42.6 / 40 = **1.07 (thus 2 units)**
10. RE input for annual conversion (only HT-SOEC systems) (SYNLINK): 8.14 kWh/kg * (701 * 10^3 kg-syngas) = **5.71 GWh**
11. RE input for annual conversion (only HT-SOEC systems) (Linde AG): 8.82 kWh/kg * (701 * 10^3 kg-syngas) = **6.18 GWh**
12. # HT-SOEC systems required (SYNLINK): (701 * 10^3 kg-syngas/year / (365 * 24)) / 354.8 kg-syngas/hr = **0.23 SYNLINK systems of 2890 kW (thus 1 system)**
13. # HT-SOEC systems required (Linde AG): (701 * 10^3 kg-syngas/year / (365 * 24)) / 16.8 kg-syngas/hr = **4.76 Linde AG systems of 150 kW (thus 5 systems)**

Appendix C: CO_2ER Potential from the Horizontal Supply Chain Perspective

C.1 Detailed Calculation and the Assumptions for the Total Investment and Average Annual Cashflow – D1 & D2

1. Syngas demand for single decentralised location: **96.4 ktpa**
2. Number of SYNLINK systems required to meet demand: $96.4 * 10^6 / 354.8 * 8760 =$ **33 units**
3. Required area: 33 * 300 = **9900 m^2**
4. Total capacity: 33 * 2890 kW = **95370 kW**
5. Required quantity of CO_2: 730 / 354.8 * 96,4 = **198 ktpa**
6. Required quantity of H_2O (electrolysis): 560 / 354.8 * 96.4 = **152 ktpa**
7. Required quantity of H_2O (HT-DAC): 4.7 * 198 = **932 ktpa**
8. Total H_2O requirements: 931 + 152 = **1084 ktpa**
9. Electricity requirements electrolyser: $8.14 * (96.4 * 10^6) =$ **784696000 kWh**

CAPEX

10. Electrolyser CAPEX: 2000 * 95370 = 190740000 €
11. HT-DAC CAPEX: $(100 * 10^3 * 365) + (98 * 10^3 * 365) = 72270000$ €
12. **Total CAPEX**: 190740000 + 72270000 = **263010000 €**

OPEX

13. Energy OPEX electrolyser: 784696000 * 0.068 = 53359328 €/year
14. Total OPEX electrolyser: 53359328 / 70 * 100 = 76227611 €/year
15. Non-energy OPEX electrolyser: 76227611 – 53359328 = 22868283 €/year
16. Energy OPEX HT-DAC: $1.46 * 10^3 * 0.068 * 198 * 10^3 = 19657440$ €/year
17. Non-energy OPEX HT-DAC: $13.51 * 198 * 10^3 = 2674980$ €/year
18. Total OPEX HT-DAC: 22331430 €/year
19. Total OPEX single PF: **98559041 €/year**

REVENUE & AVERAGE ANNUAL CASHFLOW

20. Syngas revenue: $96.4 * 10^6 * 0.053 =$ **5109200 €/year**
21. **Average Annual Cashflow**: Revenue – Total OPEX = **-93449841 €/year**

Assumptions

(i) CAPEX electrolyser: 2000 €/kW (Hauch et al., 2020)
(ii) Energy OPEX are 70% of total OPEX (Hauch et al., 2020)
(iii) Electrolyser lifetime: 4.5 years, 2030 8.5 years (Posdziech, 2021)
(iv) CAPEX HT-DAC: 365 €/tonneCO_2 (Keith et al., 2018)
(v) Syngas selling price: 0.053 €/kg (Jouny et al., 2018)
(vi) Electricity price: 0.068 €/kWh (Statista, 2022b)
(vii) Water is free
(viii) Power consumption electrolyser: 8.14 kWh/kg-syngas produced (Sunfire, 2022)
(ix) Operating days per year: 350 (Jouny et al., 2018)
(x) SYNLINK system required area: 300 m^2 (Posdziech, 2021)
(xi) Energy requirements HT-DAC: 1.46 MWh/tonne CO_2 (Keith et al., 2018)
(xii) Heat requirements of HT-DAC are met by excess heat
(xiii) Non-energy OPEX HT-DAC: 13.51 €/tonne CO_2 (Keith et al., 2018)

The calculations that were made for the **five production facilities** combined were similar to those for the single production facility. The average annual cashflow was calculated as follows:

Average Annual Cashflow: 5 * Revenue of single production facility – 5 * Total OPEX Electrolyser – 5 * Total OPEX HT-DAC = **-467249207**

Total Investment: 5 * Total CAPEX of a single production facility = **1315050000**

C.2 Detailed Calculation and the Assumptions for the Total Investment and Average Annual Cashflow – C1 & C2

1. Syngas demand for production facility: **482 ktpa**
2. Number of SYNLINK systems required to meet demand: 482 * 10^6 / 354.8 * 8760 = **162 units**
3. Required area: 162 * 300 = **48600 m^2**
4. Total capacity: 162 * 2890 kW = **468180 kW**
5. Required quantity of CO_2: 730 / 354.8 * 482 = **992 ktpa**
6. Required quantity of H_2O (electrolysis): 560 / 354.8 * 482 = **761 ktpa**
7. Electricity requirements electrolyser: 8.14 * (482 * 10^6) = **3923480000 kWh**

CAPEX

8. Electrolyser CAPEX: 2000 * 468180 = **936360000 €**

OPEX

1. Energy OPEX electrolyser: 3923480000 * 0.068 = **266796640 €/year**
2. Total OPEX electrolyser: 266796640 / 70 * 100 = **381138057 €/year**
3. Non-energy OPEX electrolyser: 381138057 - 266796640 = **114341417 €/year**
4. Costs for CO_2 feedstock: 105.06 * 992 * 10^3 = **104219520 €/year**
5. Cost for CO_2 transportation: see Assumption (vi) = 160 * 0.038 * (991 * 10^3) = **6029619 €/year**
6. Costs for H_2O feedstock: see Assumption (xiv) = **710272 €/year**
7. Total OPEX (excl. transportation): **487097469 €/year**
8. Total OPEX (incl. transportation): **492097469 €/year**

REVENUE & AVERAGE ANNUAL CASHFLOW

1. Syngas revenue: 482 * 10^6 * 0.053 = **25546000 €/year**
2. **Average Annual Cashflow**: Revenue – Total OPEX (excl. transportation) = **- 461 M €/year**
3. **Average Annual Cashflow**: Revenue – Total OPEX (incl. transportation) = **- 467M €/year**

Assumptions:

(i) CAPEX electrolyser: 2000 €/kW (Hauch et al., 2020)
(ii) Energy OPEX are 70% of total OPEX (Hauch et al., 2020)
(iii) Electrolyser lifetime: 4.5 years, 2030 8.5 years (Posdziech, 2021)
(iv) CO_2 supplied by PCC at a steel and iron manufacturing plant
(v) Costs for CO_2 in C2 – cost of capture + cost for transportation
(vi) Transportation cost for CO_2 by pipeline: 0.038 €/tonne-km (Psarras et al., 2020) – assumed 160 km.
(vii) Cost of capture: CAPEX – 23 €/tonne, E-OPEX – 10.88 €/tonne, nE-OPEX – 71.18 €/tonne (includes heat requirements) (E-OPEX based on quantification by National Petroleum Council (2019) (=0.16 MWh/tonneCO_2) & electricity price)
(viii) Total costs per tonne CO_2: 105.06 €/tonneCO_2
(ix) Syngas selling price: 0.053 €/kg (Jouny et al., 2018)
(x) Electricity price: 0.068 €/kWh (Statista, 2022b)
(xi) Power consumption electrolyser: 8.14 kWh/kg-syngas produced (Sunfire, 2022)
(xii) Operating days per year: 350 (Jouny et al., 2018)
(xiii) SYNLINK system required area: 300 m^2 (Posdziech, 2021)
(xiv) Price for H_2O: (39500 + 0.79*Quantity + 0.359*300)*1.09 (Waternet, 2022)

C.3 Adjusting Calculation Parameters

The Average Annual Cashflow and the Total Investment for adjusting the electricity price from 0.068 €/kWh to 0.018 €/kWh.

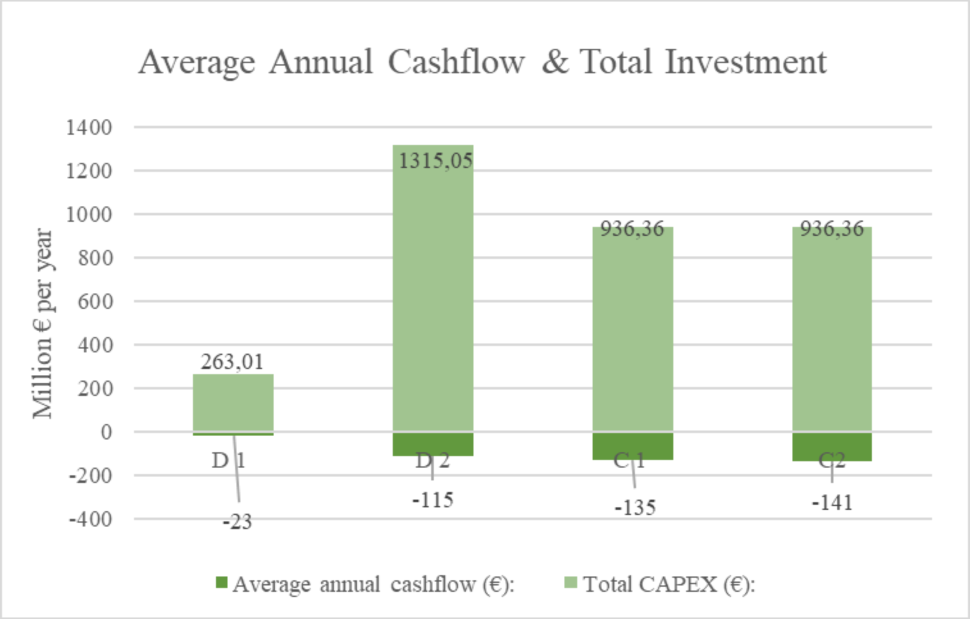

Figure A. 8 The average annual cashflow and the total investment based on the adjusted electricity price.

Appendix D: CO$_2$ER Potential from the Vertical Supply Chain Perspective

D.1 Rating of Critical Materials

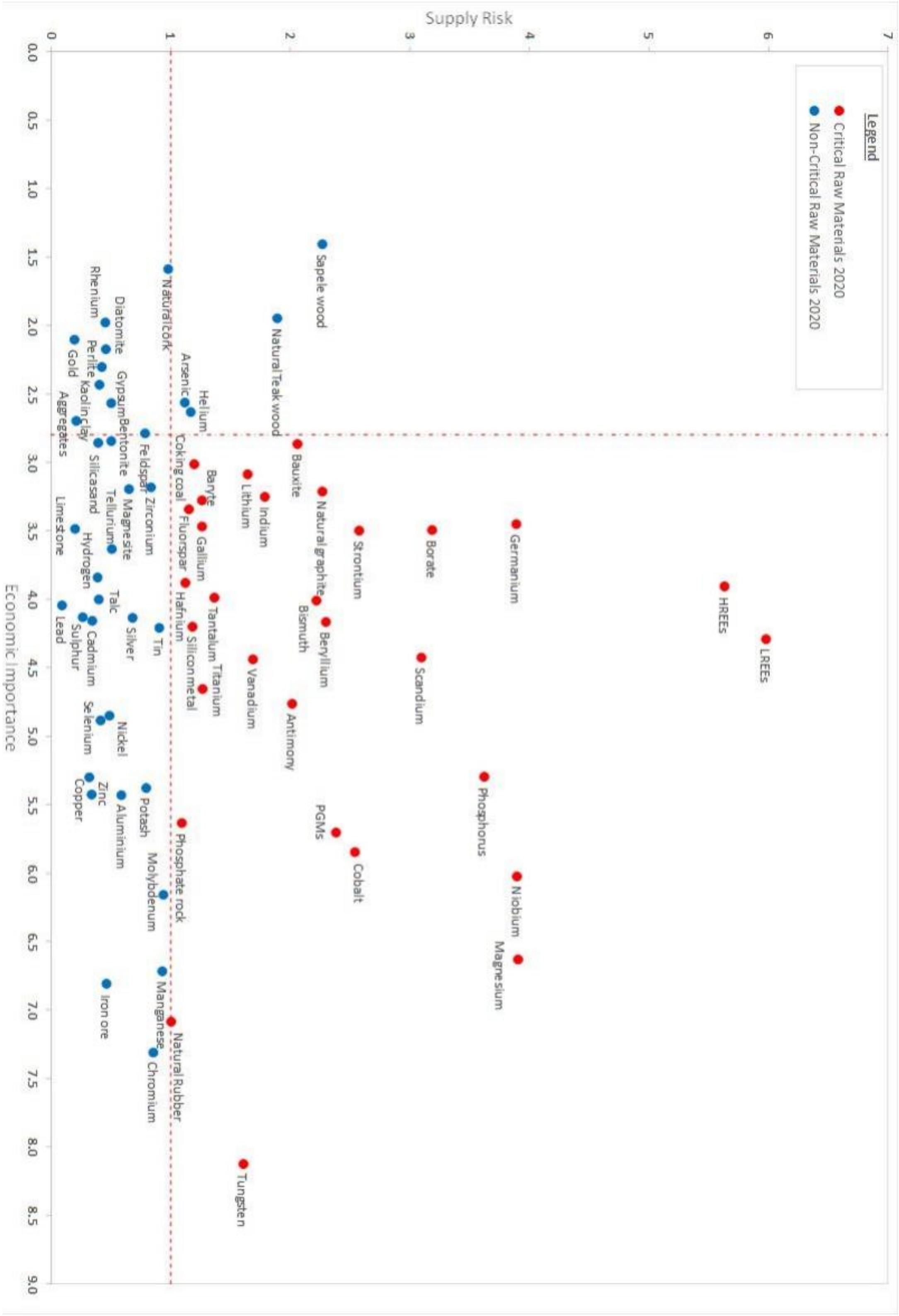

Figure A. 9 The list of critical materials based on their respective ratings on economic importance and supply risk (copied from Blengini et al. (2020)).

D.2 List of Materials that Could be Used in SOEC Technology

The complete list of materials that have been mentioned in the literature in possible SOFC and SOEC applications.

Material (Periodic System)	Common material application(s)	Explanation of application	Mentioned in:
Scandium (Sc)	Scandia (Sc_2O_3)	**Dopant** for zirconia and yttrium (currently highest oxygen ionic conductivity)	(Elder et al., 2015) (Kiemel et al., 2021) (J. B. Hansen, 2015) (HyTechCycling, 2019)
Lanthanum (La)	Doped lanthanum strontium chromite ($La_{0.9}Sr_{0.1}CrO$) (or solely lanthanum chromite $LaCrO_3$)	**Interconnect** to join individual SOECs into a stack (enhanced conductivity as lower valence ions (e.g. Ca, Mg, Sr, etc.) are substituted on either the La or Cr sites.	(Elder et al., 2015) (Kiemel et al., 2021) (HyTechCycling, 2019)
	Lanthanum gallate ($LaGaO_3$)	**Electrolyte** (oxide ion conductivity high enough for technical application)	(Elder et al., 2015)
	Lanthanum gallate doped with strontium and magnesium ($La_{0.9}Sr_{0.1}Ga_{0.8}Mg_{0.2}$) (LSGM)	**Electrolyte** - one of most promising candidates - substantially more expensive than ceria or zirconia - oxide ion conductivity above ceria and slightly below zirconia – faces some problems with formations of La-nitrate by reacting with fuel electrode	(Elder et al., 2015) (J. B. Hansen, 2015) (HyTechCycling, 2019)
	Lanthanum strontium manganite ($La_{1-x}Sr_xMnO_3$) (LSM)	Oxygen **electrode** (i.e. anode or positive) – LSM mixed with solid electrolyte materials (typically YSZ) is most common composite electrode composition (LSM electronic conductor, YSZ added as ionic phase to extend TPB region)	(Elder et al., 2015) (Kiemel et al., 2021) (J. B. Hansen, 2015) (HyTechCycling, 2019)
	Lanthanum strontium ferrite ($La_{0.8}Sr_{0.2}FeO_3$) (LSF) [ET]	Oxygen **electrode** (i.e. anode) – recently more frequently applied than LSM-YSZ composite	(Elder et al., 2015) (J. B. Hansen, 2015) (HyTechCycling, 2019)
	Lanthanum strontium cobalt ferrite (LSCF) or nickelate (LSCN) [ET]	Oxygen **electrode** (i.e. anode) – tested in various mixtures	(Elder et al., 2015) (J. B. Hansen, 2015)
	Lanthanum-doped strontium vanadate (LSV)	Fuel **electrode** (i.e. cathode) -	(J. B. Hansen, 2015)
	Strontium-doped lanthanum manganite partially substituted with chromium (LSCM)	Fuel **electrode** (i.e. cathode) – with 0.5% Palladium (Pd) very effective for CO_2 electrolysis electrodes	(J. B. Hansen, 2015)

	Lanthanum strontium manganese ferrite (LSMF)	Fuel **electrode** (i.e. cathode)	(HyTechCycling, 2019)
	Lanthanum calcium manganite (LCM)	Fuel **electrode** (i.e. cathode) – commonly used in combination with zirconia electrolytes	(HyTechCycling, 2019)
Strontium (Sr)	Niobium-doped strontium titantes (STN)	Fuel **electrode** (i.e. cathode) -	(J. B. Hansen, 2015)
	Lanthanum-doped strontium titantes with ceria (LST-ceria)	Fuel **electrode** (i.e. cathode) -	(J. B. Hansen, 2015)
	Praseodymium strontium manganite (PSM)	Fuel **electrode** (i.e. cathode) -	(HyTechCycling, 2019)
	Praseodymium strontium manganite ferrite (PSMF)	Fuel **electrode** (i.e. cathode) -	(HyTechCycling, 2019)
Yttrium (Y)	Yttrium chromite ($YCrO_3$) [IC]	**Interconnect** to join individual SOECs into a stack	(Kiemel et al., 2021)
	Yttria (or yttrium(III) oxide) (Y_2O_3) (YSZ) [EL]	**Dopant** for pure zirconia to prevent detrimental phase transitions (by stabalising cubic phase); Can also be used as **electrolyte** and uses scandia (YSZ) as dopant	(Elder et al., 2015) (Kiemel et al., 2021) (J. B. Hansen, 2015) (HyTechCycling, 2019)
Ytterbium (Yb)	Ytterbium(III) oxide (Yb_2O_3) [EL]	**Dopant** for pure zirconia to prevent detrimental phase transitions (by stabalising cubic phase)	(Elder et al., 2015)
Zirconium (Zr)	Zirconia (or zirconium dioxide) (ZrO_2) [EL]	**Electrolyte -** oxide ion conductivity high enough for technical application (most widely used)	(Elder et al., 2015) (J. B. Hansen, 2015)
Cerium (Ce)	Ceria (or cerium(IV) oxide) (CeO_2) [EL]	**Electrolyte -** oxide ion conductivity high enough for technical application – not enough stability in reducing atmosphere – see other applications (SDC & GDC)	(Elder et al., 2015) (J. B. Hansen, 2015) (HyTechCycling, 2019)
	Samarium-doped ceria (SDC) ($Sm_{0.2}Ce_{0.8}O_{2-x}$)	**Electrolyte –** shows good performance but under reducing conditions, internal short circuiting occurs which reduces the efficiency and performance of the cell (not suitable for SOEC in current status)	(J. B. Hansen, 2015) (HyTechCycling, 2019)
	Bi-layered gadolinium doped ceria (GDC)	**Electrolyte –** promising performance but at current technological status, decay fast during steam electrolysis	(Elder et al., 2015) (J. B. Hansen, 2015) (HyTechCycling, 2019)
	Bismuth oxide* (Bi_2O_3) [EL]	**Electrolyte** (oxide ion conductivity high enough for technical application) – not	(Elder et al., 2015)

		enough stability in reducing atmosphere	
	Alkaline oxides (MgO and CaO) [EL]	**Dopant** for pure zirconia to prevent detrimental phase transitions (by stabalising cubic phase) [F]	(Elder et al., 2015)
Gadolinium (Gd)	See Cerium	-	-
Samarium (Sm)	See Cerium	-	-
Nickel (Ni)	Nickel (Ni) [ET] composites of Ni & ionic conductor of electrolyte known as cermet (e.g. Ni-YSZ)	Fuel **electrode** (i.e. cathode), consisting of a composite of Ni and cermet – Ni oxidises when exposed to steam or CO_2 therefore need for recycling – also prone to carbon laydown (also valid for other iron or cobalt containing electrodes)	(Elder et al., 2015) (Kiemel et al., 2021) (HyTechCycling, 2019)
	Gallium (Ga)		
	$Ba_{0.5}Sr_{0.5}Co_{0.8}Fe_{0.2}O_{3-\delta}$ (BSCF) [ET]	Oxygen electrode (i.e. anode)– example of interesting composition that have shown excellent properties under electrolysis conditions	

D.3 Material Occurrences in Cell Configurations

List of raw materials, the frequency of their occurrences in the 8 SOEC compositions for co-electrolysis operating mode, and their classification as critical material (red) or non-critical material (green) based on Table 16 (total SOEC compositions mentioned: 9).

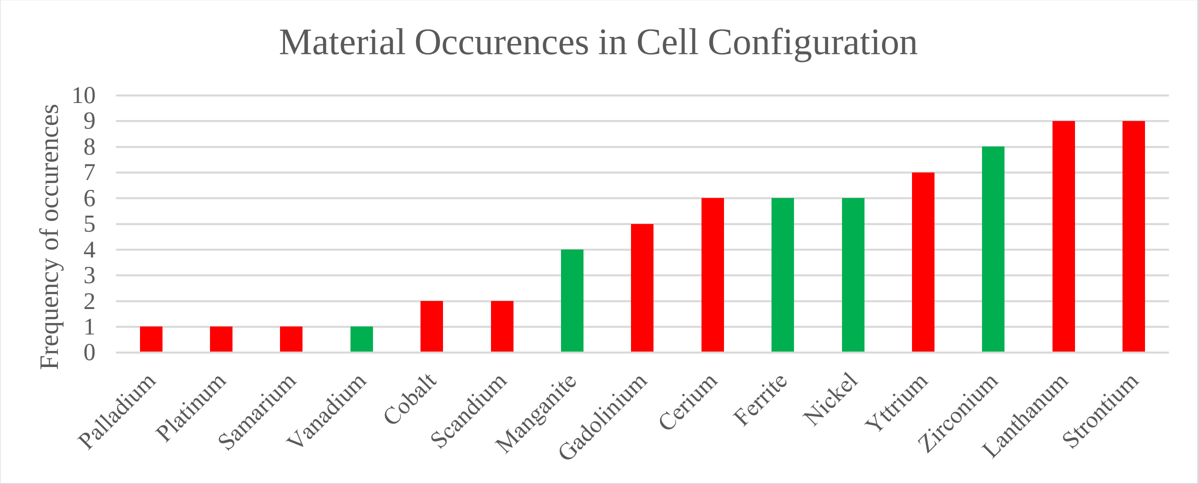

Figure A. 10 The list of raw materials and the frequency of occurrences in the 8 SOEC compositions for co-electrolysis

D.4 Quantification of Material Requirements

Schreiber et al. (2020)

The corresponding material requirements for a single cell are 0,201 g Cerium oxide, 1,98 g Lanthanum oxide, 0,053 g gadolinium oxide, 2,42 g yttrium oxide, 0,324 g Strontium carbonate, 0,389 g Iron(III) oxide-hydroxide FeO(OH), 17,9 g Nickel mix (Nickel cermet (NiO/8YSZ)), 0,394 g Cobalt hydroxide, 14,9 g Zirconium oxide. Additionally, they also specify the material requirements associated with the construction of a stack, as such, they include the interconnect but also the materials required for sealing and housing (or case) of the stack. The additional material requirements for a 150 kW HT-SOEC stack which is comprised of 960 individual cells are 19,9 g glass cermet, 3.064 kg $Mn_{1.0}Co_{1.9}Fe_{0.1}O_4$ (MCF) (for the 100 µm chromium poisoning protection layer at the anode side of the interconnector), 414 kg cast iron, 117 kg of chromium, 0,374 kg titanium, 2,84 kg of manganese, 19,8 kg Nickel (99,5%), 0,483 kg Lanthanum, 1,5 kg of Cobalt. Based on the material requirements for an individual cell, the total number of cells that are used in a stack, and the power of a stack, the material requirements in grams per kilo watt are calculated and shown in the table below.

Choe et al. (2022)

In their research, they provide a life-cycle inventory for a SOEC system which is based on the materials requirements of the research by Schreiber et al. (2020). However, unlike Schreiber et al. (2020), they specify that a single SOEC requires 0,314 kg of YSZ, 0,023 kg of NiO, and 0,052 kg of LSM. Additionally, they provide the material requirements of a stack which are 19,9 kg of glass cermet, 414 kg cast iron, 117 kg chromium, 0,374 kg of titanium, 2,84 kg of manganese, 19,8 kg of nickel (99,5%), 0,483 kg of lanthanum, 1,5 kg of cobalt and 534 kg of chromium steel. In their research, they explicitly state that the lifecycle inventory data is based on the research of Schreiber et al. (2020), and although the material requirements for the stack are identical, the material requirements for a single SOEC differ significantly.

Häfele et al. (2016)

Häfele et al. (2016), perform a life cycle assessment on the manufacturing and operation of SOE components and stacks. The functional unit in their comparison is a 1 kW single stack that consists of 5 cells, including 2 thick outer interconnects, 4 inner thin interconnects, nickel meshes and a glass sealant. Unlike the research by Schreiber et al. (2020), do not specify the thickness, width and length of a single cell, however, they do provide an active cell area, which is 100 cm^2. Furthermore, Häfele et al. (2016), primarily focus on assessing the manufacturing and operation of SOE components and stacks but they also include an analysis of H_2 production using the earlier specified cells. For the production of H_2 they assume a 100% conversion efficiency of electrical to chemical energy. The corresponding material requirements for an SOE stack of 1 kW are 20,563 g chromium steel, 38 g of LSCF/LSCo/PrNi, 425 g of YSZ, 262 g of YDC, 4 g of LSM, 59 g of glass sealant, 181 g of Ni as Ni, and 515 g of Ni as NiO (which corresponds to a total Nickel requirement of 313 g).

Kiemel et al. (2021)

The research by Kiemel et al. (2021), aims to assess CRM usage in PEM and SOEC technologies that are used for water electrolysis in the example of the German energy transition. Unlike the research by Häfele et al. (2016) and Schreiber et al. (2020), they do not specify the material requirements directly based on operation in the electrolysis mode. Instead, they use a conversion factor of approximately 3.428, based on the different power densities of SOFCs (~0.3-0.4 W/cm^2) and HT-SOECs (~1.2 W/cm^2). They use the material requirements for SOFCs provided by Marscheider-Weidermann et al. (2016), and transpose these, via the specified conversion factor, into the material requirements for SOECs. Marscheider-Weidermann et al. (2016), specify that the materials that are used in their research are 23 g/kW of scandium, 51 g/kW of cerium, 213 g/kW of lanthanum, 400 g/kW of zirconium, 13 g/kW of gadolinium, 14 g/kW of yttrium, 50.000 g/kW of aluminium, and 15.000 g/kW of chromium. The requirements that have been depicted in the table below, are these values divided by the conversion factor.

Bachmann et al. (2019)

Bachmann et al. (2019), perform a life cycle assessment on SOFC applications for domestic heat and power generation. Amongst others, their research assesses the material requirements of a SOFC system with an electric power of 5 kW. Furthermore, they assume that the power density is 0.35 W/cm^2. As such, the conversion factor that was used by Kiemel et al. (2021), can also be used to convert the material requirements as specified by Bachmann et al. (2019). They identify that, for a 5 kW fuel cell stack, 33.8 kg of stainless steel (interconnect and gas delivery), 11.6 kg of steel (case), 1.57 kg of 3YSZ (3%) (electrode material), 0.820 kg of Nickel Oxide (electrode support), 0.722 kg of LSM (Electrode material and interconnect), 0.0006 kg of Copper (case), 0.500 kg of synthetic rubber (gas delivery), and 4.95 kg of Silicium dioxide and 1.05 kg of Silicium carbide (stack insulator) are required.

Ref.	Single-cell size	System size	Efficiency	Materials	Requirements (g/kW)
(Schreiber et al., 2020)	10 x 10 x 0,05 (active cell area of 80 cm^2)	2 Stacks, 120 levels each, 960 cells in total, 150 kW	Approx.. 75%	Ceria	1,2864 g/kW
				Lanthanum oxide	12,672 g/kW
				Gadolinium oxide	0,3392 g/kW
				Yttria	15,488 g/kW
				Strontium carbonate	2,0736 g/kW
				Iron(III) oxide-hydroxide	2,4896 g/kW
				Nickel cermet	114,56 g/kW
				Cobalt hydroxide	2,5216 g/kW
				Zirconia	95,36 g/kW
				Glass cermet	132,67 g/kW
				MCF	20,43 g/kW
				Cast iron	2760 g/kW
				Chromium	780 g/kW
				Titanium	2,49 g/kW
				Manganese	18,93 g/kW
				Nickel	132 g/kW
				Lanthanum	3,22 g/kW
				Cobalt	10 g/kW
				Chromium steel	3560 g/kW
(Choe et al., 2022)	Not specified, assumed to be based on Schreiber	Not specified, assumed to be based on Schreiber	82,3 % (system efficiency)	YSZ	2009,6 g/kW
				NiO	147,2 g/kW
				LSM	332,8 g/kW
				Stack materials	n.a.
(Häfele et al., 2016)	Active cell area of 100 cm^2	1 stack, 1 level, 5 cells in total, 1 kW	100% (conversion efficiency for H_2 production)	Chromium steel	20,563 g/kW
				LSCF/LSCo/PrNi	38 g/kW
				YSZ	425 g/kW
				YDC	262 g/kW
				LSM	4 g/kW
				Glass sealant	59 g/kW
				Ni (pure)/NiO/Ni (total)	181/515/313 g/kW
	n.a.	n.a.	n.a.	Scandium	6.71 g/kW

(Kiemel et al., 2021), (Marscheider-Weidermann et al., 2016)				Cerium	14,88 g/kW
				Lanthanum	62,14 g/kW
				Zirconium	116,69 g/kW
				Gadolinium	3,79 g/kW
				Yttrium	4,08 g/kW
				Aluminium	14585,76 g/kW
				Chromium	4375,73 g/kW
(Bachmann et al., 2019)	n.a.	5 kW fuel cell stack	n.a.	Stainless steel	1972,00 g/kW
				Steel	676,78 g/kW
				YSZ (3%)	91,60 g/kW
				NiO	164 g/kW
				LSM	144.4 g/kW
				Copper	0,0006 kg
				Synthetic rubber	0,500 kg
				SiO_2	4,95 kg
				SiC	1,05 kg

D.5 Quantification of Global Annual Production, European Annual Demand and Global Availability of 15 Materials for Co-Electrolysis Applications

Material	Global Annual Production	European Annual Demand	Global Availability
Palladium	199 tonnes	59 tonnes	7200 tonnes
Platinum	178 tonnes	64 tonnes	13000 tonnes
Samarium	2498 tonnes	6.2 tonnes	n.a.
Cobalt	134 ktonnes	20 ktonnes	25 Mtonnes
Scandium	15.2 tonnes	13.7 tonnes	n.a.
Vanadium	64.4 ktonnes	12.7 ktonnes	> 63 Mtonnes
Ferrite	n.a.	n.a.	n.a.
Manganese	17.5 Mtonnes	481 tonnes	>17 Gtonnes
Cerium	51.2 ktonnes	4000 tonnes	n.a.
Gadolinium	1596 tonnes	11.3 tonnes	n.a.
Yttrium	8-10 ktonnes	520 tonnes	n.a.
Lanthanum	29 ktonnes	645 tonnes	n.a.
Nickel	>2 Mtonnes	440 ktonnes	300 Mtonnes
Strontium	160 ktonnes	49 ktonnes	> 1 Gtonnes
Zirconium	1423 ktonnes	231 ktonnes	>148 Mtonnes

D.6 List of Materials that Could be Used for Co-Electrolysis and A Brief Explanation of Their Characteristics

Material	Short Explanation
Palladium	World reserves of palladium are estimated to be 7200 tonnes in Pd content. Approximately 44% of these 7200 tonnes are located in South Africa and 41 % in Russia, European production of Pd is estimated at approximately 1 tonne per year.
Platinum	World reserves of platinum are estimated to be 13000 tonnes in Pt content. Approximately 82% of these 13000 tonnes are located in South Africa, 7% in Zimbabwe and 6% in Russia. Europe is completely reliant on imports. Much of the import is platinum waste that is being recycled for reuse.
Samarium	Classified as a rare earth element, however, it is the 40th most abundant element in the Earth's crust (more common than for example Tin). Does not occur naturally as a metallic element, it is found in several minerals. European annual demand consists of 3.8 tpa of Sm-oxide compounds and 2.4 tpa of Sm-metals and interalloys, mainly used in permanent magnets and niche applications (laser dopant, radiography, etc.).
Cobalt	World reserves of Cobalt are estimated at 25 Mtonnes, 6.9 Mtonnes of which are land-based and the remainder in Cobalt-rich crusts on the seabed. Of land-based reserves, 49% are in the Democratic Republic of Congo, 17% in Australia, and 7% in Cuba. In Europe, Cobalt resources exist in Finland which accounts for 2 tonnes per year. Cobalt is primarily used in the manufacturing of battery chemicals, turbine engine components and cutting tools.
Scandium	Is not particularly rare; abundance in the upper continental crust is 14 ppm, however, due to the small size of its ions rarely forms concentrations larger than 100 ppm, consequently, scandium deposits are rare, resulting in high market prices. EU exclusively imports Scandium, mainly used in SOFCs. Can be used as a substitute for yttrium as a stabilising agent for Zirconia.
Vanadium	Vanadium occurs in many minerals, usually obtained as a by-product in steel production. The world annual production of vanadium is concentrated 96% in three countries; China, Russia and South-Africa. In the EU Austria (6630 tonnes per year) and Germany (110 tonnes per year) produce vanadium. Mainly used in jet engines, crankshafts, gears and other critical components.
Ferrite (Fe_2O_3)	n.a.
Manganese (Mn)	Manganese is the 12th most abundant element in the Earth's upper crust (about 0.1wt%). It can be extracted from several deposit types. It is essential for the manufacturing of steel, additionally, it is being used in the production of aluminium alloys, batteries and pigments. Almost half of the global supply originates from Asia.
Cerium (Ce)	Classified as an LREE; its upper crust abundance is 63 ppm. It does not occur naturally and is mainly found in minerals. Cerium is used in many applications such as autocatalysts, glass and ceramics, and batteries. The EU consumed approximately 3700 tonnes of cerium compounds (e.g. ceria) and 305 tonnes of cerium metals.
Gadolinium (Gd)	Classified as an HREE; its upper crust abundance is 4 ppm. It does not occur naturally and is mainly found in minerals. Gadolinium can improve the workability and resistance to high-temperature oxidation of iron, and chromium and is mainly applied in magnets, lighting and metallurgy, additionally (as metal or salt) it is used in shielding for neutron radiography. The EU consumed approximately 10 tonnes of Gd-oxide compounds and 1.3 tonnes of Gd metals and interalloys.
Yttrium (Y)	Classified as an HREE; its upper crust abundance is 21 ppm. It does not occur naturally and is found mainly in minerals. Yttrium is mainly used in green phosphors (display screens and energy-efficient lighting), but it is also applied in magnets. The EU consumed approximately 450 tonnes of Y-oxide compounds and 60 tonnes of Y metals and interalloys.
Lanthanum (La)	Classified as LREE, however, with an upper crust abundance of 32 ppm, it is the 28th most abundant element in the Earth's crust. It does not occur naturally, however, can be found in several minerals. Lanthanum is used in catalysts, as an additive in

	glasses and ceramics and batteries. The EU consumes approximately 394 tonnes of La-oxide compounds and 251 tonnes of La metals and interalloys.
Nickel (Ni)	Ni occurs in nature, mainly in combined form, and as isotopes of mass numbers 58 and 60. The EU consumes approximately 65 ktonnes of mined Ni and 360 ktonnes of metal Ni per year. This Ni is mainly sourced from South Africa (28%), Greece (21%) and Finland (18%). Ni is mainly used for alloy production (i.e. stainless steel).
Strontium	Sr is a metal that is usually present in the Earth's crust as celestite or strontianite but it is also present in seawater. The main source of the EU's strontium supply is Spain (close to 100%). Sr compounds are mainly used in ceramics, glass and pyrotechnics industries. The EU consumes approximately 49 ktonnes of Sr per year.
Zirconium (Zr)	Zr is a metal that is being recovered from mineral sands and alkaline complexes. Large zirconium resources are known in Australia, Africa and Canada. The resources in the EU are negligible. Zirconium is mainly used in ceramics, refractories and foundries. One-third of the Zr is being produced in Australia and approximately 23% in South Africa and 10% in China.

D.7 Material Assessments Based on Varying Years of Global Annual Production

In the figure below, the global annual production (GAP) is based on 4.5 years. These 4.5 years are based on state-of-the-art HT-SOEC system lifetime figures that have been provided in section 4.2.2.2 by (Posdziech, 2021)

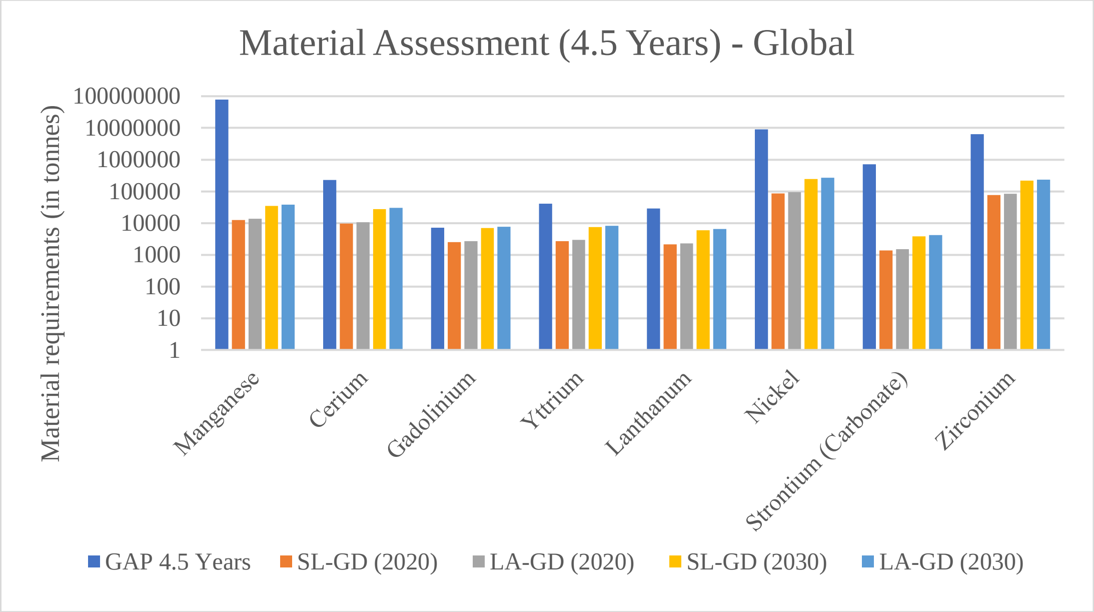

Figure A. 11 The material requirements compared with a global annual production of 4.5 years.

In the figure below, the global annual production (GAP) is based on 8.5 years. These 8.5 years are based on the information that has been provided by Posdziech (2021) as an estimation of the expected system lifetime in 2030.

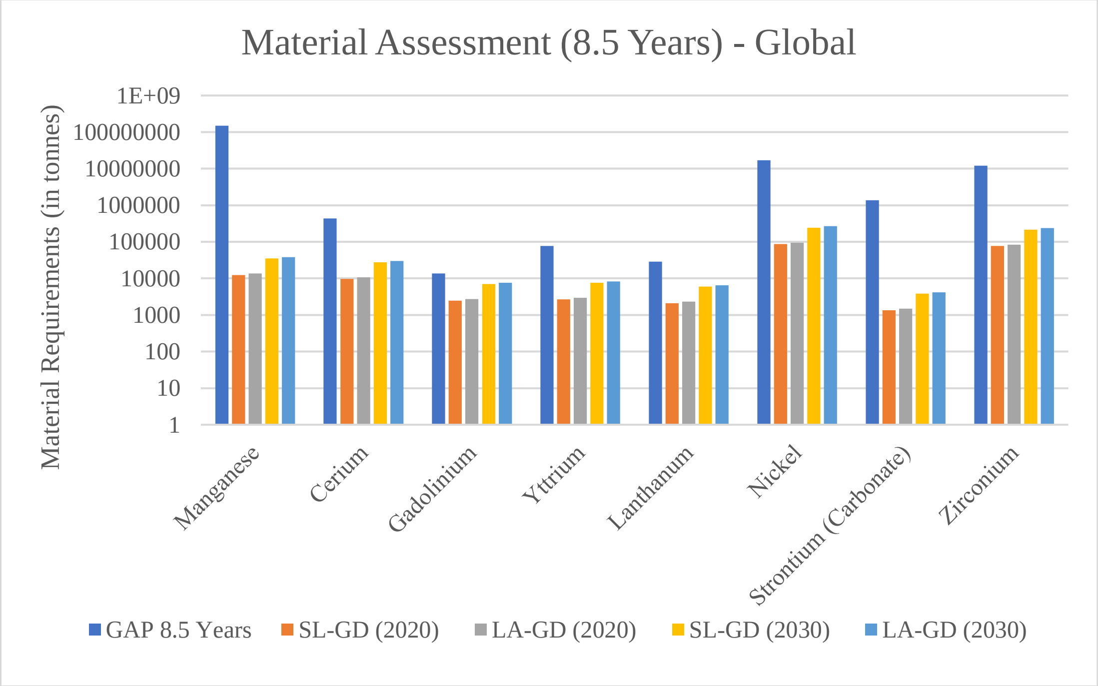

Figure A. 12 The material requirements compared with a global annual production based on 8.5 years.

In the figure below, the global annual production (GAP) is based on 10 years. These 10 years are based on the information that has been provided by Schreiber et al. (2020) as an estimation of the expected system lifetime.

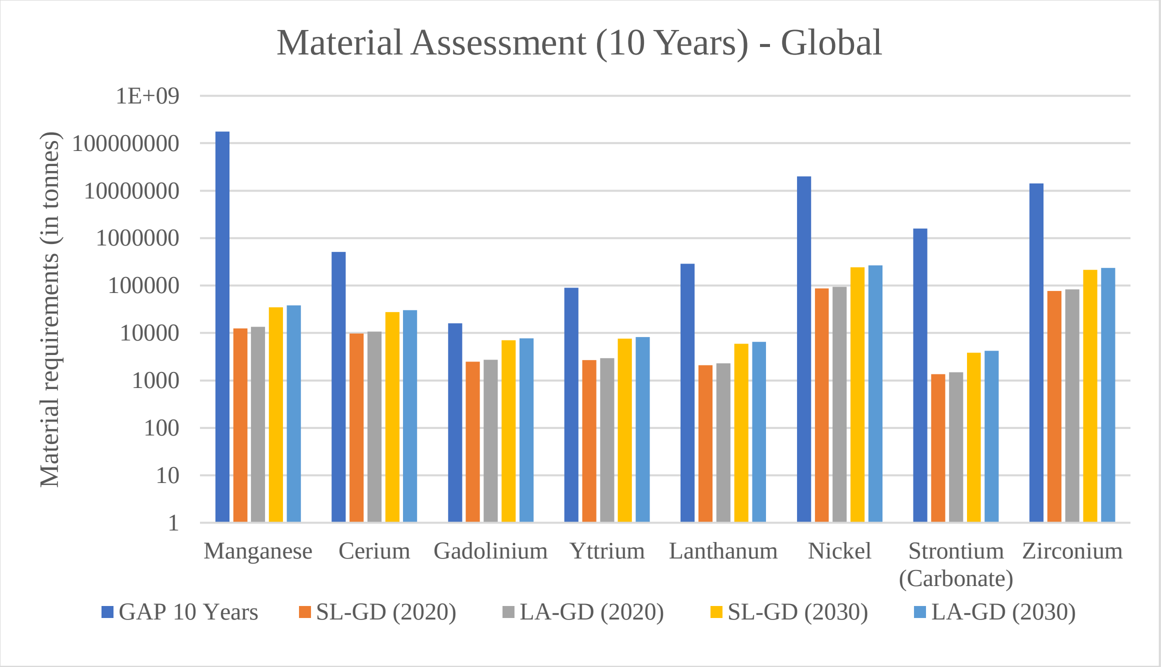

Figure A. 13 The material requirements compared with a global annual production of 10 years.

In the figure below, the European annual consumption is based on 4.5 years.

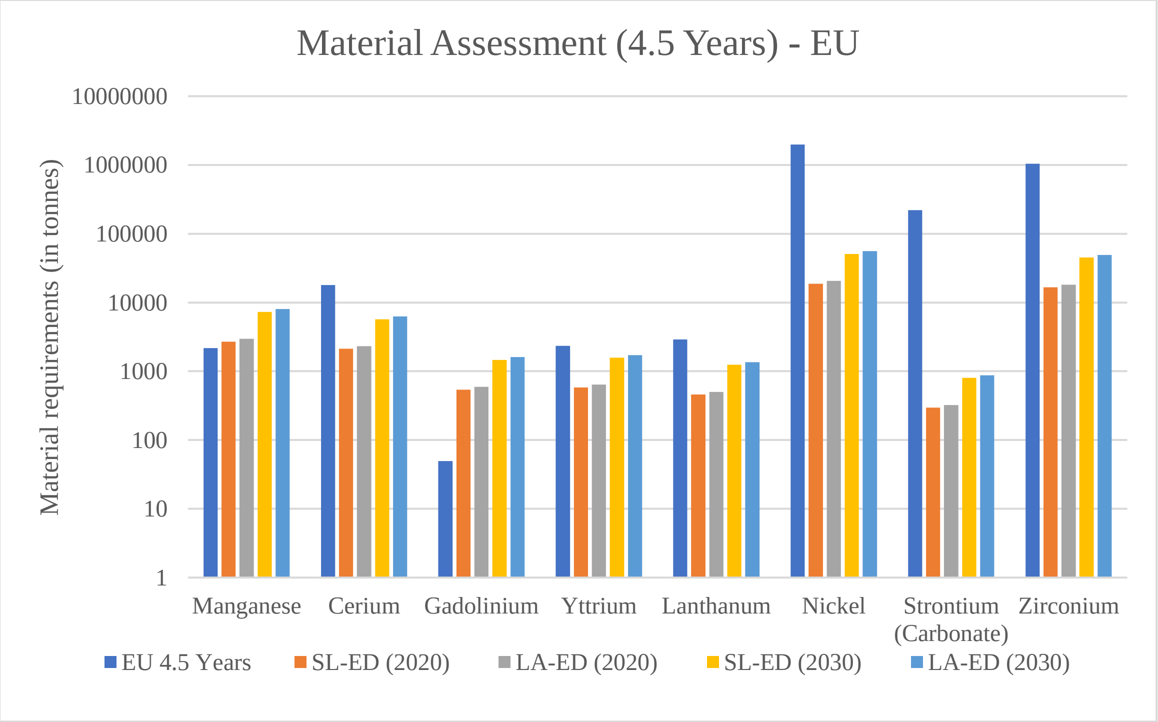

Figure A. 14 The material requirements compared with a European annual consumption of 4.5 years.

In the figure below, the European annual consumption is based on 8.5 years.

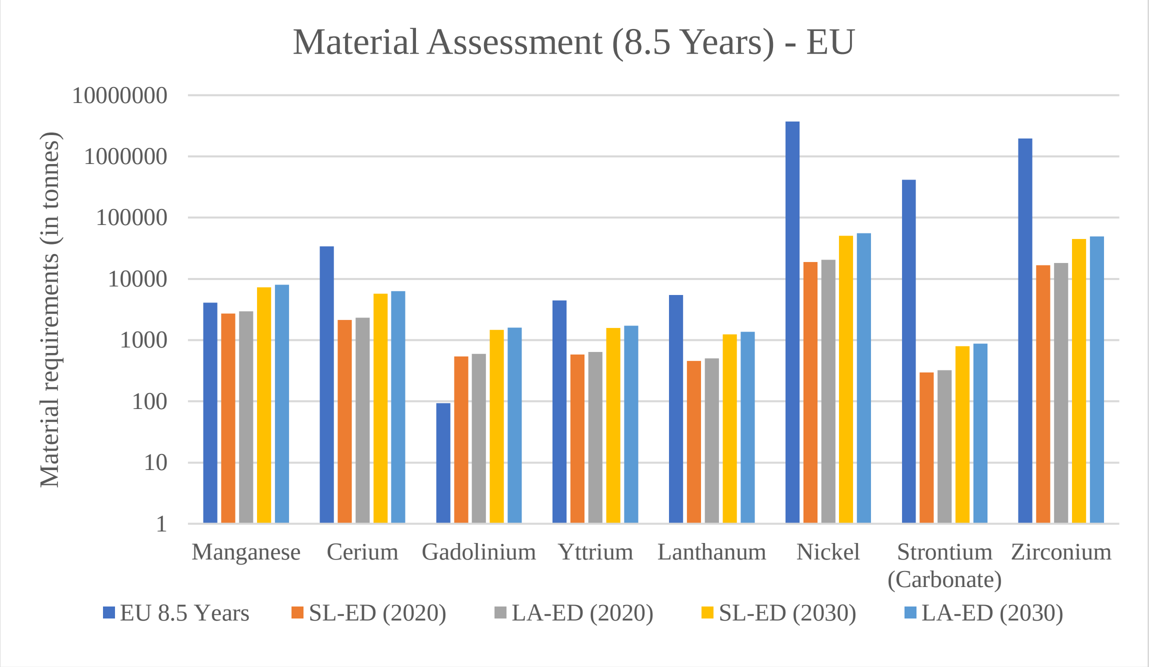

Figure A. 15 The material requirements compared with a European annual consumption of 8.5 years.

In the figure below, the European annual consumption is based on 8.5 years.

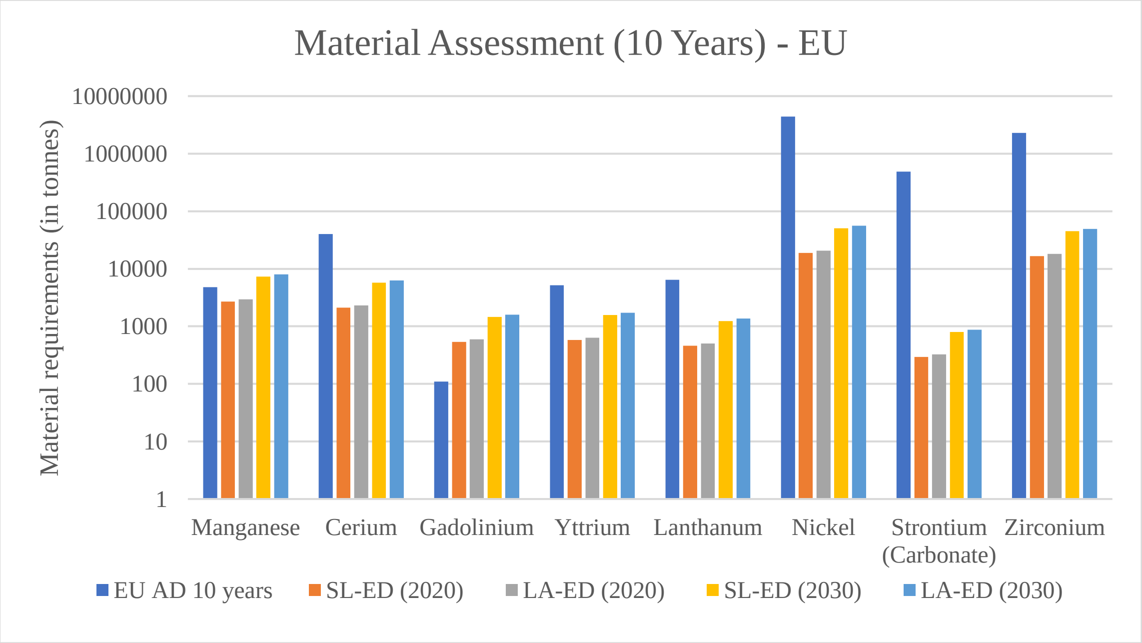

Figure A. 16 The material requirements compared with a European annual consumption of 8.5 years.

D.8 Comparing Raw Material Demand With Production

The percentage share of the demand based on the global annual production

SYNLINK:

The percentage share of the material requirements is based on the material requirements to meet the global demand in 2020 respectively 2030 and based on the **global annual production**.

	Manganese	Cerium	Gadolinium	Yttrium	Lanthanum	Nickel	Strontium	Zirconium
2020	0.07%	19%	156%	30%	7%	4%	0.85%	5%
2030	0.20%	54%	439%	84%	21%	12%	2%	15%

The percentage share of the demand is based on a **global annual production** over **4.5 years (2020)** and **8.5 years (2030)** (years are based on (expected) system lifetime that has been explained in the previous Appendix).

	Manganese	Cerium	Gadolinium	Yttrium	Lanthanum	Nickel	Strontium	Zirconium
2020	0.016%	4%	35%	7%	2%	0.96%	0.19%	1.19%
2030	0.024%	6%	52%	10%	2%	1.44%	0.28%	1.78%

The percentage share of the demand is based on **European annual demand**.

	Manganese	Cerium	Gadolinium	Yttrium	Lanthanum	Nickel	Strontium	Zirconium
2020	562%	53%	4918%	112%	71%	4%	0.60%	7%
2030	1517%	143%	13291%	303%	192%	12%	2%	19%

The percentage share of the demand based on **European annual demand** over **4.5 years (2020) and 8.5 years (2030)** (years are based on (expected) system lifetime)

	Manganese	Cerium	Gadolinium	Yttrium	Lanthanum	Nickel	Strontium	Zirconium
2020	125%	12%	1093%	25%	16%	0.95%	0.13%	2%
2030	179%	17%	1564%	36%	23%	1.36%	0.19%	2%

Linde AG:

The percentage share of the material demand is based on the material requirements to meet the global demand in 2020 respectively 2030 and based on the **global annual production**.

	Manganese	Cerium	Gadolinium	Yttrium	Lanthanum	Nickel	Strontium	Zirconium
2020	0.08%	21%	171%	33%	8%	5%	0.93%	6%
2030	0.22%	59%	482%	92%	23%	13%	3%	17%

The percentage share of the demand is based on a **global annual production** over **10 years** (years are based on (expected) system lifetime that has been explained in the previous Appendix).

	Manganese	Cerium	Gadolinium	Yttrium	Lanthanum	Nickel	Strontium	Zirconium
2020	0.008%	2%	17%	3%	1%	0.47%	0.09%	0.59%
2030	0.022%	6%	48%	9%	2%	1.33%	0.26%	2%

The percentage share of the demand is based on **European annual demand**.

	Manganese	Cerium	Gadolinium	Yttrium	Lanthanum	Nickel	Strontium	Zirconium
2020	**615%**	**58%**	**5382%**	**123%**	**78%**	**5%**	**0.66%**	**8%**
2030	**1662%**	**157%**	**14555%**	**332%**	**211%**	**13%**	**2%**	**21%**

The percentage share of the demand based on **European annual demand** over **10 years** (years are based on (expected) system lifetime)

	Manganese	Cerium	Gadolinium	Yttrium	Lanthanum	Nickel	Strontium	Zirconium
2020	**62%**	**6%**	**538%**	**12%**	**8%**	**0.47%**	**0.07%**	**0.79%**
2030	**166%**	**16%**	**1455%**	**33%**	**21%**	**1.27%**	**0.18%**	**2%**

References

Andika, R., Nandiyanto, A. B. D., Putra, Z. A., Bilad, M. R., Kim, Y., Yun, C. M., & Lee, M. (2018). Co-electrolysis for power-to-methanol applications. *Renewable and Sustainable Energy Reviews*, *95*(July), 227–241. https://doi.org/10.1016/j.rser.2018.07.030

Bachmann, T. M., Carnicelli, F., & Preiss, P. (2019). Life cycle assessment of domestic fuel cell micro combined heat and power generation: Exploring influential factors. *International Journal of Hydrogen Energy*, *44*(7), 3891–3905. https://doi.org/10.1016/j.ijhydene.2018.12.076

Badgett, A., Feise, A., & Star, A. (2022). Optimizing utilization of point source and atmospheric carbon dioxide as a feedstock in electrochemical CO2 reduction. *IScience*, *25*(5), 104270. https://doi.org/10.1016/j.isci.2022.104270

Bedon, A. (2018). *Electrolyzers*. Impact. https://wwwdisc.chimica.unipd.it/impact/SOEC.html

Bellona. (2020). *Barriers to transport and storage of CO_2 within the European Union*.

Berlin, D., Feldmann, A., & Nuur, C. (2022). Supply network collaborations in a circular economy: A case study of Swedish steel recycling. *Resources, Conservation and Recycling*, *179*(December 2021), 106112. https://doi.org/10.1016/j.resconrec.2021.106112

Beswick, R. R., Oliveira, A. M., & Yan, Y. (2021). Does the Green Hydrogen Economy Have a Water Problem? *ACS Energy Letters*, *6*(9), 3167–3169. https://doi.org/10.1021/acsenergylett.1c01375

Bianchi, F. R., & Bosio, B. (2021). Operating principles, performance and technology readiness level of reversible solid oxide cells. *Sustainability (Switzerland)*, *13*(9). https://doi.org/10.3390/su13094777

Blengini, G. A., Latunussa, C. E. L., Eynard, U., Torres de Matos, C., Wittmer, D., Georgitzikis, K., Pavel, C., Carrara, S., Mancini, L., Unguru, M., Blagoeva, D., Mathieux, F., & Pennington, D. (2020). *Study on the EU’s list of Critical Raw Materials (2020) Final Report*. https://doi.org/10.2873/904613

Bobba, S., Carrara, S., Huisman, J., Mathieux, F., & Pavel, C. (2020). Critical Raw Materials for Strategic Technologies and Sectors in the EU - a Foresight Study. In *European Commission*. https://doi.org/10.2873/58081

Bouffard, F., & Kirschen, D. S. (2008). Centralised and distributed electricity systems. *Energy Policy*, *36*(12), 4504–4508. https://doi.org/10.1016/j.enpol.2008.09.060

Bruhn, T., Naims, H., & Olfe-Kräutlein, B. (2016). Separating the debate on CO2 utilisation from carbon capture and storage. *Environmental Science and Policy*, *60*, 38–43. https://doi.org/10.1016/j.envsci.2016.03.001

Brynolf, S., Taljegard, M., Grahn, M., & Hansson, J. (2018). Electrofuels for the transport sector: A review of production costs. *Renewable and Sustainable Energy Reviews*, *81*(May 2017), 1887–1905. https://doi.org/10.1016/j.rser.2017.05.288

Budinis, S. (2022). *Direct Air Capture: Tracking Report*. International Energy Agency. https://www.iea.org/reports/direct-air-capture

Bui, M., Adjiman, C. S., Bardow, A., Anthony, E. J., Boston, A., Brown, S., Fennell, P. S., Fuss, S., Galindo, A., Hackett, L. A., Hallett, J. P., Herzog, H. J., Jackson, G., Kemper, J., Krevor, S., Maitland, G. C., Matuszewski, M., Metcalfe, I. S., Petit, C., … Mac Dowell, N. (2018). Carbon capture and storage (CCS): The way forward. *Energy and Environmental Science*, *11*(5), 1062–1176. https://doi.org/10.1039/c7ee02342a

Capuder, T., & Mancarella, P. (2014). Techno-economic and environmental modelling and optimization of flexible distributed multi-generation options. *Energy*, *71*, 516–533. https://doi.org/10.1016/j.energy.2014.04.097

Carbon Engineering. (2018). *Direct Air Capture*. Squamish Canada. https://carbonengineering.com/our-technology/

CHEManager. (2011). *AkzoNobel's On-Site Chlorine Solution*. Chemicals & Distribution. https://www.chemanager-online.com/en/products/akzonobels-site-chlorine-solution

Chen, C., Khosrowabadi Kotyk, J. F., & Sheehan, S. W. (2018). Progress toward Commercial Application of Electrochemical Carbon Dioxide Reduction. *Chem*, *4*(11), 2571–2586. https://doi.org/10.1016/j.chempr.2018.08.019

Chen, X., Guan, C., Xiao, G., Du, X., & Wang, J. Q. (2015). Syngas production by high temperature steam/CO2 coelectrolysis using solid oxide electrolysis cells. *Faraday Discussions*, *182*, 341–351. https://doi.org/10.1039/c5fd00017c

Choe, C., Cheon, S., Gu, J., & Lim, H. (2022). Critical aspect of renewable syngas production for power-to-fuel via solid oxide electrolysis: Integrative assessment for potential renewable energy source. *Renewable and Sustainable Energy Reviews*, *161*(March), 112398. https://doi.org/10.1016/j.rser.2022.112398

Dahlgren, E., Göçmen, C., Lackner, K., & Van Ryzin, G. (2013). Small modular infrastructure. *Engineering Economist*, *58*(4), 231–264. https://doi.org/10.1080/0013791X.2013.825038

Daneshvar, E., Wicker, R. J., Show, P. L., & Bhatnagar, A. (2022). Biologically-mediated carbon capture and utilization by microalgae towards sustainable CO2 biofixation and biomass valorization – A review. *Chemical Engineering Journal*, *427*(April 2021), 130884. https://doi.org/10.1016/j.cej.2021.130884

Davidsson, S., & Höök, M. (2017). Material requirements and availability for multi-terawatt deployment of photovoltaics. *Energy Policy*, *108*(June), 574–582. https://doi.org/10.1016/j.enpol.2017.06.028

Department of Energy, U. (2009). *Energy.gov*. FE Implementation of the Recovery Act. https://www.energy.gov/fecm/fe-implementation-recovery-act

Durán, I., Rubiera, F., & Pevida, C. (2017). Separation of CO2 in a solid waste management incineration facility using activated carbon derived from pine sawdust. *Energies*, *10*(6). https://doi.org/10.3390/en10060827

Durusut, E., & Joos, M. (2018). *Shipping CO2 - UK Cost Estimation Study* (Issue November). https://assets.publishing.service.gov.uk/government/uploads/system/uploads/attachment_data/file/761762/BEIS_Shipping_CO2.pdf

Ebbehøj, S. L. (2015). *Integration of CO2 air capture and solid oxide electrolysis for methane production*. Department of Energy Conversion and Storage, Technical University of Denmark.

Elder, R., Cumming, D., & Mogensen, M. B. (2015). High Temperature Electrolysis. In *Carbon Dioxide Utilisation: Closing the Carbon Cycle: First Edition*. Elsevier B.V. https://doi.org/10.1016/B978-0-444-62746-9.00011-6

Environmental Protection Agency, U. (2019). *Greenhouse Gas Reporting Program: Industrial Profile: Power Plants Sector*. *September*. http://www.eia.gov/electricity/data/browser/#/topic/0?agg=2.

EurEau. (2021). *Europe ' s Water in Figures An overview of the* (2021 Editi).

European Commission. (2019a). *Demonstration of large-scale co-electrolysis for the Industrial Power-to-X market*. Cordis EU Research Results. https://cordis.europa.eu/programme/id/H2020_FCH-02-8-2020

European Commission. (2019b). *Press remarks by President von der Leyen on the occasion of the adoption of the European Green Deal Communication*. https://ec.europa.eu/commission/presscorner/detail/en/speech_19_6749

European Commission. (2020a). Critical Raw Materials Factsheets (2020). In *Critical Raw Materials Factsheets*. https://doi.org/10.2873/92480

European Commission. (2020b). *Study on the EU's list of Critical Raw Materials (2020), Factsheets on Non-critical Raw Materials*. https://doi.org/10.2873/867993

European Commission. (2022). *Carbon capture, use and storage*. https://ec.europa.eu/clima/eu-action/carbon-capture-use-and-storage_en#:~:text=The CCS Directive enables carbon,specific EU legislation for CCU.

European Industrial Gasses Association. (2004). *CARBON MONOXIDE AND SYNGAS PIPELINE SYSTEMS* (Vol. 303, Issue 7860). https://doi.org/10.1016/S0140-6736(74)92974-2

Fasihi, M., Efimova, O., & Breyer, C. (2019). Techno-economic assessment of CO 2 direct air capture plants. *Journal of Cleaner Production*, *224*, 957–980. https://doi.org/10.1016/j.jclepro.2019.03.086

Fernández-González, J., Rumayor, M., Domínguez-Ramos, A., & Irabien, Á. (2022). CO2 electroreduction: Sustainability analysis of the renewable synthetic natural gas. *International Journal of Greenhouse Gas Control*, *114*. https://doi.org/10.1016/j.ijggc.2021.103549

Fu, Q., Mabilat, C., Zahid, M., Brisse, A., & Gautier, L. (2010). Syngas production via high-temperature steam/CO2 co-electrolysis: An economic assessment. *Energy and Environmental Science*, *3*(10), 1382–1397. https://doi.org/10.1039/c0ee00092b

Gallandat, N., Romanowicz, K., & Züttel, A. (2017). An Analytical Model for the Electrolyser Performance Derived from Materials Parameters. *Journal of Power and Energy Engineering*, *05*(10), 34–49. https://doi.org/10.4236/jpee.2017.510003

Gao, L., Fang, M., Li, H., & Hetland, J. (2011). Cost analysis of CO2 transportation: Case study in China. *Energy Procedia*, *4*, 5974–5981. https://doi.org/10.1016/j.egypro.2011.02.600

Gao, N., Quiroz-Arita, C., Diaz, L. A., & Lister, T. E. (2020). Intensified co-electrolysis process for syngas production from captured CO2. *Journal of CO2 Utilization*, *43*(May 2020), 101365. https://doi.org/10.1016/j.jcou.2020.101365

Garg, S., Li, M., Weber, A. Z., Ge, L., Li, L., Rudolph, V., Wang, G., & Rufford, T. E. (2020). Advances and challenges in electrochemical CO2 reduction processes: An engineering and design perspective looking beyond new catalyst materials. *Journal of Materials Chemistry A*, *8*(4), 1511–1544. https://doi.org/10.1039/c9ta13298h

Garrehy, P. (2016). *Centralized vs Decentralized Manufacturing*. Industry Today. https://industrytoday.com/centralized-vs-decentralized-manufacturing/

Gokhberg, L, Fursov, K., Miles, L., & Perani, G. (2013). *Handbook of innovation indicators and measurement*.

Gómez, E., del Teso, R., Cabrera, E., Cabrera, E., & Soriano, J. (2018). Labeling Water Transport efficiencies. *Water (Switzerland)*, *10*(7). https://doi.org/10.3390/w10070935

Graves, C., Ebbesen, S. D., Mogensen, M., & Lackner, K. S. (2011). Sustainable hydrocarbon fuels by recycling CO2 and H 2O with renewable or nuclear energy. *Renewable and Sustainable Energy Reviews*, *15*(1), 1–23. https://doi.org/10.1016/j.rser.2010.07.014

Gutiérrez-Sánchez, O., Bohlen, B., Daems, N., Bulut, M., Pant, D., & Breugelmans, T. (2022). A State-of-the-Art Update on Integrated CO2 Capture and Electrochemical Conversion Systems. *ChemElectroChem*, *9*(5). https://doi.org/10.1002/celc.202101540

Häfele, S., Hauck, M., & Dailly, J. (2016). Life cycle assessment of the manufacture and operation of solid oxide electrolyser components and stacks. *International Journal of Hydrogen Energy*, *41*(31), 13786–13796. https://doi.org/10.1016/j.ijhydene.2016.05.069

Hansen, J. B. (2015). Solid oxide electrolysis - a key enabling technology for sustainable energy scenarios. *Faraday Discussions*, *182*, 9–48. https://doi.org/10.1039/c5fd90071a

Hansen, J., Kharecha, P., Sato, M., Masson-Delmotte, V., Ackerman, F., Beerling, D. J., Hearty, P. J., Hoegh-Guldberg, O., Hsu, S. L., Parmesan, C., Rockstrom, J., Rohling, E. J., Sachs, J., Smith, P., Steffen, K., Van Susteren, L., Von Schuckmann, K., & Zachos, J. C. (2013). Assessing “dangerous climate change”: Required reduction of carbon emissions to protect young people, future generations and nature. *PLoS ONE*, *8*(12). https://doi.org/10.1371/journal.pone.0081648

Hauch, A., Küngas, R., Blennow, P., Hansen, A. B., Hansen, J. B., Mathiesen, B. V., & Mogensen, M. B. (2020). Recent advances in solid oxide cell technology for electrolysis. *Science*, *370*(6513). https://doi.org/10.1126/science.aba6118

Haugen, H. A., Eldrup, N. H., Fatnes, A. M., & Leren, E. (2017). Commercial Capture and Transport of CO2 from Production of Ammonia. *Energy Procedia*, *114*(1876), 6133–6140. https://doi.org/10.1016/j.egypro.2017.03.1750

Heijnen, P., Chappin, E., & Nikolic, I. (2014). Infrastructure network design with a multi-model approach: Comparing geometric graph theory with an agent-based implementation of an ant colony optimization. *Jasss*, *17*(4). https://doi.org/10.18564/jasss.2533

Hong, W. Y. (2022). A techno-economic review on carbon capture, utilisation and storage systems for achieving a net-zero CO2 emissions future. *Carbon Capture Science & Technology*, *3*(March), 100044. https://doi.org/10.1016/j.ccst.2022.100044

Hussain, S., & Yangping, L. (2020). Review of solid oxide fuel cell materials: cathode, anode, and electrolyte. *Energy Transitions*, *4*(2), 113–126. https://doi.org/10.1007/s41825-020-00029-8

HyTechCycling. (2019). *Assessment of critical materials and components in FCH technologies*. *700190*, 1–33.

IEA. (2020). Special Report on Carbon Capture Utilisation and Storage. In *Energy Technology Perspectives 2020*. https://doi.org/10.1787/9789264109834-en

IEA. (2021). The Role of Critical Minerals in Clean Energy Transitions. *The Role of Critical Minerals in Clean Energy Transitions*. https://doi.org/10.1787/f262b91c-en

IMARC. (2021). *Syngas Market: Global Industry Trends, Share, Size, Growth, Opportunity and Forecast 2022-2027*. Press Release. https://www.imarcgroup.com/syngas-market

Ingvarsdóttir, A. (2020). Comparison of direct air capture technology to point source CO2 capture in Iceland. *Kith Royal Institute for Technology*.

Inkwood Research. (2017). *Syngas Market - Global Trends, Size Share, Analysis Report 2017-2026*. https://inkwoodresearch.com/reports/europe-syngas-market/#report-summary

International Energy Agency. (2020). Energy Technology Perspectives 2020 - Special Report on Carbon Capture Utilisation and Storage. *Energy Technology Perspectives 2020 - Special Report on Carbon Capture Utilisation and Storage*. https://doi.org/10.1787/208b66f4-en

International Energy Agency. (2021). *Net zero targets drive new momentum for CCUS*. https://www.iea.org/fuels-and-technologies/carbon-capture-utilisation-and-storage

Jiang, K., Ashworth, P., Zhang, S., Liang, X., Sun, Y., & Angus, D. (2020). China's carbon capture, utilization and storage (CCUS) policy: A critical review. *Renewable and Sustainable Energy Reviews*, *119*. https://doi.org/10.1016/j.rser.2019.109601

Jiang, Y., Chen, F., & Xia, C. (2021). A review on cathode processes and materials for electro-reduction of carbon dioxide in solid oxide electrolysis cells. *Journal of Power Sources*, *493*(96), 229713. https://doi.org/10.1016/j.jpowsour.2021.229713

Jin, S., Hao, Z., Zhang, K., Yan, Z., & Chen, J. (2021). Advances and Challenges for the Electrochemical Reduction of CO2 to CO: From Fundamentals to Industrialization. *Angewandte Chemie - International Edition*, *60*(38), 20627–20648. https://doi.org/10.1002/anie.202101818

Jones, C. R., Olfe-Kräutlein, B., Naims, H., & Armstrong, K. (2017). The social acceptance of carbon dioxide utilisation: A review and research Agenda. In *Frontiers in Energy Research* (Vol. 5, Issue JUN). Frontiers Media S.A. https://doi.org/10.3389/fenrg.2017.00011

Jouny, M., Luc, W., & Jiao, F. (2018). General Techno-Economic Analysis of CO2 Electrolysis Systems. *Industrial and Engineering Chemistry Research*, *57*(6), 2165–2177. https://doi.org/10.1021/acs.iecr.7b03514

Junne, T., Wulff, N., Breyer, C., & Naegler, T. (2020). Critical materials in global low-carbon energy scenarios: The case for neodymium, dysprosium, lithium, and cobalt. *Energy*, *211*, 118532. https://doi.org/10.1016/j.energy.2020.118532

Kearns, D., Liu, H., & Consoli, C. (2021). Technology Readiness and Costs of CCS - Global CCS Institute. *Global CCS Insitute*, *March*, 50. https://www.globalccsinstitute.com/wp-content/uploads/2021/03/Technology-Readiness-and-Costs-for-CCS-2021-1.pdf

Keith, D. W., Holmes, G., St. Angelo, D., & Heidel, K. (2018). A Process for Capturing CO2 from the Atmosphere. *Joule*, *2*(8), 1573–1594. https://doi.org/10.1016/j.joule.2018.05.006

Kiemel, S., Smolinka, T., Lehner, F., Full, J., Sauer, A., & Miehe, R. (2021). Critical materials for water electrolysers at the example of the energy transition in Germany. *International Journal of Energy Research*, *45*(7), 9914–9935. https://doi.org/10.1002/er.6487

Kujanpää, L., Rauramo, J., & Arasto, A. (2011). Cross-border CO2 infrastructure options for a CCS demonstration in Finland. *Energy Procedia*, *4*, 2425–2431. https://doi.org/10.1016/j.egypro.2011.02.136

Küngas, R. (2020). Review—Electrochemical CO 2 Reduction for CO Production: Comparison of Low- and High-Temperature Electrolysis Technologies . *Journal of The Electrochemical Society*, *167*(4), 044508. https://doi.org/10.1149/1945-7111/ab7099

Lam, C., Meinert, E., Yang, A., & Cui, Z. (2021). Comparison between centralized and decentralized supply chains of autologous chimeric antigen receptor T-cell therapies: a UK case study based on discrete event simulation. *Cytotherapy*, *23*(5), 433–451. https://doi.org/10.1016/J.JCYT.2020.08.007

Larson, A. (2017). *World's Largest Post-Combustion Carbon Capture Project Completed*. Power Magazine. https://www.powermag.com/worlds-largest-post-combustion-carbon-capture-project-completed/

Lee, D. Y., Mehran, M. T., Kim, J., Kim, S., Lee, S. B., Song, R. H., Ko, E. Y., Hong, J. E., Huh, J. Y., & Lim, T. H. (2020). Scaling up syngas production with controllable H2/CO ratio in a highly efficient, compact, and durable solid oxide coelectrolysis cell unit-bundle. *Applied Energy*, *257*(October 2019), 114036. https://doi.org/10.1016/j.apenergy.2019.114036

Lee, M. Y., Park, K. T., Lee, W., Lim, H., Kwon, Y., & Kang, S. (2020). Current achievements and the future direction of electrochemical CO2 reduction: A short review. *Critical Reviews in Environmental Science and Technology*, *50*(8), 769–815. https://doi.org/10.1080/10643389.2019.1631991

Li, M., Irtem, E., Iglesias Van Montfort, H. P., & Burdyny, T. (2021). *Sequential vs integrated CO 2 capture and electrochemical conversion: An energy comparison*. 1–15.

Li, Q., & Hu, G. (2016). Techno-economic analysis of biofuel production considering logistic configurations. *Bioresource Technology*, *206*, 195–203. https://doi.org/10.1016/j.biortech.2016.01.101

Li, W., Shi, Y., Luo, Y., & Cai, N. (2013). Elementary reaction modeling of CO2/H2O co-electrolysis cell considering effects of cathode thickness. *Journal of Power Sources*, *243*, 118–130. https://doi.org/10.1016/j.jpowsour.2013.05.119

Lim, C. K., Liu, Q., Zhou, J., Sun, Q., & Chan, S. H. (2017). High-temperature electrolysis of synthetic seawater using solid oxide electrolyzer cells. *Journal of Power Sources*, *342*, 79–87. https://doi.org/10.1016/j.jpowsour.2016.12.019

Lo, S. L. Y., How, B. S., Teng, S. Y., Lam, H. L., Lim, C. H., Rhamdhani, M. A., & Sunarso, J. (2021). Stochastic techno-economic evaluation model for biomass supply chain: A biomass gasification case study with supply chain uncertainties. *Renewable and Sustainable Energy Reviews*, *152*(July), 111644. https://doi.org/10.1016/j.rser.2021.111644

Lotrič, A., Sekavčnik, M., Kuštrin, I., & Mori, M. (2021). Life-cycle assessment of hydrogen technologies with the focus on EU critical raw materials and end-of-life strategies. *International Journal of Hydrogen Energy*, *46*(16), 10143–10160. https://doi.org/10.1016/j.ijhydene.2020.06.190

Lu, S., Shi, Y., Meng, N., Lu, S., Yu, Y., & Zhang, B. (2020). Electrosynthesis of Syngas via the Co-Reduction of CO2 and H2O. *Cell Reports Physical Science*, *1*(11), 100237. https://doi.org/10.1016/j.xcrp.2020.100237

Mahmood, A., Bano, S., Yu, J. H., & Lee, K. H. (2019). Performance evaluation of SOEC for CO2/H2O co-electrolysis: Considering the effect of cathode thickness. *Journal of CO2 Utilization*, *33*(November 2018), 114–120. https://doi.org/10.1016/j.jcou.2019.05.014

Marscheider-Weidermann, F., Langkau, S., & Hummen, E. (2016). *Rohstoffe für Zukunftstechnologien 2016* (Rohstoffin). DERA.

Marufuzzaman, M., Li, X., Yu, F., & Zhou, F. (2016). Supply Chain Design and Management for Syngas Production. *ACS Sustainable Chemistry and Engineering*, *4*(3), 890–900. https://doi.org/10.1021/acssuschemeng.5b00944

McCollum, D. L., & Ogden, J. M. (2006). *Correlations for Estimating Carbon Dioxide Density and Viscosity*. 87. https://escholarship.org/uc/item/1zg00532

Mcqueen, N., Gomes, K. V., Mccormick, C., & Blumanthal, K. (2021). A review of direct air capture (DAC): scaling up commercial technologies and innovating for the future Progress in Energy. *Progress in Energy*, *3*(3).

Mehmeti, A., Angelis-Dimakis, A., Arampatzis, G., McPhail, S. J., & Ulgiati, S. (2018). Life cycle assessment and water footprint of hydrogen production methods: From conventional to emerging technologies. *Environments - MDPI*, *5*(2), 1–19. https://doi.org/10.3390/environments5020024

Metz, B., Davidson, O., de Coninck, H., Loos, M., & Meyer, L. (2005). *Carbon Dioxide Capture and Storage* (1st ed., Vol. 1). Cambridge University PRess. https://doi.org/10.1016/bs.ache.2021.10.005

Mohammed, S. A. S., Yahya, W. Z. N., Bustam, M. A., & Kibria, M. G. (2021). Elucidation of the roles of ionic liquid in co2 electrochemical reduction to value-added chemicals and fuels. *Molecules*, *26*(22), 1–23. https://doi.org/10.3390/molecules26226962

Münch, M. (2018). Report on Large Scale Manufacturing Strategy for Solid Oxide Fuel Cells (SOFC). *Co-Funded by the European Commission within the H2020 Programme the Fuel Cells and Hydrogen 2 Joint Undertaking*, *2019*, 13.

National Petroleum Council. (2019). *Meeting the Dual Challenge: A Roadmap to At-Scale Deployment of Carbon Capture, Use, and Storage Key Excerpts from National Petroleum Council Report: Chapter 6: CO 2 Transport*.

Nechache, A., & Hody, S. (2021). Alternative and innovative solid oxide electrolysis cell materials: A short review. *Renewable and Sustainable Energy Reviews*, *149*. https://doi.org/10.1016/j.rser.2021.111322

NETL. (2014). Costs of Capturing CO2 from Industrial Sources. *U.S Department of Energy- National Energy Technology Laboratory*, 1–144. https://sequestration.mit.edu/pdf/2013_Summers_Capture_Costs_Industrial_Sources.pdf

Newcomer, A., & Apt, J. (2007). Storing syngas lowers the carbon price for profitable coal gasification. *Environmental Science and Technology*, *41*(23), 7974–7979. https://doi.org/10.1021/es070956a

Nibud. (2022). *Kosten van Energy en Water*. https://www.nibud.nl/onderwerpen/uitgaven/kosten-energie-water/

Nicodemus, J. H., McGuinness, M., & Maharjan, R. (2014). A thermodynamic and cost analysis of solar syngas from the zinc/zinc-oxide cycle. *ASME 2014 8th International Conference on Energy Sustainability, ES 2014 Collocated with the ASME 2014 12th International Conference on Fuel Cell Science, Engineering and Technology*, *2*(July). https://doi.org/10.1115/ES2014-6389

Ozden, A., García de Arquer, F. P., Huang, J. E., Wicks, J., Sisler, J., Miao, R. K., O’Brien, C. P., Lee, G., Wang, X., Ip, A. H., Sargent, E. H., & Sinton, D. (2022). Carbon-efficient carbon dioxide electrolysers. *Nature Sustainability*, *5*(July). https://doi.org/10.1038/s41893-022-00879-8

Ozkan, M., Nayak, S. P., Ruiz, A. D., & Jiang, W. (2022). Current status and pillars of direct air capture technologies. *IScience*, *25*(4), 103990. https://doi.org/10.1016/j.isci.2022.103990

Pace, G., & Sheehan, S. W. (2021). Scaling CO2 Capture With Downstream Flow CO2 Conversion to Ethanol. *Frontiers in Climate*, *3*(May), 1–9. https://doi.org/10.3389/fclim.2021.656108

Park, S., Wijaya, D. T., Na, J., & Lee, C. W. (2021). Towards the large-scale electrochemical reduction of carbon dioxide. *Catalysts*, *11*(2), 1–30. https://doi.org/10.3390/catal11020253

Parra, D., & Patel, M. K. (2016). Techno-economic implications of the electrolyser technology and size for power-to-gas systems. *International Journal of Hydrogen Energy*, *41*(6), 3748–3761. https://doi.org/10.1016/j.ijhydene.2015.12.160

Pei, P., Korom, S. F., Ling, K., & Nasah, J. (2016). Cost comparison of syngas production from natural gas conversion and underground coal gasification. *Mitigation and Adaptation Strategies* *for Global Change*, *21*(4), 629–643. https://doi.org/10.1007/s11027-014-9588-x

Pérez-Fortes, M., Laínez-Aguirre, J. M., Arranz-Piera, P., Velo, E., & Puigjaner, L. (2012). Design of regional and sustainable bio-based networks for electricity generation using a multi-objective MILP approach. *Energy*, *44*(1), 79–95. https://doi.org/10.1016/j.energy.2012.01.033

Pérez-Fortes, M., Schöneberger, J. C., Boulamanti, A., Harrison, G., & Tzimas, E. (2016). Formic acid synthesis using CO2 as raw material: Techno-economic and environmental evaluation and market potential. *International Journal of Hydrogen Energy*, *41*(37), 16444–16462. https://doi.org/10.1016/j.ijhydene.2016.05.199

Pieri, T., Nikitas, A., Castillo-Castillo, A., & Angelis-Dimakis, A. (2018). Holistic assessment of carbon capture and utilization value chains. *Environments - MDPI*, *5*(10), 1–17. https://doi.org/10.3390/environments5100108

Posdziech, O. (2021). Production of renewable hydrogen and syngas via high-temperature electrolysis. *Workshop on Advanced PtG and PtL Technologies*. https://multiplhy-project.eu/Documents/Workshop on Advanced PtG and PtL Technologies High-Temperature Electrolysis_Posdziech.pdf

Psarras, P., He, J., Pilorgé, H., McQueen, N., Jensen-Fellows, A., Kian, K., & Wilcox, J. (2020). Cost Analysis of Carbon Capture and Sequestration from U.S. Natural Gas-Fired Power Plants. *Environmental Science and Technology*, *54*(10), 6272–6280. https://doi.org/10.1021/acs.est.9b06147

Rahman, M. M., Khan, I., Field, D. L., Techato, K., & Alameh, K. (2022). Powering agriculture: Present status, future potential, and challenges of renewable energy applications. *Renewable Energy*, *188*, 731–749. https://doi.org/10.1016/j.renene.2022.02.065

Redissi, Y., & Bouallou, C. (2013). Valorization of carbon dioxide by co-electrolysis of CO2/H2O at high temperature for syngas production. *Energy Procedia*, *37*, 6667–6678. https://doi.org/10.1016/j.egypro.2013.06.599

ReportLinker. (2022). *Syngas Market - Growth, Trends, COVID-19 Impact, and Forecasts (2022 - 2027)*. GlobalNewswire. https://www.globenewswire.com/news-release/2022/10/04/2527997/0/en/Syngas-Market-Growth-Trends-COVID-19-Impact-and-Forecasts-2022-2027.html

Reytier, M., Di Iorio, S., Chatroux, A., Petitjean, M., Cren, J., De Saint Jean, M., Aicart, J., & Mougin, J. (2015). Stack performances in high temperature steam electrolysis and co-electrolysis. *International Journal of Hydrogen Energy*, *40*(35), 11370–11377. https://doi.org/10.1016/j.ijhydene.2015.04.085

Ridjan, I. (2015). *Integrated electrofuels and renewable energy systems*.

Ridjan, I., Mathiesen, B. V., Connolly, D., Ridjan, I., Mathiesen, B. V., & Connolly, D. (2013). SOEC pathways for the production of synthetic fuels. In *SOEC pathways for the production of synthetic fuels*.

Schreiber, A., Peschel, A., Hentschel, B., & Zapp, P. (2020). Life Cycle Assessment of Power-to-Syngas: Comparing High Temperature Co-Electrolysis and Steam Methane Reforming. *Frontiers in Energy Research*, *8*(November), 1–17. https://doi.org/10.3389/fenrg.2020.533850

Serpa, J., Morbee, J., & Tzimas, E. (2011). *Technical and economic characteristics of a CO2 transmission pipeline infrastructure*. https://doi.org/10.2790/30861

Shell Global. (2012). *Pearl GTL - Overview*. Major Projects. https://www.shell.com/about-us/major-projects/pearl-gtl/pearl-gtl-an-overview.html

Simoes, S. G., Catarino, J., Picado, A., Lopes, T. F., di Berardino, S., Amorim, F., Gírio, F., Rangel, C. M., & Ponce de Leão, T. (2021). Water availability and water usage solutions for electrolysis in hydrogen production. *Journal of Cleaner Production*, *315*(June). https://doi.org/10.1016/j.jclepro.2021.128124

Smedley, T. (2017). *Is the world running out of fresh water?* BBC Future Now. https://www.bbc.com/future/article/20170412-is-the-world-running-out-of-fresh-water

Smith, E., Morris, J., Kheshgi, H., Teletzke, G., Herzog, H., & Paltsev, S. (2021). The cost of CO2 transport and storage in global integrated assessment modeling. *International Journal of Greenhouse Gas Control*, *109*, 1–76. https://doi.org/10.1016/j.ijggc.2021.103367

Smith, W. A., Burdyny, T., Vermaas, D. A., & Geerlings, H. (2019). Pathways to Industrial-Scale Fuel Out of Thin Air from CO2 Electrolysis. *Joule*, *3*(8), 1822–1834. https://doi.org/10.1016/j.joule.2019.07.009

Song, Y., Zhang, X., Xie, K., Wang, G., & Bao, X. (2019). High-Temperature CO2 Electrolysis in Solid Oxide Electrolysis Cells: Developments, Challenges, and Prospects. *Advanced Materials*, *31*(50), 1–18. https://doi.org/10.1002/adma.201902033

Statista. (2020). *Carbon dioxide emissions in 2010 and 2020, by select country*. Energy & Environment. https://www.statista.com/statistics/270499/co2-emissions-in-selected-countries/

Statista. (2022a). *Cumulative renewable energy capacity worldwide from 2009 to 2021*. Energy. https://www.statista.com/statistics/1094331/global-renewable-capacity-cumulative/

Statista. (2022b). *Prices of electricity for industry in the Netherlands from 2008 to 2021*. https://www.statista.com/statistics/596254/electricity-industry-price-netherlands/

Sunfire. (2022). *Renewable syngas for e-fuel and chemicals production*.

The Engineering ToolBox. (2022a). *Fuel Gases - Heating Values*. https://www.engineeringtoolbox.com/heating-values-fuel-gases-d_823.html

The Engineering ToolBox. (2022b). *Fuels - Higher and Lower Calorific Values*. https://www.engineeringtoolbox.com/fuels-higher-calorific-values-d_169.html

The Engineering ToolBox. (2022c). *Gas Mixtures - Properties*. Gas Mixtures and the Ideal Gas Law, Mass Calculations, the Individual Gas Constant and Density. https://www.engineeringtoolbox.com/gas-mixture-properties-d_586.html

The White House. (2021). *FACT SHEET: President Biden Sets 2030 Greenhouse Gas Pollution Reduction Target Aimed at Creating Good-Paying Union Jobs and Securing U.S. Leadership on Clean Energy Technologies*. https://www.whitehouse.gov/briefing-room/statements-releases/2021/04/22/fact-sheet-president-biden-sets-2030-greenhouse-gas-pollution-reduction-target-aimed-at-creating-good-paying-union-jobs-and-securing-u-s-leadership-on-clean-energy-technologies/#:~:te

Thorvaldson Aursland, K. M. (2016). *Train transport of CO_2 – a key to enable CCS from small European emitters?* https://blog.sintef.com/sintefenergy/ccs/train-transport-of-co2-a-key-to-enable-ccs-from-small-european-emitters/

Tiseo, I. (2022). *Emission in the EU - Statistics & Facts*. Energy & Environment. https://www.statista.com/topics/4958/emissions-in-the-european-union/#topicHeader__wrapper

Towler, G., & Sinnott, R. (2022). Economic evaluation of projects. In *Chemical Engineering Design*. https://doi.org/10.1016/b978-0-12-821179-3.00009-1

United Nations. (2022). *For a livable climate: Net-zero commitments must be backed by credible action*. Climate Action. https://www.un.org/en/climatechange/net-zero-coalition

United States Environmental Protection Agency. (2022). *Overview of Greenhouse Gases*. Greenhouse Gas Emissions. https://www.epa.gov/ghgemissions/overview-greenhouse-gases

Valero, A., Valero, A., & Calvo, G. (2021). Summary and critical review of the International Energy Agency's special report: The role of critical minerals in clean energy transitions. *Revista de Metalurgia*, *57*(2). https://doi.org/10.3989/REVMETALM.197

van 't Noordende, H., & Ripson, P. (2022). *A One-GigaWatt Green-Hydrogen Plant: Advanced Design and Total Installed-Capital Costs*. https://ispt.eu/media/ISPT-public-report-gigawatt-green-hydrogen-plant.pdf

Von Der Assen, N., & Bardow, A. (2014). Life cycle assessment of polyols for polyurethane production using CO 2 as feedstock: Insights from an industrial case study. *Green Chemistry, 16*(6), 3272–3280. https://doi.org/10.1039/c4gc00513a

Voxco. (2021). *Pros And Cons of Exploratory Research*. https://www.voxco.com/blog/exploratory-research-pros-and-cons/

Wang, L., Chen, M., Küngas, R., Lin, T. E., Diethelm, S., Maréchal, F., & Van herle, J. (2019). Power-to-fuels via solid-oxide electrolyzer: Operating window and techno-economics. *Renewable and Sustainable Energy Reviews, 110*(April), 174–187. https://doi.org/10.1016/j.rser.2019.04.071

Wang, Yao, Liu, T., Lei, L., & Chen, F. (2017). High temperature solid oxide H2O/CO2 co-electrolysis for syngas production. *Fuel Processing Technology*, *161*, 248–258. https://doi.org/10.1016/j.fuproc.2016.08.009

Wang, Yuan, Zhao, L., Otto, A., Robinius, M., & Stolten, D. (2017). A Review of Post-combustion CO2 Capture Technologies from Coal-fired Power Plants. *Energy Procedia, 114*(November 2016), 650–665. https://doi.org/10.1016/j.egypro.2017.03.1209

Waternet. (2022). *Zakelijke Kosten Drinkwater*. https://www.waternet.nl/zakelijk/drinkwater-voor-bedrijven/kosten-met-watermeter/

Witvoet, G. (2018). *Do you know the difference between demineralised water and distilled water?* Bronkhorst Instruments. https://www.bronkhorst.com/int/blog-1/do-you-know-the-difference-between-demineralised-water-and-distilled-water/#:~:text=Demineralised water is water that,demi water or deionised water.

Yaashikaa, P. R., Senthil Kumar, P., Varjani, S. J., & Saravanan, A. (2019). A review on photochemical, biochemical and electrochemical transformation of CO2 into value-added products. *Journal of CO2 Utilization*, *33*(May), 131–147. https://doi.org/10.1016/j.jcou.2019.05.017

Zero Emissions Platform. (2010). The Costs of CO 2 Storage Post-demonstration CCS in the EU. *Ieaghg*, 1–53.

Zhang, H., Wang, L., Van, J., Mar, F., & Desideri, U. (2019). *Techno-economic Optimization of CO2-to-Methanol with Solid-Oxide Electrolyzer*.

Zheng, Yao, Vasileff, A., Zhou, X., Jiao, Y., Jaroniec, M., & Qiao, S. Z. (2019). Understanding the Roadmap for Electrochemical Reduction of CO2 to Multi-Carbon Oxygenates and Hydrocarbons on Copper-Based Catalysts. *Journal of the American Chemical Society*, *141*(19), 7646–7659. https://doi.org/10.1021/jacs.9b02124

Zheng, Yun, Wang, J., Yu, B., Zhang, W., Chen, J., Qiao, J., & Zhang, J. (2017). A review of high temperature co-electrolysis of H2O and CO2 to produce sustainable fuels using solid oxide electrolysis cells (SOECs): Advanced materials and technology. *Chemical Society Reviews*, *46*(5), 1427–1463. https://doi.org/10.1039/c6cs00403b